

For Reference

NOT TO BE TAKEN FROM THIS ROOM

For Reference

NOT TO BE TAKEN FROM THIS ROOM

Ex LIBRIS
UNIVERSITATIS
ALBERTAEANAE



THE UNIVERSITY OF ALBERTA

STEADY LINEAR GAS FLOW THROUGH POROUS MEDIA

BY

L.J. KOLADA



A THESIS

SUBMITTED TO THE FACULTY OF GRADUATE STUDIES
IN PARTIAL FULFILLMENT OF THE REQUIREMENTS FOR
THE DEGREE OF MASTER OF SCIENCE
IN PETROLEUM ENGINEERING

FACULTY OF ENGINEERING
DEPARTMENT OF CHEMICAL AND PETROLEUM ENGINEERING

EDMONTON, ALBERTA

DECEMBER, 1967

UNIVERSITY OF ALBERTA

FACULTY OF GRADUATE STUDIES

The undersigned certify that they have read, and recommend to the Faculty of Graduate Studies for acceptance, a thesis entitled "Steady Linear Gas Flow Through Porous Media", submitted by L.J. Kolada in partial fulfillment of the requirements for the degree of Master of Science in Petroleum Engineering.

ABSTRACT

An evaluation of the currently accepted visco-inertial flow theory has indicated that in normal laboratory determination of the absolute permeability and the inertial resistance coefficient a correction for molecular streaming is warranted. Modified forms of the visco-inertial theory have been developed considering molecular streaming for flow under both low and high pressure gradients.

A graphical means of solution for the aforementioned parameters of a medium has been proposed for flow at a low pressure gradient, and a general numerical technique has been developed for use with both modified flow equations.

It has been shown that the theory developed also applies for gas flowing in the presence of a static liquid phase. Experimental determination of the effective permeability, the Klinkenberg b-factor and the coefficient of inertial resistance has indicated that these parameters are continuous functions of the liquid saturation. While the effective permeability has been found to decrease with saturation and the Klinkenberg b-factor to remain relatively constant, the inertial resistance coefficient has been found to increase at an increasing rate.

ACKNOWLEDGEMENTS

The author wishes to express appreciation for the cooperation of many individuals and organizations in the course of this study. He is especially grateful for the capable guidance of his supervisor, Professor P.M. Dranchuk, of the Department of Chemical and Petroleum Engineering, and for the helpful suggestions of Dr. D.L. Flock, Dr. A.C. Saxena, J.K. Donnelly, and other members of the Department of Chemical and Petroleum Engineering.

Acknowledgement is made to Chevron Standard Limited, the Research Council of Alberta, the Province of Alberta, and the National Research Council for providing financial assistance.

TABLE OF CONTENTS

	<u>Page</u>
LIST OF TABLES	iii
LIST OF FIGURES	v
INTRODUCTION	1
LITERATURE REVIEW	3
Visco-Inertial Flow	3
Viscous Flow	6
Gas Flow in the Presence of a Second Phase	9
EVALUATION OF THE CURRENT THEORY	13
Analysis of Laboratory Flow Tests	13
Examining the Implications of Slippage on the Interpretation of Visco-Inertial Flow Data	15
PROPOSED THEORY	22
Modification of the Visco-Inertial Flow Theory	22
Methods for Solving the Modified Equations	25
Estimation of the Parameters	28
EXPERIMENTAL APPARATUS	30
EXPERIMENTAL PROCEDURE	33
TREATMENT OF DATA	36
RESULTS	38
Reanalysis of the Data of Previous Investigators	38
Present Experimental Results	40
Modification of the Correlation of the Inertial Resistance Coefficient	69
DISCUSSION OF RESULTS	73

CONCLUSIONS AND RECOMMENDATIONS	79
Conclusions	79
Recommendations	80
NOMENCLATURE	82
BIBLIOGRAPHY	84
APPENDIX A - A MODIFIED VERSION OF THE VISCO-INERTIAL FLOW THEORY ACCOUNTING FOR SLIPPAGE EFFECTS AT HIGH FLOW RATES	A-1
APPENDIX B - DEVELOPMENT OF A GENERAL NUMERICAL PROCEDURE TO SOLVE THE MODIFIED FORCHHEIMER EQUATIONS	B-1
APPENDIX C - APPLICATION OF THE NUMERICAL TECHNIQUE TO TWO MODIFIED FORMS OF THE FORCHHEIMER EQUATION	C-1
APPENDIX D - TABULATED DATA	D-1

LIST OF TABLES

<u>Table No.</u>	<u>Title</u>	<u>Page</u>
1	A Summary of Results for Core 20 of Sadiq	38
2	Quasilinearization Results for Samples 20 and 14 of Cornell	39
3	Physical Properties of the Samples	40
4	A Summary of Results for Core 1	52
5	Permeability and Inertial Resistance Coefficient Distribution for Core 1	54
6	A Summary of Results for Core 2	63
7	Permeability and Inertial Resistance Coefficient Distribution for Core 2	64
8	Effective Permeability, Klinkenberg b-factor and Inertial Resistance Coefficient as a Function of Liquid Saturation for Core 3	67
9	A Comparison of Inertial Resistance Coefficient Estimations	72
10	Experimental Gas Flow Data for Core 1	D-2
11	Experimental Gas Flow Data for Core 1 Section 1	D-6
12	Experimental Gas Flow Data for Core 1 Section 2	D-8
13	Experimental Gas Flow Data for Core 1 Section 3	D-10
14	Experimental Gas Flow Data for Core 1 Section 4	D-12
15	Experimental Gas Flow Data for Core 2	D-14

Table
No.

Title

Page

16	Experimental Gas Flow Data for Core 2 Section 1	D-18
17	Experimental Gas Flow Data for Core 2 Section 2	D-20
18	Experimental Gas Flow Data for Core 2 Section 3	D-22
19	Experimental Gas Flow Data for Core 2 Section 4	D-24
20	Experimental Gas Flow Data for Core 3 Dry	D-26
21	Experimental Gas Flow Data for Core 3 Liquid Saturation .0765	D-28
22	Experimental Gas Flow Data for Core 3 Liquid Saturation .124	D-30
23	Experimental Gas Flow Data for Core 3 Liquid Saturation .205	D-32
24	Experimental Gas Flow Data for Core 3 Liquid Saturation .253	D-34

LIST OF FIGURES

<u>Figure No.</u>	<u>Title</u>	<u>Page</u>
1	Flow Coefficients for Brown Dolomite Core 20 of Cornell Using Standard Visco-Inertial Flow Plot Technique	18
2	Flow Coefficients for Outcrop Sandstone Core 14 of Cornell Using Standard Visco- Inertial Flow Plot Technique	19
3	Sleeve Type Core Holder	32
4	Backpressure Plot for Core 1	41
5	Klinkenberg Permeability Plot for Core 1	43
6	Klinkenberg Permeability Plot Coefficients for Core 1	44
7	Standard Visco-Inertial Flow Plot for Core 1	45
8	Flow Coefficients for Core 1 Using Standard Visco-Inertial Flow Plot Technique	47
9	Modified Visco-Inertial Flow Plot for Core 1	48
10	Modified Visco-Inertial Flow Equation Coefficients for Core 1	49
11	Results from Quasilinearization of Equation (32) for Core 1	51
12	Pressure Drop Profile for Core 1	53
13	Backpressure Plot for Core 2	55
14	Klinkenberg Permeability Plot for Core 2	56
15	Klinkenberg Permeability Plot Coefficients for Core 2	57
16	Standard Visco-Inertial Flow Plot for Core 2	59

<u>Figure No.</u>	<u>Title</u>	<u>Page</u>
17	Modified Visco-Inertial Flow Plot for Core 2	60
18	Flow Coefficients for Core 2 Using Standard Visco-Inertial Flow Plot Technique	61
19	Modified Visco-Inertial Flow Equation Coefficients for Core 2	62
20	Pressure Drop Profile for Core 2	65
21	Pressure Drop Profile for Core 2	66
22	Visco-Inertial Flow Plot for Core 3	68
23	Effective Permeability, Klinkenberg b-Factor and Inertial Resistance Coefficient as a Function of Liquid Saturation for Core 3	70

INTRODUCTION

For some time now flow of a single phase fluid through saturated porous media has been studied rigorously. It has been customary to describe flow in the viscous and visco-inertial flow regions by means of Darcy's Law and the Forchheimer equation respectively^(1,2). The Klinkenberg b-factor, the permeability and the inertial resistance coefficient are empirical constants used to characterize a porous medium.

Generally the presence of a connate water is inherent to those formations which contain petroleum hydrocarbon deposits. Hence, it is important to predict the flow behavior of a gas in the presence of a liquid such as a connate water or a hydrocarbon.

The theory describing flow in a dry porous medium has been extended to describe the phenomenon of flow in the presence of a second phase. Under viscous flow conditions this type of analysis has been verified experimentally⁽³⁾. The conclusions which have been made are that the permeability to the gas is a continuously decreasing function of the liquid saturation, unique for each sample, while the Klinkenberg b-factor remains essentially constant. An attempt has also been made to apply the visco-inertial flow theory to gas flow in the presence of a second phase⁽⁴⁾.

The object of this study was to theoretically and experimentally verify the visco-inertial flow theory and to determine the effect that an increasing liquid saturation has upon the characteristic parameters of a porous medium under visco-inertial flow conditions.

LITERATURE REVIEW

Visco-Inertial Flow

According to Scheidegger⁽⁵⁾, Forchheimer, drawing an analogy with the phenomenon occurring in tubes, suggested that high velocity flow through porous media may be described by an expression of the form

$$\frac{(p_1 - p_2)}{L} = aq + bq^2 \quad (1)$$

where q is the seepage velocity and a and b are thought to be constants.

From a development based on Reynold's theory of resistance to flow and the Kozeny assumption that a porous medium is analogous to parallel capillaries with common hydraulic radius, Ergun and Orning⁽⁶⁾ presented an expression of the form

$$\frac{(p_1 - p_2)}{L} = c\mu q + d\rho q^2 \quad (2)$$

where c and d are constants and functions of the medium. They illustrated the validity of this expression by showing the linearity of $(p_1 - p_2)/q_O L$ versus ρq_O for flow through unconsolidated porous media of fluids which were assumed to behave ideally.

Green and Duwez⁽⁷⁾ characterized the structure of a porous medium with two length parameters F_A and F_B , using

the quadratic equation

$$-\frac{dp}{dx} = F_A \mu q + F_B \rho q^2 \quad (3)$$

F_A is the viscous resistance coefficient and F_B is the inertial resistance coefficient, both independent of the fluid properties. Using a form of Equation (3) integrated for a constant mass flow rate of an ideal gas, they evaluated the resistance coefficients for four sintered porous metal specimens.

Cornell and Katz⁽⁸⁾ conducted a study of "inertial, quasi turbulent or turbulent" flow of various gases through twenty-four consolidated samples of sandstone, limestone, and dolomite. They concluded that an expression of the form of Equation (3) is valid.

The motion of ordinary Newtonian fluids can be described by means of the Navier-Stokes equation. In a porous medium gross simplifications must be made in order to formulate boundary conditions. Irmay⁽⁹⁾ analyzed an idealized pore system of spherical particles, and Tek⁽¹⁰⁾ represented the flow channels by a sequence of truncated cones, giving rise to successive restrictive orifices along the channel. They both indicated the validity of an expression similar to Equation (3) which may be written as

$$-\frac{dp}{dx} = F_A \mu q + F_B \rho q |q| \quad (4)$$

where F_A and F_B are dependent upon the nature of the pore geometry. The conditions imposed in arriving at Equation (4) are horizontal steady linear isothermal flow of a single phase Newtonian fluid through chemically inactive homogeneous isotropic geometrically stable saturated media.

Equation (3), the differential form which will be referred to as the Forchheimer equation, has been put into a more useful form by combining with the modified gas law and integrating for a constant mass flow rate. Realizing that viscosity μ and compressibility Z are pressure dependent under isothermal conditions, Mackett⁽¹¹⁾ used

$$\frac{Z_0 T_0 p_c^2 A}{\rho_0 \mu_0 T_c Q_0 \bar{T}_r L} \left(\int_0^{p_{r1}} \frac{p_r}{Z \mu_r} dp_r - \int_0^{p_{r2}} \frac{p_r}{Z \mu_r} dp_r \right) \\ = F_A + F_B \frac{Q_0 \rho_0}{A \mu_{ia}} \quad (5)$$

where the integrated average viscosity μ_{ia} was taken as

$$\mu_{ia} = \mu_0 \frac{\int_0^{p_{r1}} \frac{p_r}{Z} dp_r - \int_0^{p_{r2}} \frac{p_r}{Z} dp_r}{\int_0^{p_{r1}} \frac{p_r}{Z \mu_r} dp_r - \int_0^{p_{r2}} \frac{p_r}{Z \mu_r} dp_r} \quad (6)$$

where $\mu_r = \frac{\mu}{\mu_0}$

He evaluated the isothermal variation of viscosity and compressibility of nitrogen with pressure to investigate

the magnitude of errors resulting from the assumption of average fluid properties. He concluded that under normal laboratory conditions it was valid to use values of viscosity and compressibility evaluated at the arithmetic mean pressure and temperature. This indicated that the integrated form used by Cornell⁽¹²⁾ is valid

$$\frac{M(p_1^2 - p_2^2)}{2\bar{\mu}ZRTL w/A} = F_A + F_B \frac{w}{A\bar{\mu}} \quad (7)$$

The non-rigorous nature of the derivation of the Forchheimer equation left open the question whether the factors F_A and F_B were geometrical and structural variables or were dependent upon pressure or velocity. Since structure itself may change to a certain extent with varying ambient conditions, changes in temperature and pressure may affect F_A and F_B .

Greenberg and Weger⁽¹³⁾ studied the constancy of F_A and F_B for flow through porous metals at high rates and pressures up to 2000 psi. They concluded that these coefficients remained constant under isothermal conditions.

Viscous Flow

The criterion for kinematic similarity has been applied by Hubbert⁽¹⁴⁾ to define the Reynolds Number, N_{Re} , which is a measure of the ratio of inertial effects to the

viscous effects. From Equation (7) this may be written as

$$N_{Re} = \frac{F_B}{F_A} \frac{w}{A\mu} \quad (8)$$

At very low rates, for example at Reynolds Numbers less than 0.01, the portion of the pressure drop due to inertial effects is very small compared to that due to the viscous effects. Hence, the inertial effects may be neglected in Equation (3) resulting in

$$-\frac{dp}{dx} = F_A \mu q \quad (9)$$

When a comparison is made with Darcy's Law⁽¹⁵⁾

$$-\frac{dp}{dx} = \frac{l}{k} \mu q \quad (10)$$

the viscous resistance coefficient is found to be the inverse of permeability k.

For linear flow of a constant mass flow rate, Mackett⁽¹⁶⁾ again indicated the validity of using values of the viscosity and compressibility evaluated at the mean temperature and pressure. The resulting integrated forms are

$$\frac{M(p_1^2 - p_2^2)}{2\mu Z R T L w/A} = \frac{1}{k} \quad (11)$$

$$\frac{AT_o Z_o (p_1^2 - p_2^2)}{2\mu Z \bar{T} P_o L Q_o} = \frac{1}{k} \quad (12)$$

Following the investigation of Kundt and Warburg, Klinkenberg⁽¹⁷⁾ observed that as the mean free path length of the fluid approaches the dimensions of the flow conduit, the gas layer immediately adjacent to the wall of a capillary has a finite velocity in the direction of flow. The mean free path length or the average distance travelled by a gas molecule between intermolecular collisions is a function of the pressure, temperature and the nature of the gas⁽¹⁸⁾.

$$\lambda = \frac{1}{\sqrt{2} \pi d^2 n} = \frac{RT}{\sqrt{2} \pi p N d^2} \quad (13)$$

Drawing an analogy to the flow in glass capillary tubes, Klinkenberg corrected the apparent permeability of a porous medium to the absolute permeability exhibited to a fluid of a very low mean free path. On the basis of the theory and extensive experimentation he proposed that the apparent permeability k_a , calculated from Darcy's law using Equations (11) and (12), be related to the absolute permeability by

$$k_a = k \left(1 + \frac{4c\bar{\lambda}}{r} \right) \quad (14)$$

For any gas c is a constant and is approximately equal to 1.0. Substituting for the mean free path length in Equation (14)

$$k_a = k \left(1 + \frac{4cRT}{\sqrt{2} \pi d^2 N \bar{p} r} \right) \quad (15)$$

Under isothermal conditions the factor $\frac{4cRT}{\sqrt{2} \pi d^2 Nr}$

is a constant for a given gas and medium. This is referred to as the Klinkenberg b-factor, which is inversely proportional to an effective path radius r. Therefore equation (15) may be written

$$k_a = k(1 + \frac{b}{\bar{p}}) \quad (16)$$

where \bar{p} is the arithmetic mean pressure.

Emphasis has been placed on slippage because of its presence under normal laboratory conditions. Stewart and Owens⁽¹⁹⁾ performed tests on heterogeneous limestones to investigate the extent to which slippage and inertial effects can exist simultaneously. Slippage was controlled by maintaining constant mean free path conditions. At very large Reynolds Numbers the slippage effect disappeared. Nevertheless at high flow rates it was found that both slippage and inertial effects contributed significantly to the phenomenon observed.

Gas Flow in the Presence of a Second Phase

Experimental evidence has indicated that relationships similar to those obtained to predict gas flow behavior through dry porous media are valid in describing the flow of gas in the presence of a liquid phase.

Rose⁽²⁰⁾ and Estes and Fulton⁽²¹⁾ showed that Klinkenberg's interpretation of slippage could be applied to both homogeneous gas flow and flow of gas in a liquid saturated porous medium. It was observed that under isothermal conditions the relative effect of slippage was constant as the Klinkenberg b-factor remained relatively constant for various saturations. The permeability was found to decrease continuously with increasing liquid saturation.

Hamm and Eilerts⁽²²⁾ studied the effects of a condensate saturation in typical sandstone and limestone reservoir rocks on the mobility of gas. Under viscous flow conditions they investigated the effects of pressure, liquid saturation and velocity on the mobility, which is defined as the ratio of the permeability to the viscosity. They concluded that increased gas velocity, increased liquid saturation and increased pressure would decrease the mobility. These effects are attributable respectively to inertial effects, the influence of the liquid saturation and the reduction of slippage effects and increase of gas viscosity with increasing pressure.

Using a sample of heterogeneous limestone which exhibited negligible slippage effects, Stewart and Owens⁽²³⁾ studied two-phase flow of gas and oil under external gas drive. They found two regions of flow similar to those which are evident in single-phase flow.

Iffly and Naville⁽²⁴⁾ presented an equation, describing visco-inertial flow, which was accredited to Houpeurt

$$v(1 + \phi U - \frac{\rho}{\mu} |v|) = - \frac{k_g}{\phi \mu} \text{grad } \vec{p} \quad (17)$$

U and k_g , the effective permeability to the gas, are the two length parameters. The integrated form of the equation for linear flow of an ideal gas was used

$$w(1 + \frac{U w}{\mu A}) = \frac{k_g A}{\mu} \int_{p_1}^{p_2} \rho dp = \frac{k_g A M(p_1^2 - p_2^2)}{2\mu LRT} \quad (18)$$

Flow tests were performed on a sandstone sample at various saturations of a frozen immobilized second phase. For all saturations a plot of $(p_1^2 - p_2^2)/w$ versus w appeared to be linear. The parameters U and k_g were evaluated for all saturations. With an increasing saturation of the second phase k_g was found to decrease continuously while U increased in magnitude.

Results were found to compare favorably with those obtained for simultaneous flow of two phases. This procedure was not recommended because of instability, but served to indicate that the phenomenon observed occurs independently of the saturating medium.

Nichol⁽²⁵⁾ also studied visco-inertial flow behavior in the presence of an immobile second phase. He investigated

the variation of the inertial resistance coefficient F_B , as defined in Equation (7), with an increasing saturation of glycerin, the second phase. The coefficient was found to decrease slightly at low saturations but increase sharply thereafter.

EVALUATION OF THE CURRENT THEORY

Analysis of Laboratory Flow Tests

The dynamic flow equations may be applied to predict gas flow behavior in a porous medium under the conditions of viscous and visco-inertial flow provided the three parameters absolute permeability, the Klinkenberg b-factor and the inertial resistance coefficient are known. It has been found advantageous to obtain these parameters from laboratory tests upon representative samples.

At first the permeability of a test specimen was determined by conducting a single laboratory flow test and applying Darcy's Law to the resulting data.

Klinkenberg⁽²⁶⁾ observed that this apparent permeability of a porous medium to a gas was dependent upon the nature of the medium, the mean flowing pressure and the nature of the gas. He proposed that the absolute permeability be determined by means of a multiple point flow test. By Equation (16), from a plot of k_a versus $1/\bar{p}$, termed a Klinkenberg plot, the absolute permeability is the extrapolated intercept and the Klinkenberg b-factor is the slope divided by the absolute permeability.

For flow in the visco-inertial region Equation (7) may be modified, recalling that F_A is the reciprocal permeability.

$$\frac{M(p_1^2 - p_2^2)}{2\bar{\mu}ZRTL w/A} = \frac{1}{k} + F_B \frac{w}{A\bar{\mu}} \quad (19)$$

Examination of Equation (19) indicates that a plot of the left hand side versus $w/A\bar{\mu}$, termed a visco-inertial flow plot⁽²⁷⁾, is linear with slope F_B and intercept $1/k$.

In many instances application of these graphical techniques yields anomalous results as evidenced by appreciable departures from linearity in both the Klinkenberg and visco-inertial flow plots⁽²⁸⁾. In view of the fact that a Klinkenberg extrapolation is invalid if the data are not in the viscous flow region, recent studies have revealed that departures from linearity exhibited by the Klinkenberg plot at high mean pressures may be attributed to the inclusion of visco-inertial data observations⁽²⁹⁾. Hence, the departures may be avoided, provided the data points to be used are restricted to the viscous flow region. For flow in the viscous region, examination of Equation (12) indicates that if permeability, viscosity, compressibility, and temperature can be assumed constant for a series of data runs upon a specimen, a plot of $\log(p_1^2 - p_2^2)$ versus $\log Q_o$ will be linear with slope of 1. This plot is termed the backpressure plot. A departure from linearity at higher flow rates is assumed to represent the existence of significant inertial effects. Consequently, in order to delineate the viscous and visco-inertial flow regions, Dranchuk and Sadiq⁽³⁰⁾ have suggested

that data be first plotted on a backpressure plot. Data on the straight line portion of the curve may be taken to lie in the viscous flow region.

For data taken in the visco-inertial flow region, downwarping of the data plot at low Reynolds Numbers and corresponding low mean pressures has been attributed to molecular streaming. However, no attempt has been made to correct for this effect. The approach in most cases has been to ignore the effect or extrapolate supposedly unaffected data.

Examining the Implications of Slippage on the Interpretation of Visco-Inertial Flow Data

Cornell⁽³¹⁾ attributed the downwarping on the visco-inertial data plot to molecular streaming but chose to avoid the effects by extrapolating unaffected data. No rigid criterion for delineation of the region of linearity has been established for the visco-inertial flow plot. This makes one wonder how unaffected data may be chosen. It is equally likely that some, all or none of the data are affected. Even though slippage may contribute to the phenomenon observed, the basic theory of visco-inertial flow may not adequately describe the phenomenon occurring. With this in mind, several sets of the data presented by Cornell were examined.

Results are presented for two samples which exhibited peculiar characteristic curves. Data observations had been taken with very similar gases so that the Klinkenberg b-factor could be taken as one constant for each sample.

If the observed data were consistent with the theory, evaluation of the parameters for portions of the data should yield the same values obtained using the entire data set. Standard experimental procedure is such that the mean pressure decreases as the flow rate decreases. Thus, the effect of slippage would become more significant as the flow rate is decreased. Therefore, on a visco-inertial flow plot, inclusion of data points at successively lower values of the abscissa $w/A\bar{\mu}$ would increase the effect of slippage on the determination of permeability and the inertial resistance coefficient. Hence, the data were processed by first analyzing the two highest flow rate data points and successively adding the lower flow rate data points, one at a time, until all of the data had been included. The coefficients k and F_B , evaluated from a linear least squares fit for each group of data, have been plotted at the corresponding smallest value of $w/A\bar{\mu}$ in the group analyzed. Thus, this plot indicates the values obtained for the parameters using all available data taken at values of $w/A\bar{\mu}$ above that used for the abscissa. The difference between any two successive points indicates the effect which the addition of one more data point at a lower flow rate would have.

Results for sample 20⁽³²⁾ are presented graphically in Figure (1). The values presented by Cornell are a permeability k of 1.01 md and a "turbulence factor" F_B of $7.25 \times 10^{10} \text{ ft}^{-1}$. However, it would appear that at high values of the independent variable $w/A\bar{\mu}$ the proper extrapolated values are a permeability k of 0.65 md and a "turbulence factor" F_B of $5.4 \times 10^{10} \text{ ft}^{-1}$. Generally it appears that the results for this sample exhibit internal inconsistencies. It is not immediately evident whether slippage alone or discrepancies in the basic theory cause the deviation.

For core sample 14⁽³³⁾, Cornell presented values of 20.9 md for the permeability and $8.2 \times 10^8 \text{ ft}^{-1}$ for the "turbulence factor". Results obtained from a linear least squares fit of the data are presented in Figure (2). It appears that extrapolation should yield a permeability of 16.5 md and a "turbulence factor" of $7.0 \times 10^8 \text{ ft}^{-1}$.

Hence, the ramifications of not being able to distinguish which, if any, data are unaffected by slippage are clearly illustrated by indicating the error introduced each time an additional data point is included in the evaluation. There is a definite trend as the permeability and "turbulence factor" presented by Cornell are consistently higher than those thought to be correct.

The theory indicates that both the Klinkenberg and visco-inertial graphical approaches should yield the permeability of the sample. The approach of Sadiq⁽³⁴⁾ was to check

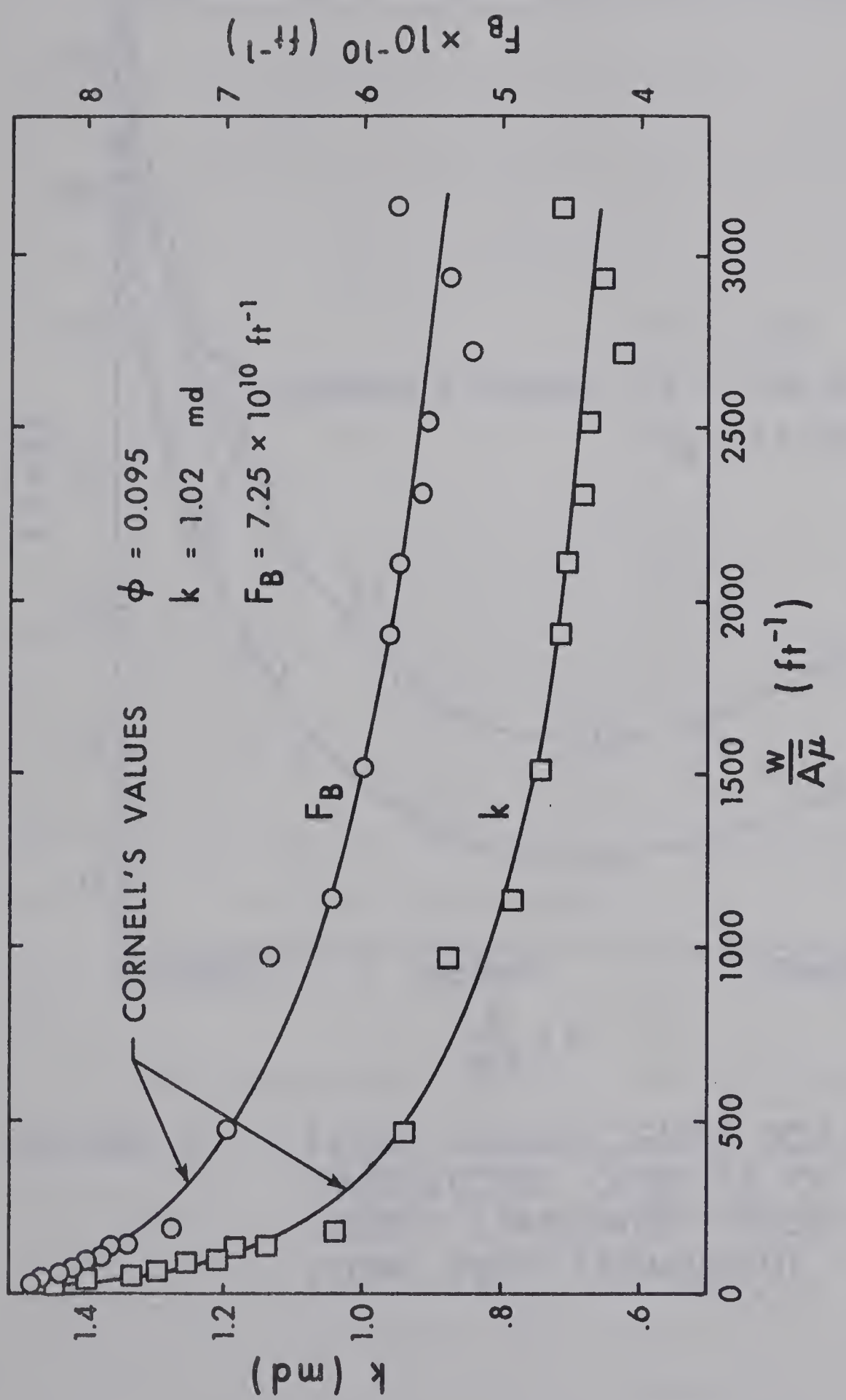


FIGURE 1
FLOW COEFFICIENTS FOR BROWN DOLOMITE CORE
20. OF CORNELL USING STANDARD VISCO-INERTIAL
FLOW PLOT TECHNIQUE

FIGURE 1

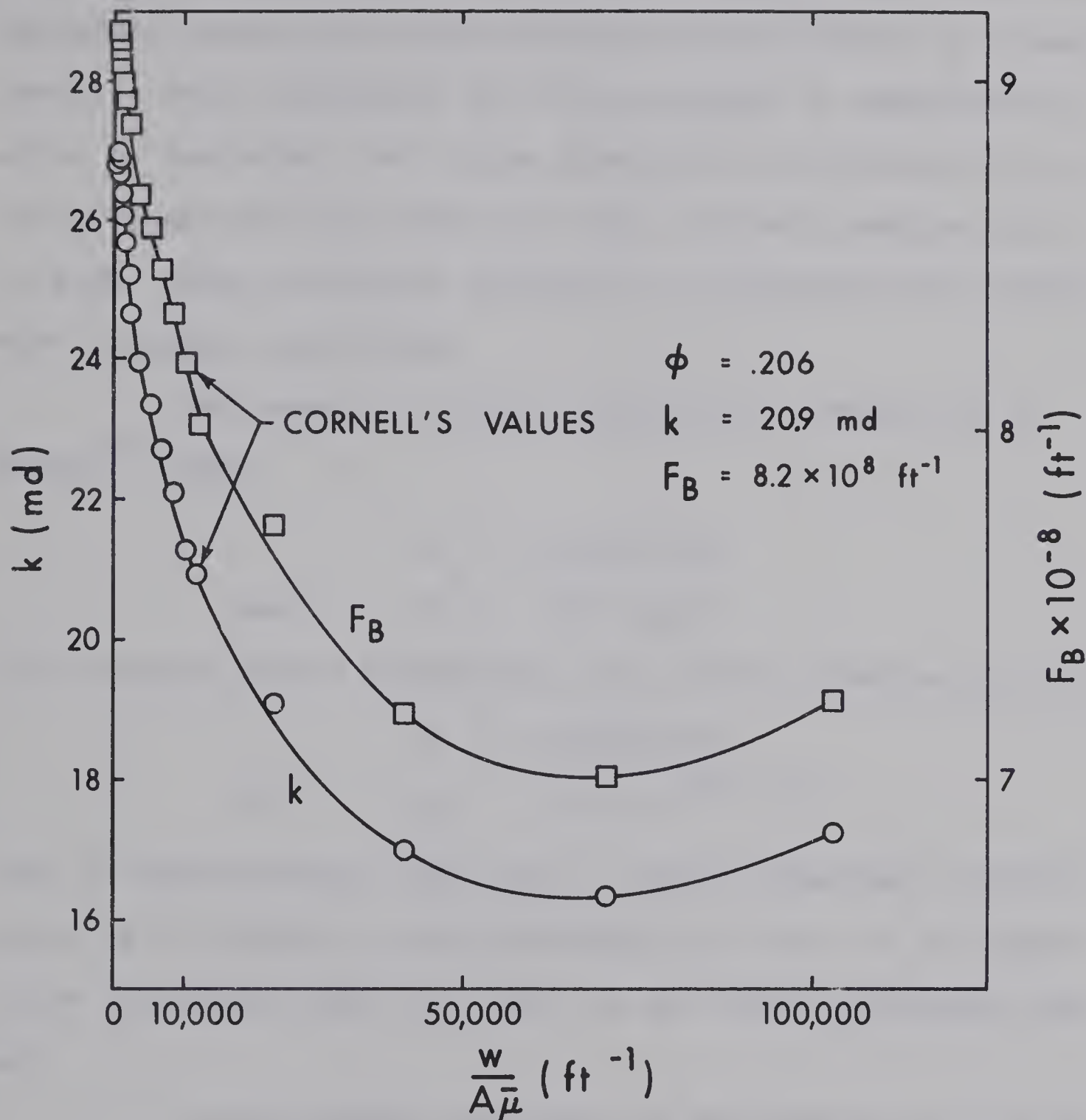


FIGURE 2

FLOW COEFFICIENTS FOR OUTCROP
SANDSTONE CORE 14. OF CORNELL
USING STANDARD VISCO-INERTIAL
FLOW PLOT TECHNIQUE

the visco-inertial theory by comparing to Klinkenberg plot results of viscous data. He found that generally the two independent means yield permeabilities which differ by a small amount. This difference may be attributed to experimental error or neglected, but close observation indicates that invariably permeability obtained from the visco-inertial plot is high. When molecular streaming is pronounced the difference is quite significant.

For example, results obtained for sample 20 of Sadiq⁽³⁵⁾ were

$$k = 0.000127 \text{ md}$$

$$\text{and } b = 160.4 \text{ psia}$$

for nitrogen from a Klinkenberg plot of the viscous data and

$$k = 0.000184 \text{ md}$$

$$\text{and } F_B = 8.01 \times 10^{16} \text{ ft}^{-1}$$

from a visco-inertial flow plot. Having observed a discrepancy of 45 percent in the permeability value, it is impossible to predict what the error in the other parameters may be.

In the present case and for the others presented the discrepancies are great enough to warrant performing a correction for slippage. The delineation of unaffected data on a visco-inertial flow plot has been shown to be very difficult, if not impossible, since it is within the realm of possibility that in some cases all data are affected.

Correcting for slip should enable the use of all data taken and ensure that the analysis of viscous data and the analysis of visco-inertial data yield consistent results.

PROPOSED THEORY

Modification of the Visco-Inertial Flow Theory

The Forchheimer equation

$$-\frac{dp}{dx} = F_A \mu q + F_B \rho q^2 \quad (20)$$

has been used to describe visco-inertial flow under the conditions of no slip. Klinkenberg's modification of Darcy's Law has also been used to adequately describe the slip phenomenon under strictly viscous flow conditions.

$$k_a = k \left(1 + \frac{b}{p}\right) \quad (21)$$

The contribution of slip may be incorporated in the viscous term of the basic Forchheimer equation. Klinkenberg's modification of Darcy's Law, Equation (10), may be written as

$$-\frac{dp}{dx} = \frac{\mu q}{k_a} = \frac{\mu q}{k \left(1 + \frac{b}{p}\right)} \quad (22)$$

From a comparison to Equation (9), the truncated form of the Forchheimer equation, it becomes obvious that

$$F_A = \frac{1}{k_a} = \frac{1}{k \left(1 + \frac{b}{p}\right)} \quad (23)$$

Forchheimer's equation written in terms of the absolute permeability k is

$$-\frac{dp}{dx} = \frac{\mu q}{k \left(1 + \frac{b}{p}\right)} + F_B \rho q^2 \quad (24)$$

Multiplying through by ρ/μ , which is equal to $\rho M/\mu ZRT$ according to the modified gas law, and defining the constant mass flow rate as

$$\rho q = \frac{w}{A} \quad (25)$$

results in

$$\frac{-M}{\mu ZRT} \frac{w}{A} pdp = \left(\frac{1}{k(1 + \frac{b}{p})} + \frac{F_B w}{A\mu} \right) dx \quad (26)$$

In order to facilitate the solution of this equation the apparent permeability may be taken as a function of the arithmetic mean pressure. Essentially this means replacing p in the viscous term by \bar{p} . Substituting $pd़p = dp^2/2$ and taking integrals,

$$\frac{-M}{2R} \frac{\frac{p_2^2}{2} - \frac{p_1^2}{2}}{\frac{w}{A}} \frac{dp^2}{\mu ZT} = \int_0^L \left(\frac{1}{k(1 + \frac{b}{\bar{p}})} + \frac{F_B w}{\mu A} \right) dx \quad (27)$$

When constant values of the viscosity and compressibility, both evaluated at the arithmetic mean pressure and temperature, are used the integrated form becomes

$$\frac{M(p_1^2 - p_2^2)}{2\bar{\mu}ZRT L} \frac{\frac{w}{A}}{\bar{A}} = \frac{1}{k(1 + \frac{b}{\bar{p}})} + \frac{F_B w}{A\bar{\mu}} \quad (28)$$

At this point it is suitable to restate the Reynolds Number, on the basis of this development, as

$$N_{Re} = \frac{k F_B w}{A\bar{\mu}} \left(1 + \frac{b}{\bar{p}} \right) \quad (29)$$

It is also appropriate to restate the integrated forms of the viscous flow equations in the light of Klinkenberg's modification of Darcy's Law. Equations (11) and (12) become

$$\frac{M(p_1^2 - p_2^2)}{2\bar{\mu}ZRTL \frac{W}{A}} = \frac{1}{k_a} = \frac{1}{k(1 + \frac{b}{\bar{p}})} \quad (30)$$

$$\frac{AT_oZ_o(p_1^2 - p_2^2)}{2\bar{\mu}ZT P_o L Q_o} = \frac{1}{k_a} = \frac{1}{k(1 + \frac{b}{\bar{p}})} \quad (31)$$

According to Equation (31) it is interesting to note that a plot of $\log((1 + \frac{b}{\bar{p}})(p_1^2 - p_2^2))$ versus $\log Q_o$, which may be termed a modified backpressure plot, should be linear of slope 1.

These relationships have been derived under the premises of a low overall pressure drop as the questionable assumption that \bar{p} is not a function of p has been made. To check the ramifications of this assumption the theory was rederived to account for large pressure drops. This resulted in the modified form, derived in detail in Appendix A

$$\frac{M(p_1^2 - p_2^2)}{2\bar{\mu}ZRTL \frac{W}{A}} = \frac{\gamma^3}{\gamma^2 - \frac{2ab^2}{k(p_1^2 - p_2^2)} \ln \frac{(ab+p_1\gamma)}{(ab+p_2\gamma)} + \frac{b\gamma}{kp}} \quad (32)$$

where

$$\alpha = \frac{F_B W}{A\bar{\mu}}$$

and

$$\gamma = \frac{1}{k} + \alpha$$

Methods for Solving the Modified Equations

In normal laboratory analysis, when access to a digital computer is not available, it is convenient to have a graphical means of solution. Then a linear fit may be estimated by observation if necessary.

Advantage may be taken of the linearity of Equation (28). From a plot of the left hand side versus $\frac{w}{A\mu} (1 + \frac{b}{p})$, referred to as a modified visco-inertial flow plot, the absolute permeability is the reciprocal of the intercept and the inertial resistance coefficient is the slope. Use of this technique requires the prior knowledge of b. The modified graphical technique may now be applied as follows:

- 1) The data are plotted on a conventional backpressure plot.
- 2) The viscous and visco-inertial flow regions are tentatively delineated by conservatively picking the lowest flow rate at which departure from linearity appears to occur.
- 3) A Klinkenberg plot is performed for the data in the viscous region, and tentative values of b and k are determined from a linear least squares fit of the data.
- 4) A modified backpressure plot is constructed and the regions of viscous and visco-inertial flow are again delineated. If the point of departure agrees with that established in 2) above, the tentative values as determined in 3) are assumed correct. If not, the procedure

is repeated until agreement is achieved.

- 5) The final value of b is used to construct a modified visco-inertial plot for all data except those which have been found to be in the viscous region. Now k and F_B are determined from a linear least squares fit of the data.

Graphical techniques generally employed have shortcomings since the method is time-consuming and the data must be split requiring a large number of observations in both the viscous and visco-inertial flow regions. It would be highly desirable to use all of the available data in evaluating each parameter. This would add considerably more weight to the values obtained.

The modified form of the Forchheimer equation derived to describe flow under relatively high pressure differentials is not readily amenable to graphical treatment.

Provided access to a digital computer is available a numerical procedure may be developed to solve for the best values of the parameters. From an examination of the equations presented it is obvious that in general the relationship may be represented by

$$\frac{M(p_1^2 - p_2^2)}{2\bar{\mu}ZRTL \frac{W}{A}} = fcn(k, b, F_B) \quad (33)$$

The functional relationship is non-linear with respect to the three constants k , b and F_B . Now it is necessary to determine values of the parameters k , b and F_B to make the assumed functional relationship optimal for experimentally

determined values of $\frac{M(p_1^2 - p_2^2)}{2\bar{\mu}ZRTL \frac{w}{A}}$, $\frac{w}{A\bar{\mu}}$, \bar{p} and $p_1 - p_2$

for each of a series of data points. The criterion of optimization which may be used for the estimation of the best fit parameters is minimization of the residual sum of squares of the left hand side.

Since this type of solution hinges upon linearity, quasilinearization, a combination of linear approximation techniques with the capabilities of the digital computer, may be applied. The Newton-Raphson approximation scheme⁽³⁶⁾, by analogy with the sequence of approximations to the zeros of a function, may be applied to present an expansion about a set of parameter values. This results in the iterative solution of a set of linear equations. Thus, given initial estimates one may apply linear least squares to determine corrections to the guesses. Convergence is not always achieved and is related to the selection of initial guesses. If the initial parameter estimates are good, convergence will occur rapidly.

Application of this technique, which is described in detail in Appendix B, requires evaluation of several derivatives of the functional relationship with respect to

the parameters. In Appendix C the necessary relationships are developed for the two equations presented previously.

Estimation of the Parameters

In order to assure convergence in the interpretation of data by the numerical technique proposed it is extremely important to have good initial guesses of the unknown parameters. In a re-evaluation of the results of previous studies, the values presented in the original work leave no guess work for good initial guesses. However, in the case of recent tests, where only basic physical data are available, a simple technique must be determined for making good estimations of the parameters.

Permeability may be approximated from a single point test. Any single point could do but it is suggested the lowest flow rate observation be used.

The Klinkenberg b-factor for air has been correlated with absolute permeability by Heid et al⁽³⁷⁾ as

$$b = 0.777 k^{-0.39} \quad (34)$$

for b in international atmospheres and k in millidarcies. It is suggested that b, calculated from this equation using the single point permeability, be used as a starting value.

As reported by Sadiq⁽³⁸⁾ many attempts have been made to predict the inertial resistance coefficient. From a dimensional analysis he proposed

$$F_B = \frac{1.617 \times 10^5}{k^{.5} \phi^{5.07}} \quad (35)$$

where F_B is in ft^{-1} and k in md, as a general correlation of F_B with the absolute permeability and the effective porosity. It is therefore suggested that this relationship be used to obtain a good initial guess of F_B using the single point permeability evaluation.

EXPERIMENTAL APPARATUS

A gas expansion porosimeter, calibrated with solid blanks of known dimensions, was used to measure the gross grain volume of the cores prior to mounting.

Accurate determination of the characteristic flow parameters of the samples tested required precise measurement and control of temperature, pressure and volumetric flow rate over an extensive range of values for each data set.

The temperature of the flowing fluid immediately upstream and downstream of the endface flow taps was measured with calibrated iron constantan thermocouples, inserted in the flow line. Control of the mean temperature was effected by passing the fluid through a copper coil, immersed in a constant temperature glycol bath, before entering the sample.

Water and mercury manometers were used to obtain pressure readings up to 30 psig, whereas higher pressures were measured with a variety of calibrated bourdon-tube pressure gauges. Control of the upstream pressure was effected by means of pressure regulators in series between the gas supply cylinders and the sample holder. Downstream pressure could be controlled by a backpressure regulator in the flow line.

Several calibrated volumetric flow measuring devices were used so that an extensive range could be covered adequately. Flow rates below 15 cc/sec were measured by timing

the displacement of soap-film in a burette. Rates between 15 cc/sec and 180 cc/sec were measured with a wet test meter and higher rates to 1650 cc/sec were measured using a dia-phragm meter.

The coreholders used were of a rubber sleeve construction and a resin mounted type. For the sleeve type of core holder illustrated in Figure (3) a 1/8-inch neoprene sleeve was used satisfactorily with nitrogen as the pressurizing fluid, effecting a seal around the core and maintaining a longitudinal compression on the core. The core holder was modified by penetrating the rubber sleeve with 1/8 inch stainless steel Autoclave tubing to enable the measurement of the pressure distribution along the length of the sample.

The resin mounted core holder has been described by Mackett⁽³⁹⁾.

The inlet and outlet flow lines and all pressure taps consisted of 1/8-inch stainless steel Autoclave tubing. Tygon tubing was used to connect the flow measuring devices. The entire apparatus was enclosed in a thermostatically controlled constant temperature cabinet.

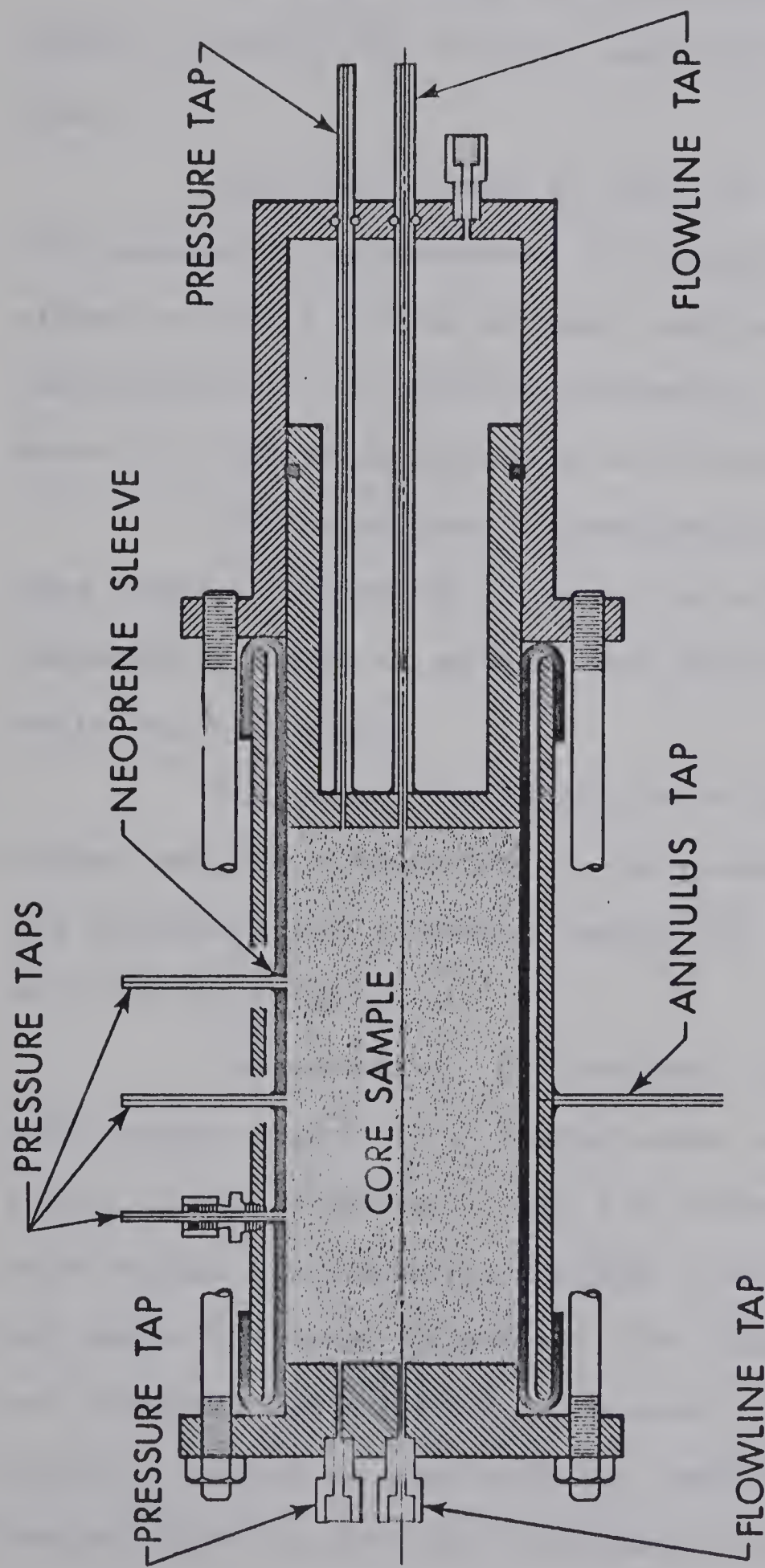


FIGURE 3
SLEEVE TYPE CORE HOLDER

EXPERIMENTAL PROCEDURE

The core samples were cleaned by refluxing toluene vapors at 240°F for 20 hours and drying at 220°F for 24 hours.

The bulk volume of each of the cores was evaluated from extensive measurements of length and diameter. The effective grain volume of each sample was determined using a calibrated gas expansion porosimeter. From these measurements the effective porosity was evaluated.

The cores were subsequently mounted in the sleeve type holder or mounted in resin in a similar fashion to that proposed by Mackett, except that the filler in the Hysol 4160 resin was excluded.

Following the insertion of the core into the core holder and the connection of the pressure taps and flow lines, the apparatus was pressure tested for leaks using a soap solution type detector.

Subsequently, the desired flow tests were run, with data points chosen in a random order as a check for any internal inconsistencies. For all tests on the sleeve type core holder the pressurizing fluid pressure was maintained 100 psi above the inlet pressure. The temperature of the cabinet was observed periodically to ensure that it remained constant during a series of runs and the temperature of the glycol bath was adjusted so that the arithmetic mean temperature of the

flowing fluid, nitrogen, was constant.

For each run, after adjustment of the pressure regulating equipment, when observation of the inlet and outlet pressures and volumetric flow rate indicated that stabilized conditions prevailed, values were recorded of 1) barometric pressure and ambient temperature, 2) inlet and outlet thermocouple readings, 3) inlet, outlet and intermediate pressure readings, and 4) volumetric flow rate reading with the corresponding pressure and temperature readings for the particular measuring device.

For those series of runs in which a resident uniform liquid saturation was desired 2-octanol, a chemically inactive fluid possessing a low vapor pressure, was used as the saturating fluid. In order that the proper proportions of this fluid be deposited within the core it was found necessary to mix with a non-reacting solvent of high vapor pressure, such as pentane, which could easily be removed from the core.

Hence, the entire procedure consisted of first evacuating the core sample in situ. Then a deaerated solution of the fluids, containing the saturating fluid in the desired proportion, was injected into the sample with a Ruska proportioning pump to a pressure higher than that encountered under flow conditions, noting in each case the volume required to fill the holder and sample. Saturations required were generally below the minimum saturation for liquid flow, hence,

an immobile saturation of mixture was established by flowing in both directions at a high pressure and a considerably higher rate than those expected under test conditions. Then the solvent was removed by flowing at low pressures and under vacuum for sufficient periods of time. Between series of runs the sample was removed from the coreholder and weighed to determine the resident liquid saturation.

TREATMENT OF DATA

A general computer program was written to process the recorded experimental gas flow data. Observed pressure readings and volumetric flow rate readings were corrected and reduced to standard conditions by applying the appropriate conversion and calibration factors. Volumetric flow rate was recorded at the reference conditions of 1 international atmosphere and 520°R.

In determining fluid properties the values of viscosity and compressibility were evaluated at the arithmetic mean temperature and pressure. The relationship used for the viscosity of nitrogen was that suggested by Kestin and Wang⁽⁴⁰⁾

$$\begin{aligned}\mu = & 1778 \times 10^{-7} (1 + 8.958 \times 10^{-4} (p-1) \\ & + 6.120 \times 10^{-7} (p-1)^2 + 3.997 \times 10^{-8} (p-1)^3) \\ & + 4.55 \times 10^{-7} (T - 25)\end{aligned}\quad (36)$$

for viscosity μ in poise, pressure p in international atmospheres and temperature T in °C.

Compressibility was evaluated by four-point Lagrangian interpolation of curve fitted data of Hilsenrath et al⁽⁴¹⁾ at temperatures of 280, 290, 300, and 310°K.

The expressions necessary for performing graphical plots and mathematical fits of the processed data were recorded on IBM cards to facilitate their use in further processing.

Programs were also written to perform least squares fit of viscous data on a Klinkenberg plot, least squares fit of Forchheimer equation visco-inertial flow plot and modified visco-inertial flow plot, quasilinearization of the modified visco-inertial flow equation for low pressure gradients and the modified visco-inertial flow equation for high pressure gradients. The quasilinearization technique was programmed for an IBM 7040 using the method of determinants and Cramers Rule for the simultaneous solution of the linear equations. A sample of the program and related nomenclature appears in Appendix C.

RESULTS

Reanalysis of the Data of Previous Investigators

In order to apply the modified visco-inertial flow graphical technique it is necessary to have a value of the Klinkenberg b-factor. For sample 20 of Sadiq a Klinkenberg extrapolation had been performed on the viscous data and b had been evaluated as 160.4 psi for nitrogen. Therefore, the modified technique was applied to the visco-inertial flow data of sample 20⁽⁴²⁾.

The numerical technique was applied to both modified visco-inertial flow equations, using the original determinations for initial guesses⁽⁴³⁾. A summary of the results obtained is presented in Table 1.

Table 1

A Summary of Results for Core 20 of Sadiq

Method	k (md)	b (psi)	F_B^{-1} (ft ⁻¹)
Klinkenberg Plot	0.000127	160.4	
Visco-Inertial Flow Plot	0.000184		8.01×10^{16}
Modified Visco-Inertial Flow Plot	0.000124	(160.4)	2.58×10^{16}
Quasilinearization of Eqn. (28)	0.000125	172.3	3.18×10^{16}
Quasilinearization of Eqn. (32)	0.000126	171.3	3.22×10^{16}

Since sufficient viscous data were not available for the two samples of Cornell, quasilinearization was performed on both modified equations. The values presented by Cornell were used as initial guesses and b was estimated using the correlation previously proposed. A summary of results obtained for samples 20 and 14 is presented in Table 2.

Table 2
Quasilinearization Results for
Samples 20 and 14 of Cornell

Method	k (md)	b (psi)	F_B^{-1} (ft $^{-1}$)
<u>Sample 20</u>			
Cornell	1.01		7.25×10^{10}
Estimation	0.65		5.4×10^{10}
Quasilinearization of Eqn. (28)	0.595	67.5	5.66×10^{10}
Quasilinearization of Eqn. (32)	0.614	65.0	5.75×10^{10}
<u>Sample 14</u>			
Cornell	20.9		8.2×10^8
Estimation	16.5		7.0×10^8
Quasilinearization of Eqn. (28)	18.28	11.97	7.79×10^8
Quasilinearization of Eqn. (32)	18.35	11.89	7.8×10^8

Present Experimental Results

Sufficient data were taken for several core samples so that a careful evaluation of the basic theory and the slip correction for flow both in a dry core sample and in the presence of an immobile liquid phase could be made. The physical properties of these samples are listed in Table 3.

Table 3
Physical Properties of the Samples

Sample	1	2	3
Description	Berea Sandstone	Gilwood Sandstone	Swan Hills Limestone
Diameter (cm)	8.93	8.82	8.66
Length (cm)	21.8	18.3	19.9
Area (cm^2)	62.7	61.2	58.9
Pore Volume (cm^3)	293.	276.	165.
Porosity	0.214	0.246	0.141

A low permeability berea sandstone, sample 1, was chosen for a series of runs because of the probable homogeneity of the sample. The basic flow data appear in Table 10, Appendix D and are presented graphically on a standard backpressure plot in Figure (4). As expected, the viscous data do not lie on a 45° straight line. The departure from linearity and

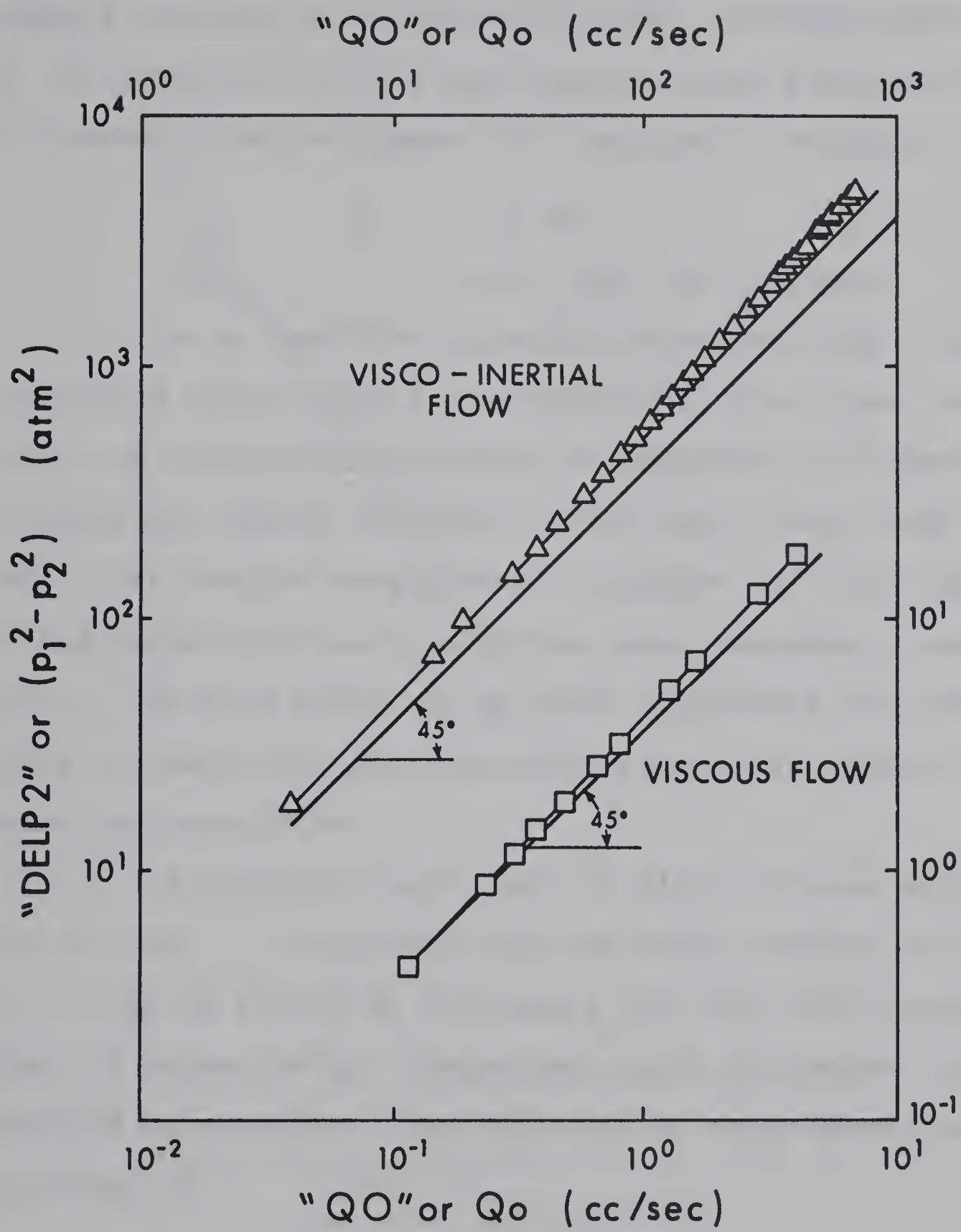


FIGURE 4

BACKPRESSURE PLOT FOR CORE 1

hence the transition between viscous and visco-inertial flow appears to occur at a rate of 4 cc/sec. A least squares fit of the tentative viscous data observations, presented on a Klinkenberg plot in Figure (5), resulted in values of

$$k = 2.29 \text{ md}$$

$$\text{and } b = 0.610 \text{ atm. for nitrogen.}$$

As a check for internal inconsistencies k and b were calculated using the six observations at the lowest mean pressures and thereafter for groups of observations formed by successively adding one point at the next higher mean pressure. The results were plotted in Figure (6) with the abscissa being the lowest reciprocal mean pressure in each group. The data appear to be quite consistent and the results presented for the tentative viscous data appear to be quite representative.

A standard visco-inertial flow plot was performed for all data. It appeared that the data, plotted in Figure (7), could be fitted by a straight line for $w/A\bar{\mu}$ greater than $0.3 \text{ gm/sec cm}^2 \text{ cp}$. These data could be assumed unaffected by slippage. Extrapolation of these data resulted in values of

$$k = 2.20 \text{ md}$$

$$\text{and } F_B = 143. \text{ atm sec}^2/\text{gm} = 4.42 \times 10^9 \text{ ft}^{-1}$$

A check was made using all nonviscous data, a linear fit yielding values of

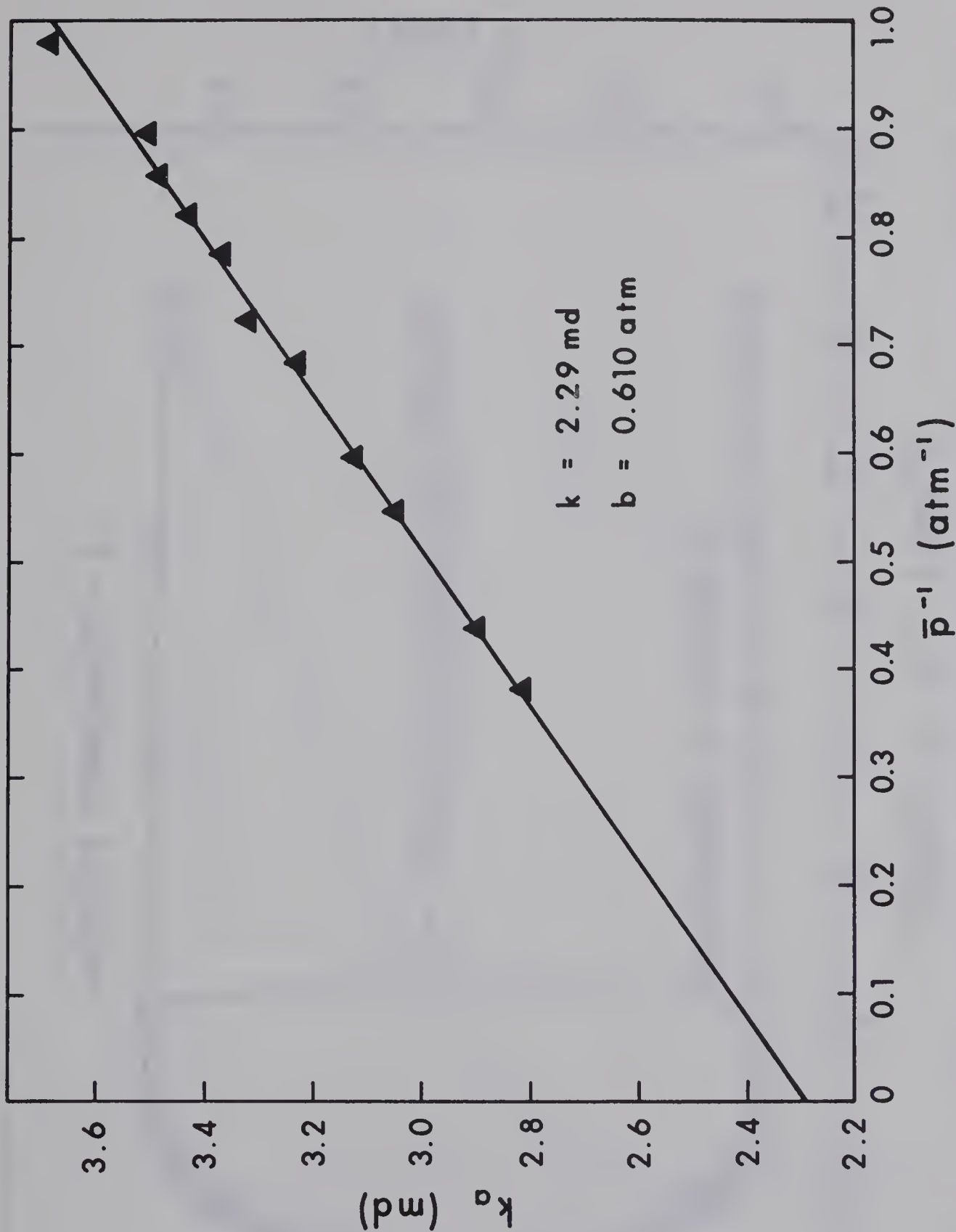


FIGURE 5 KLINKENBERG PERMEABILITY PLOT FOR CORE 1.

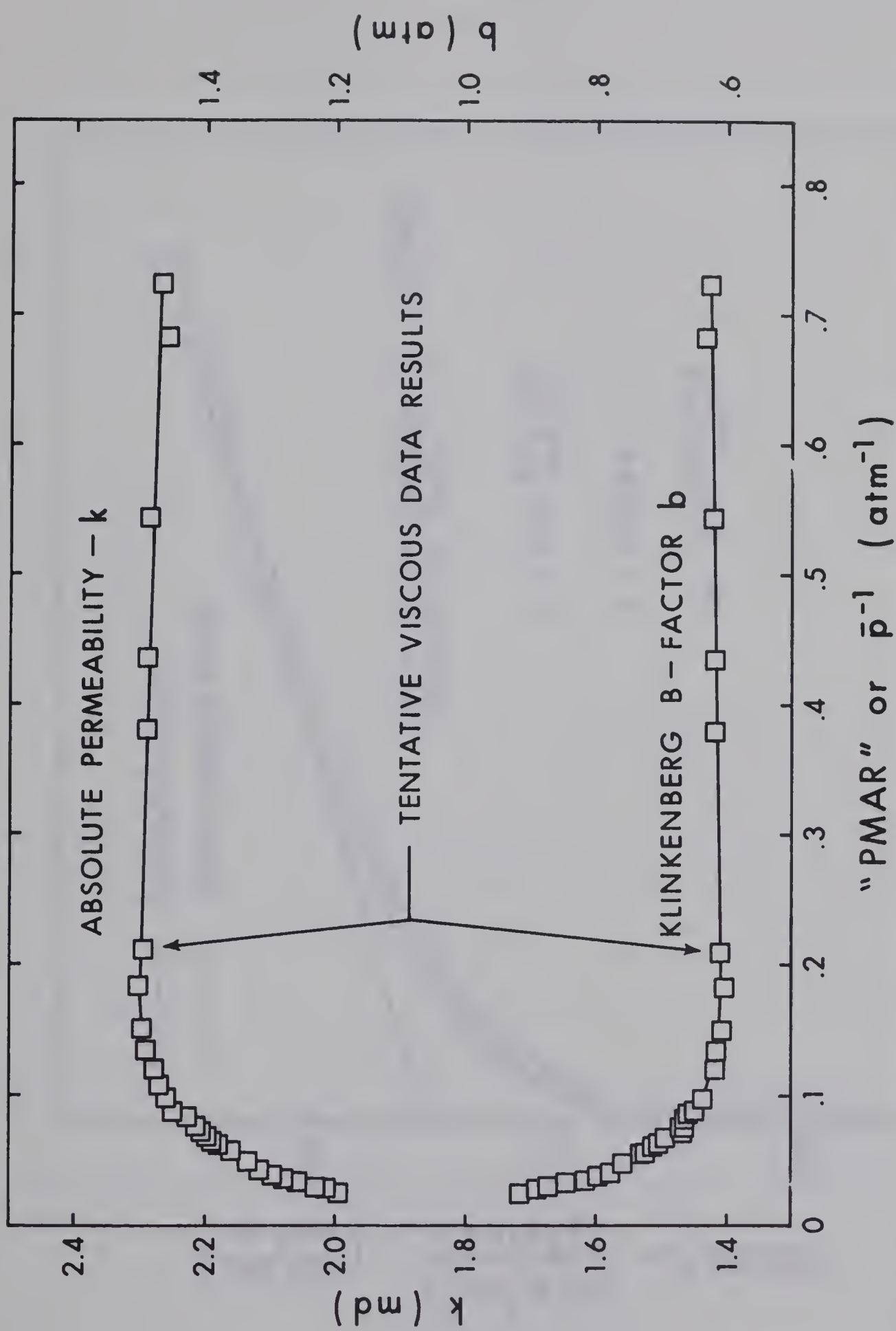


FIGURE 6 KLINKENBERG PERMEABILITY PLOT COEFFICIENTS FOR CORE 1.

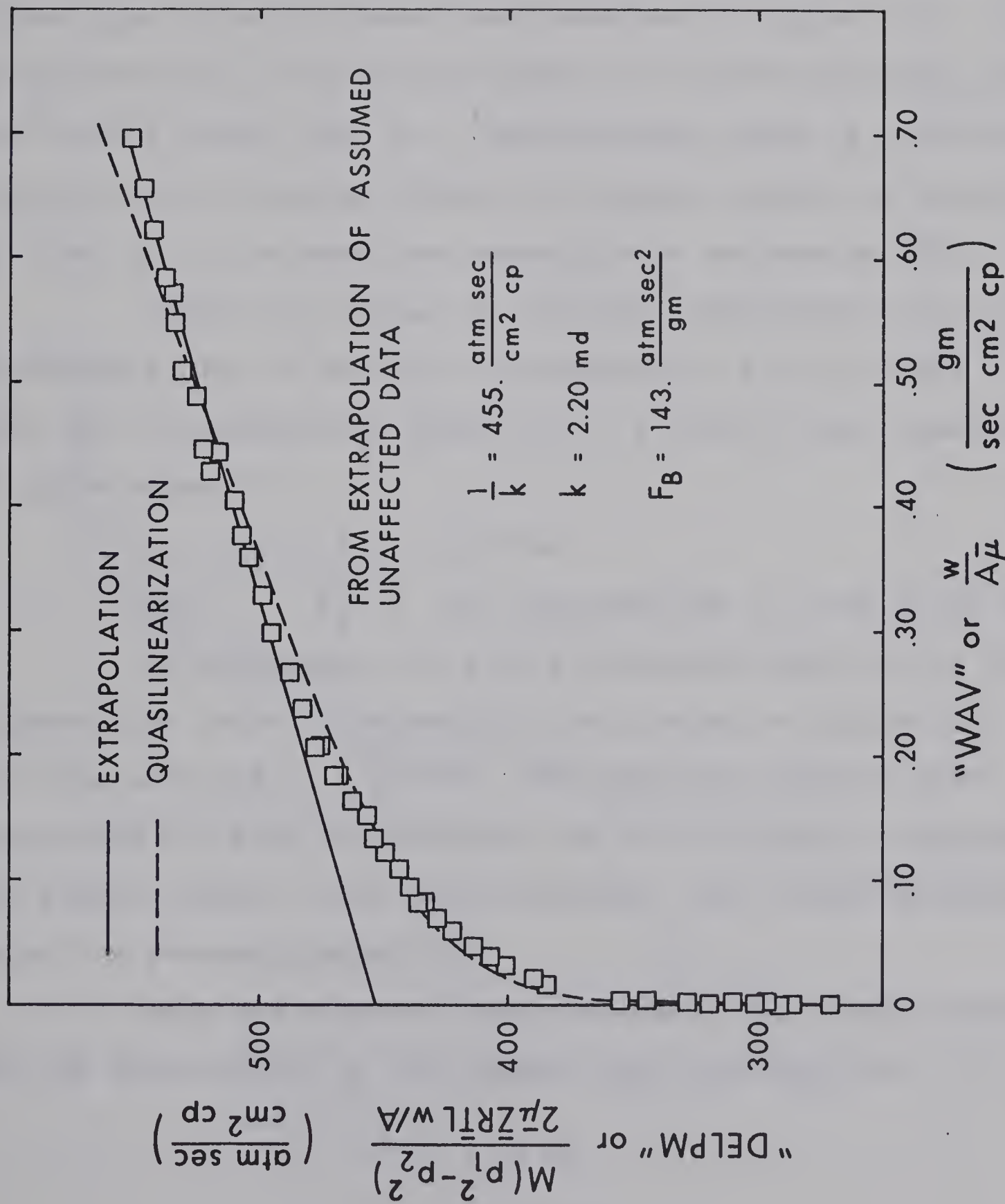


FIGURE 7 STANDARD VISCO-INERTIAL FLOW PLOT FOR CORE 1.

$$k = 2.41 \text{ md}$$

$$\text{and } F_B = 225. \text{ atm sec}^2/\text{gm} = 6.95 \times 10^9 \text{ ft}^{-1}$$

The results of an analysis, identical to that performed upon Cornell's data, are presented in Figure (8). As noted previously, the results seem to be quite consistent for $w/A\bar{\mu}$ values larger than 0.3. Nevertheless there is a definite trend as the increasing effect of slippage causes the values of k and F_B to increase continuously with decreasing $w/A\bar{\mu}$.

Using the b value of .610 atm, determined from the Klinkenberg plot, a modified visco-inertial flow plot was made and is presented in Figure (9). A linear least squares fit gave values of

$$k = 2.26 \text{ md}$$

$$\text{and } F_B = 184. \text{ atm sec}^2/\text{gm} = 5.69 \times 10^9 \text{ ft}^{-1}$$

As previously, data were processed beginning at the highest flow rates. The results are plotted in Figure (10) with the abscissa $(1 + \frac{b}{p})w/A\bar{\mu}$. The modified analysis technique does not seem to correlate the data very well although the results appear to be more consistent than those obtained using the standard technique.

From the proposal made previously the initial guesses for the coefficients of this sample were evaluated as

$$k = 3.69 \text{ md}$$

$$b = 0.467 \text{ atm}$$

$$\text{and } F_B = 6.66 \text{ atm sec}^2/\text{gm} = 2.06 \times 10^8 \text{ ft}^{-1}$$

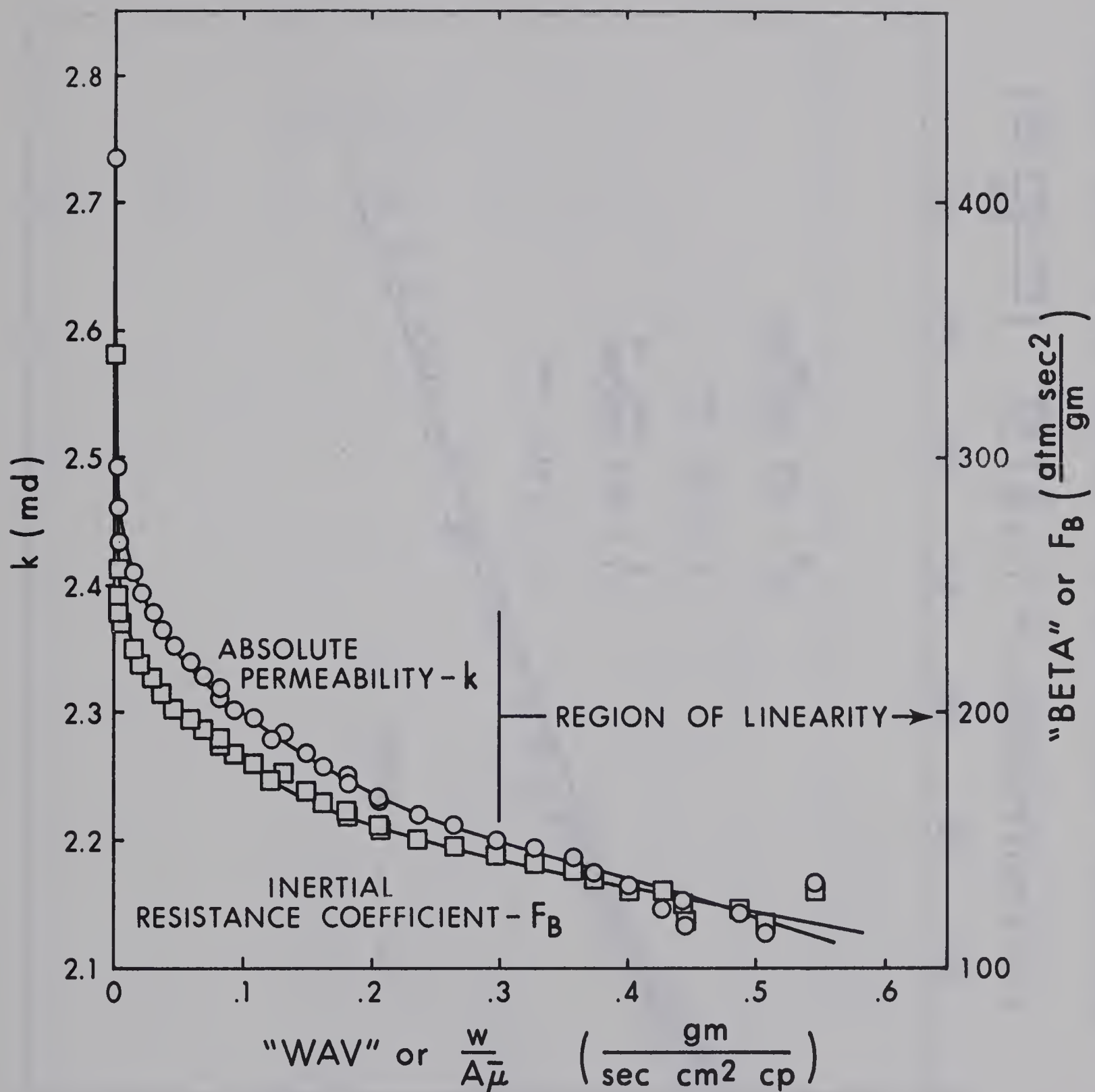
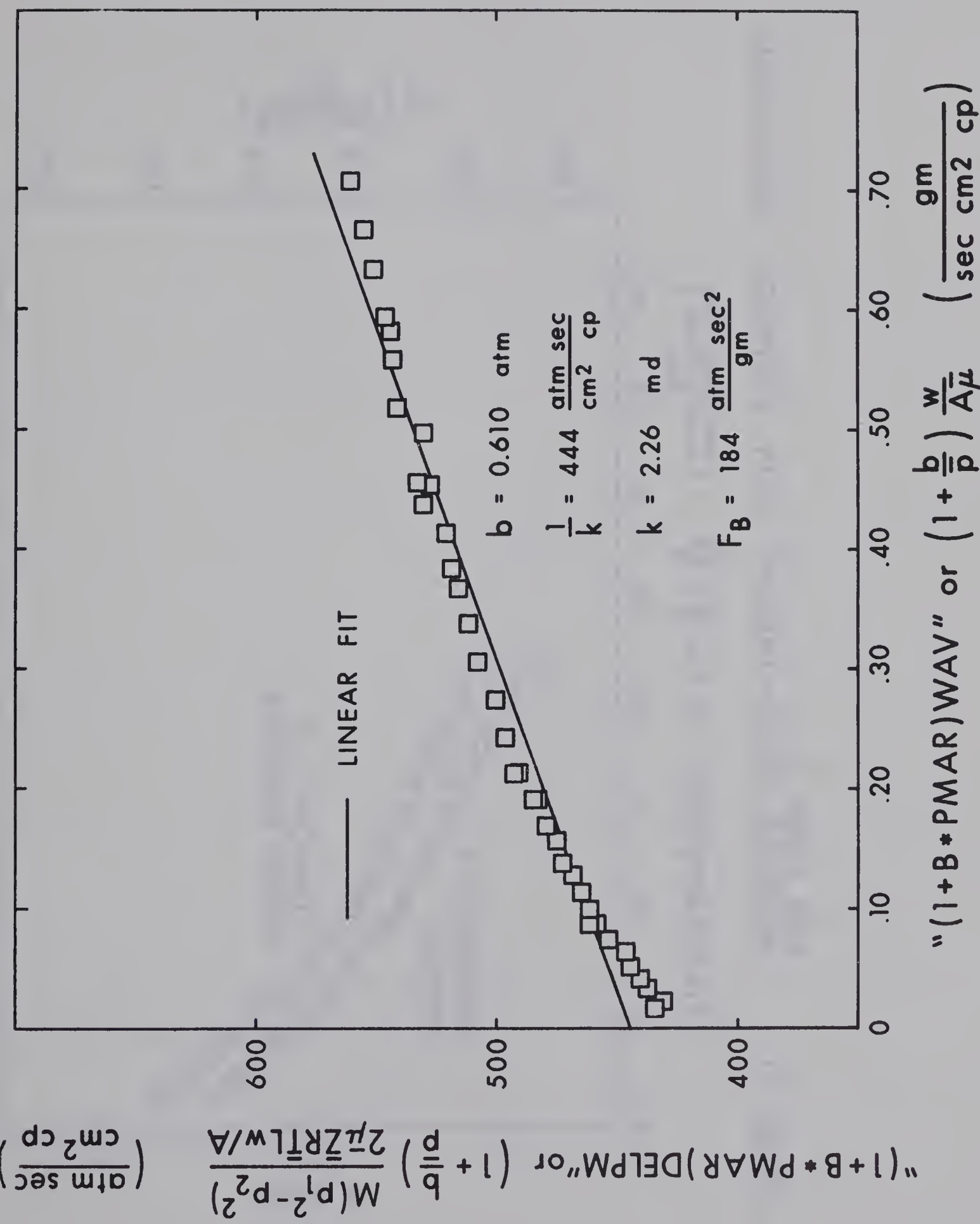


FIGURE 8 FLOW COEFFICIENTS FOR CORE 1. USING STANDARD VISCO-INERTIAL FLOW PLOT TECHNIQUE



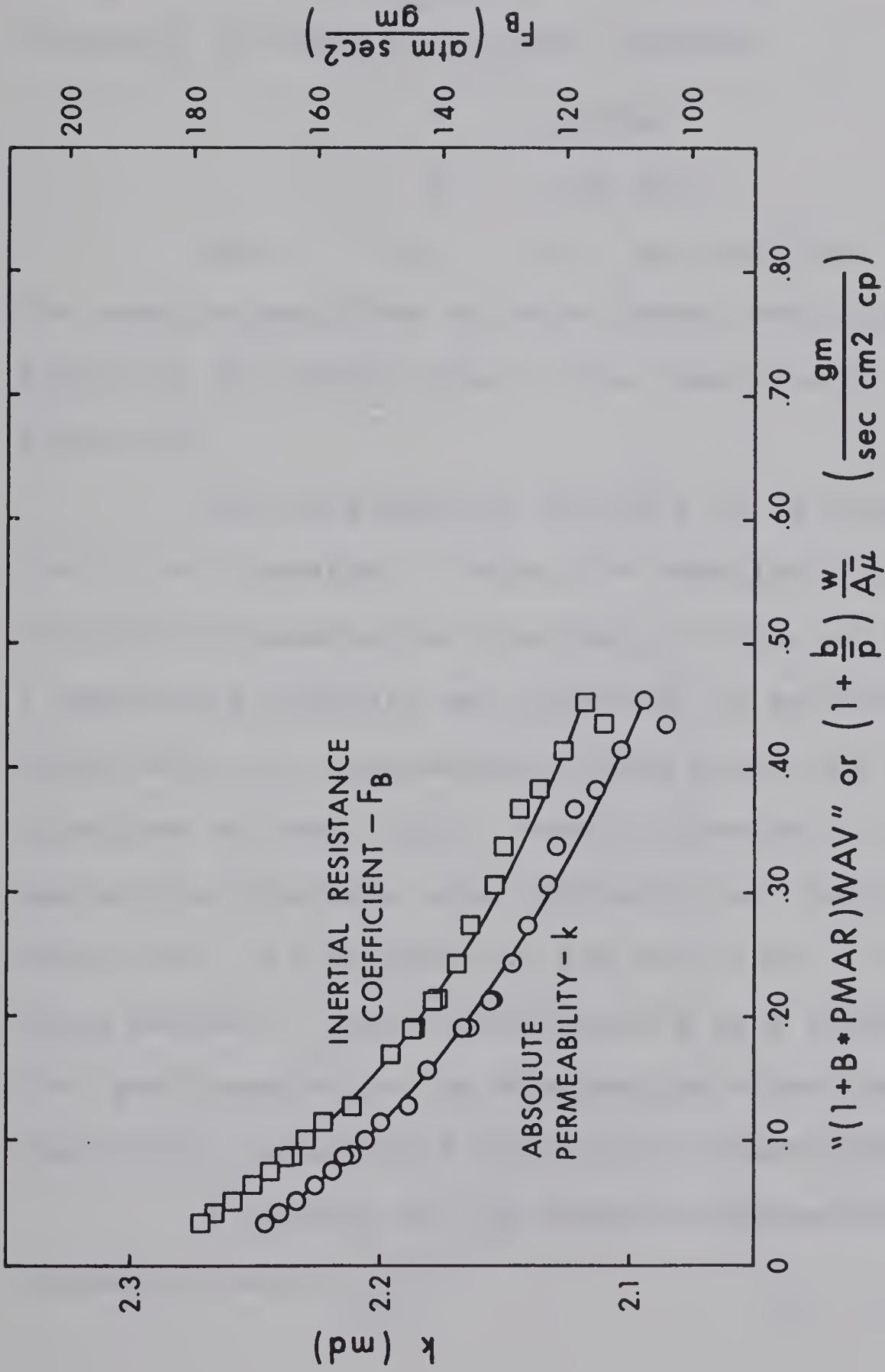


FIGURE 10 MODIFIED VISCO-INERTIAL FLOW EQUATION COEFFICIENTS FOR CORE 1.

Quasilinearization was performed on both Equations (28) and (32). With a convergence criterion $\epsilon = 10^{-4}$, 6 iterations were required in each case to converge to similar results, identical to three significant figures,

$$k = 2.24 \text{ md}$$

$$b = .670 \text{ atm}$$

$$\text{and } F_B = 177. \text{ atm sec}^2/\text{gm} = 5.47 \times 10^9 \text{ ft}^{-1}$$

The results predicted by using these coefficients are represented by the dashed line on the visco-inertial flow plot, Figure (7).

In the graphical analysis it is necessary to assume that b is a constant. Using the numerical technique it is possible to examine the constancy of b as well as k and F_B . A repetitive analysis was performed in solving Equation (32) numerically, by successively using more data points in the direction of lower $w/A\bar{\mu}$. Results plotted in Figure (11) against the abscissa $w/A\bar{\mu}$ indicate that there is no consistency until all of the data has been used. A check made using series of four representative data points indicated that good results may be obtained provided the data observations fully cover the flow regions investigated.

A summary of the results obtained for Core 1 is listed in Table 4.

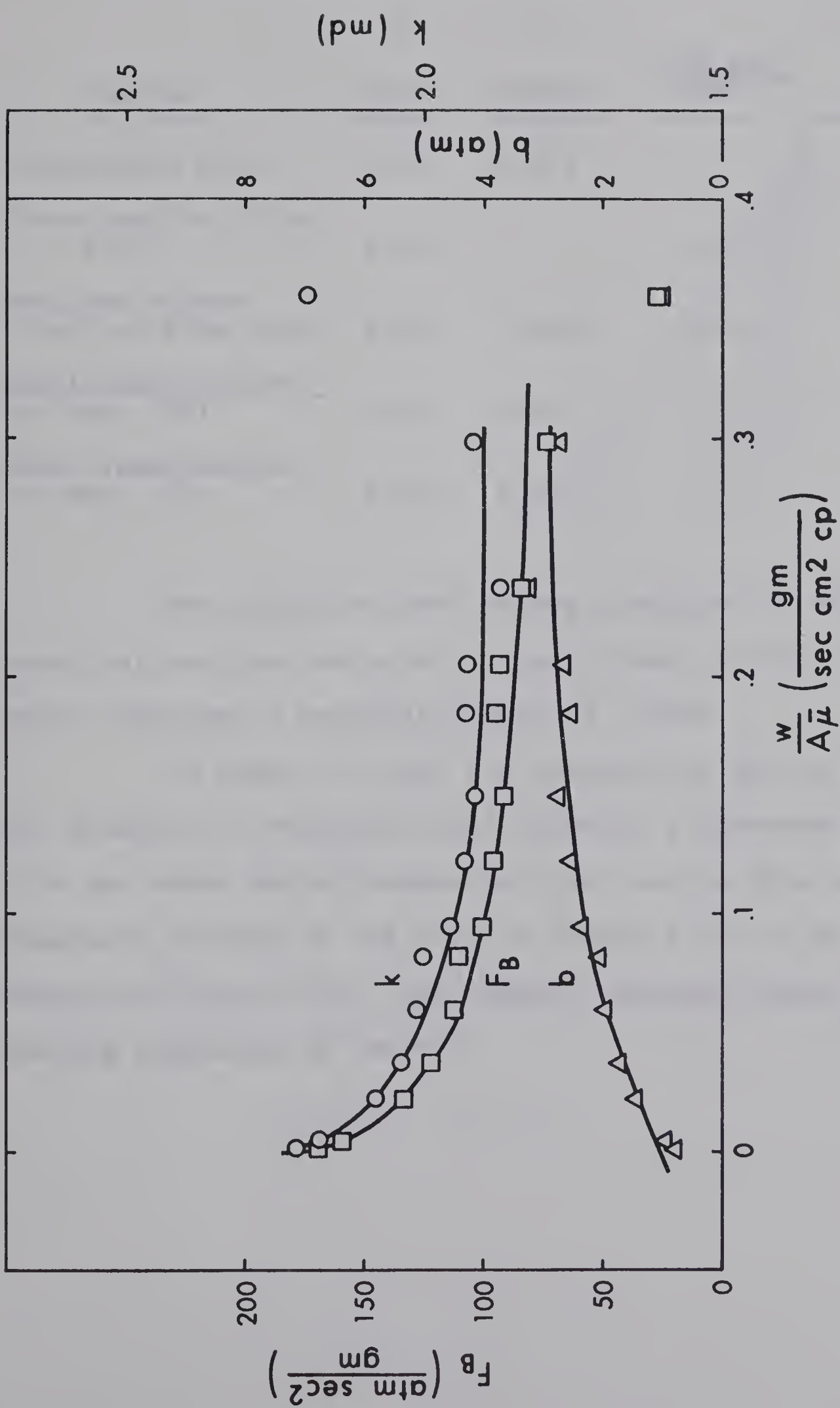


FIGURE 11 RESULTS FROM QUASILINEARIZATION OF EQUATION (32)
FOR CORE 1.

Table 4
A Summary of Results for Core 1

Method	k (md)	b (atm.)	$\frac{\text{atm sec}^2}{\text{gm}}$	F_B ft^{-1}
Klinkenberg Plot	2.29	0.610		
Visco-Inertial Flow Plot	2.20		143.	4.42×10^9
Modified Visco-Inertial Flow Plot	2.26	(.610)	184.	5.69×10^9
Quasilinearization of Eqn. (38)	2.24	0.670	177.	5.47×10^9
Quasilinearization of Eqn. (32)	2.24	0.670	177.	5.47×10^9

Now using the best values, obtained from the numerical analysis using all data, a check on the cut-off point indicated a Reynolds Number of .00199.

In order to check for homogeneity of the sample and the presence of mechanical end effects, a pressure drop profile was taken during several of the runs on this sample. Graphical results of the data in Tables 11 to 14 are presented in Figure (12). The results obtained using $b = 0.610$ atm are presented in Table 5.

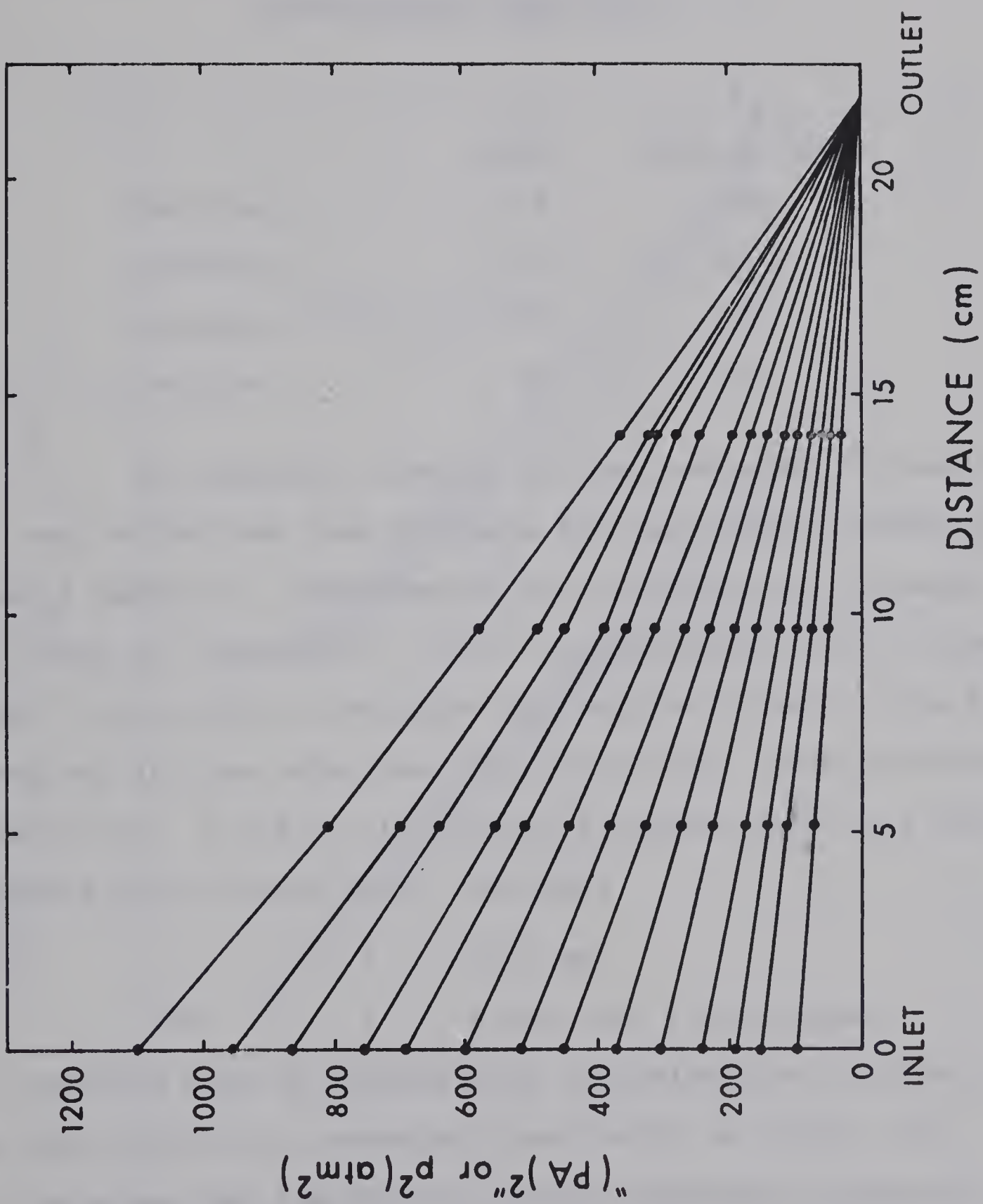


FIGURE 12 PRESSURE DROP PROFILE FOR CORE 1.

Table 5

Permeability and Inertial Resistance Coefficient

Distribution for Core 1

	<u>k</u> (md)	<u>F_B</u> (atm sec ² /gm)
Section 1	2.15	340.
Section 2	2.10	200.
Section 3	2.44	255.
Section 4	2.50	290.

An analysis, similar to that performed for sample 1, was carried out upon the data for the Gilwood sandstone sample number 2. Experimental gas flow data are presented in Table 15, Appendix D. From a backpressure plot of these data, Figure (13), a straight line may be fitted to the data obtained at flow rates less than 40 cc/sec. under reference conditions. A fit of the tentative viscous data on a Klin-kenberg plot, Figure (14), indicated

$$k = 36.5 \text{ md}$$

$$\text{and } b = 0.401 \text{ atm. for nitrogen}$$

An analysis made by successively including more data points in the evaluation, presented graphically in Figure (15), illustrates that the data are quite consistent internally and that the tentative results are representative.

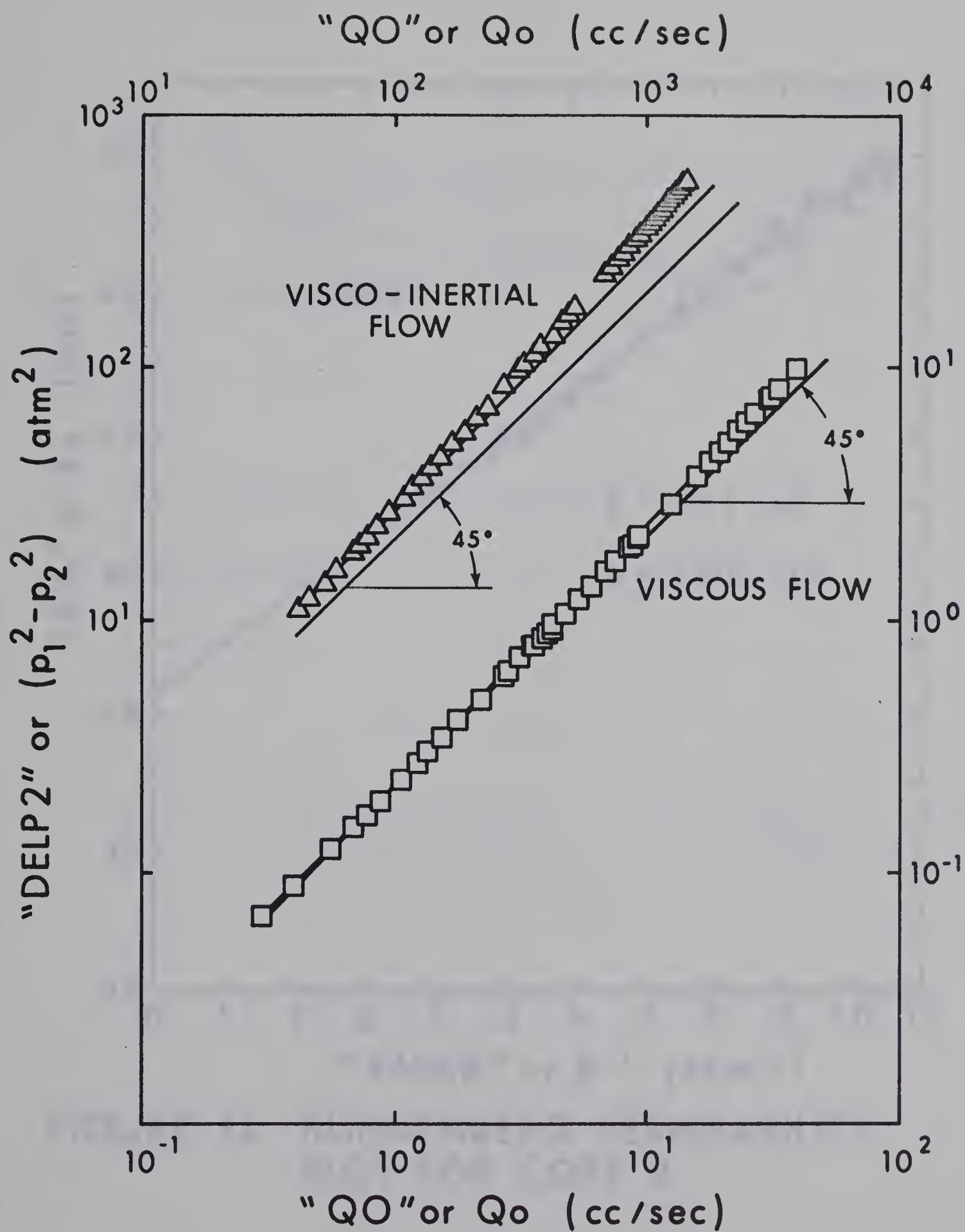


FIGURE 13

BACKPRESSURE PLOT FOR CORE 2.

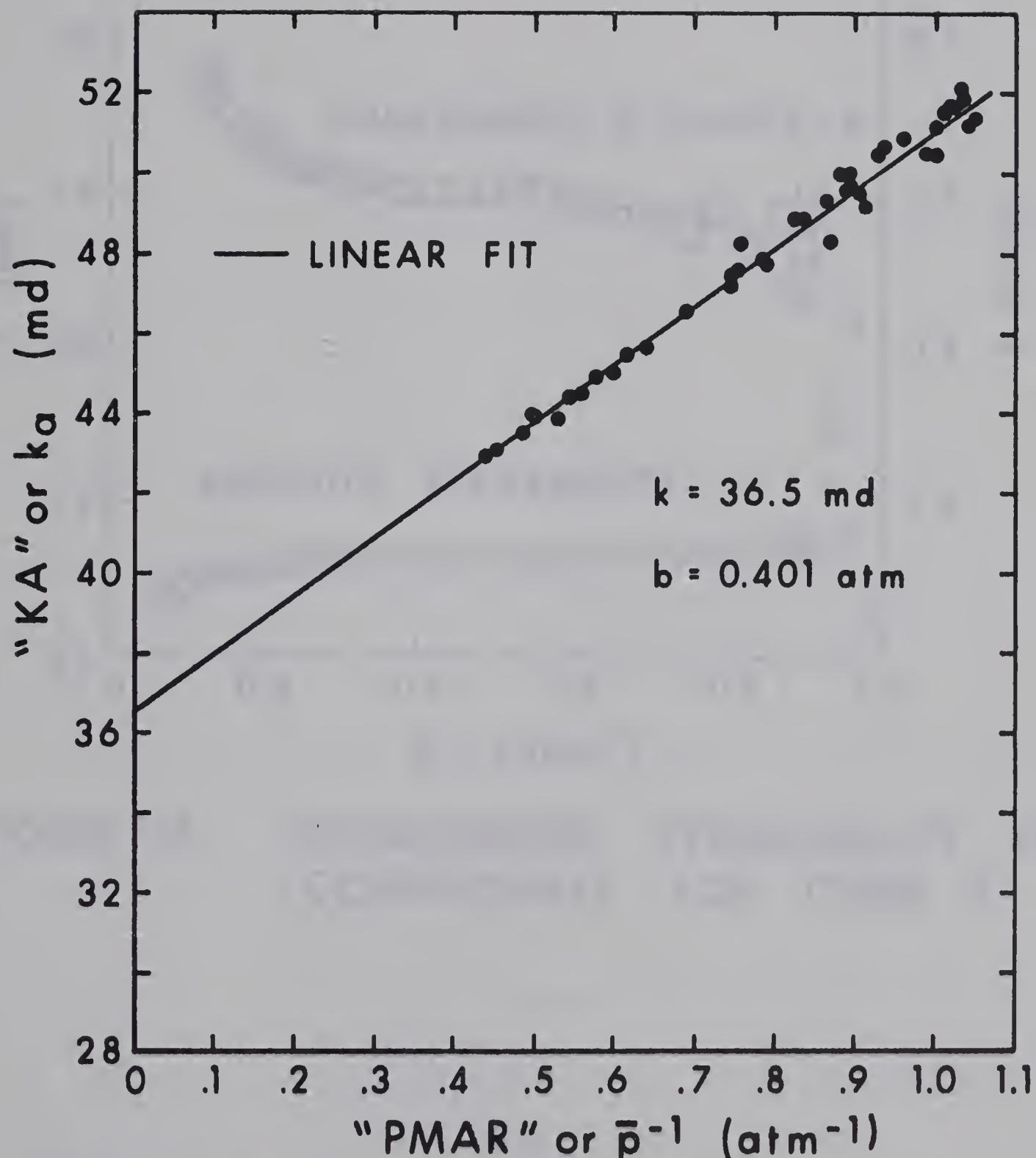


FIGURE 14 KLINKENBERG PERMEABILITY PLOT FOR CORE 2

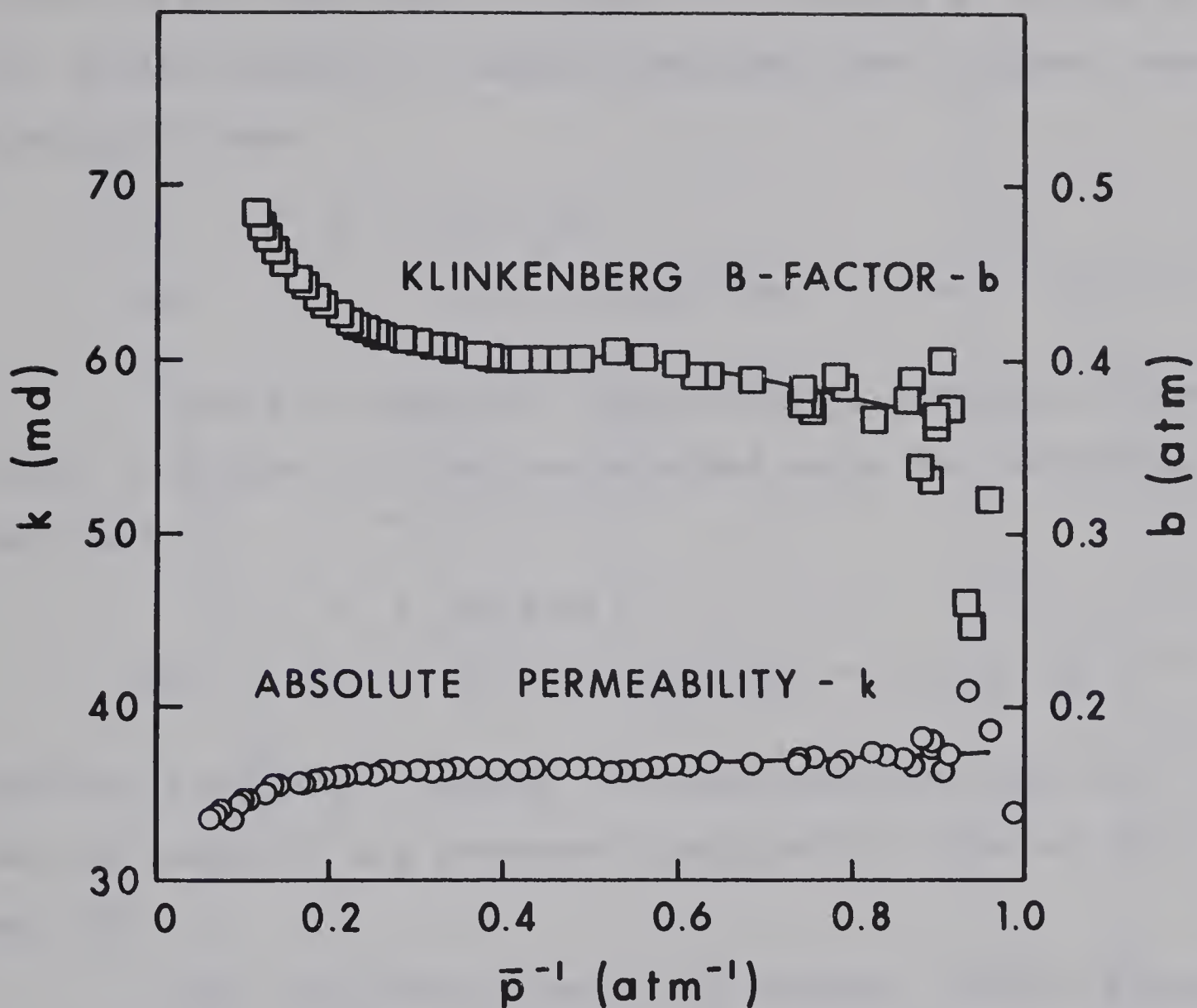


FIGURE 15 KLINKENBERG PERMEABILITY PLOT
COEFFICIENTS FOR CORE 2

The apparently straight line portion of the standard visco-inertial flow plot in Figure (16) occurs at values of $w/A\mu$ greater than 0.7. Results obtained from a linear least squares fit were

$$k = 35.8 \text{ md}$$

and $F_B = 4.80 \text{ atm sec}^2/\text{gm} = 1.48 \times 10^8 \text{ ft}^{-1}$

Using the modified visco-inertial technique illustrated in Figure (17), values obtained using the nonviscous data were

$$k = 36.4 \text{ md}$$

and $F_B = 5.78 \text{ atm sec}^2/\text{gm} = 1.79 \times 10^8 \text{ ft}^{-1}$

Results of analyses, similar to those performed upon the data of sample 1, are presented graphically in Figures (18) and (19).

For the quasilinearization schemes, initial guesses were obtained using the correlations previously presented

$$k = 51.5 \text{ md}$$
$$b = 0.166 \text{ atm}$$

and $F_B = 0.874 \text{ atm sec}^2/\text{gm} = 2.70 \times 10^7 \text{ ft}^{-1}$

For a convergence criterion ϵ of 10^{-4} , solution of Equations (28) and (32) both yielded the results

$$k = 36.2 \text{ md}$$
$$b = 0.423 \text{ atm for nitrogen}$$

and $F_B = 5.62 \text{ atm sec}^2/\text{gm} = 1.74 \times 10^8 \text{ ft}^{-1}$

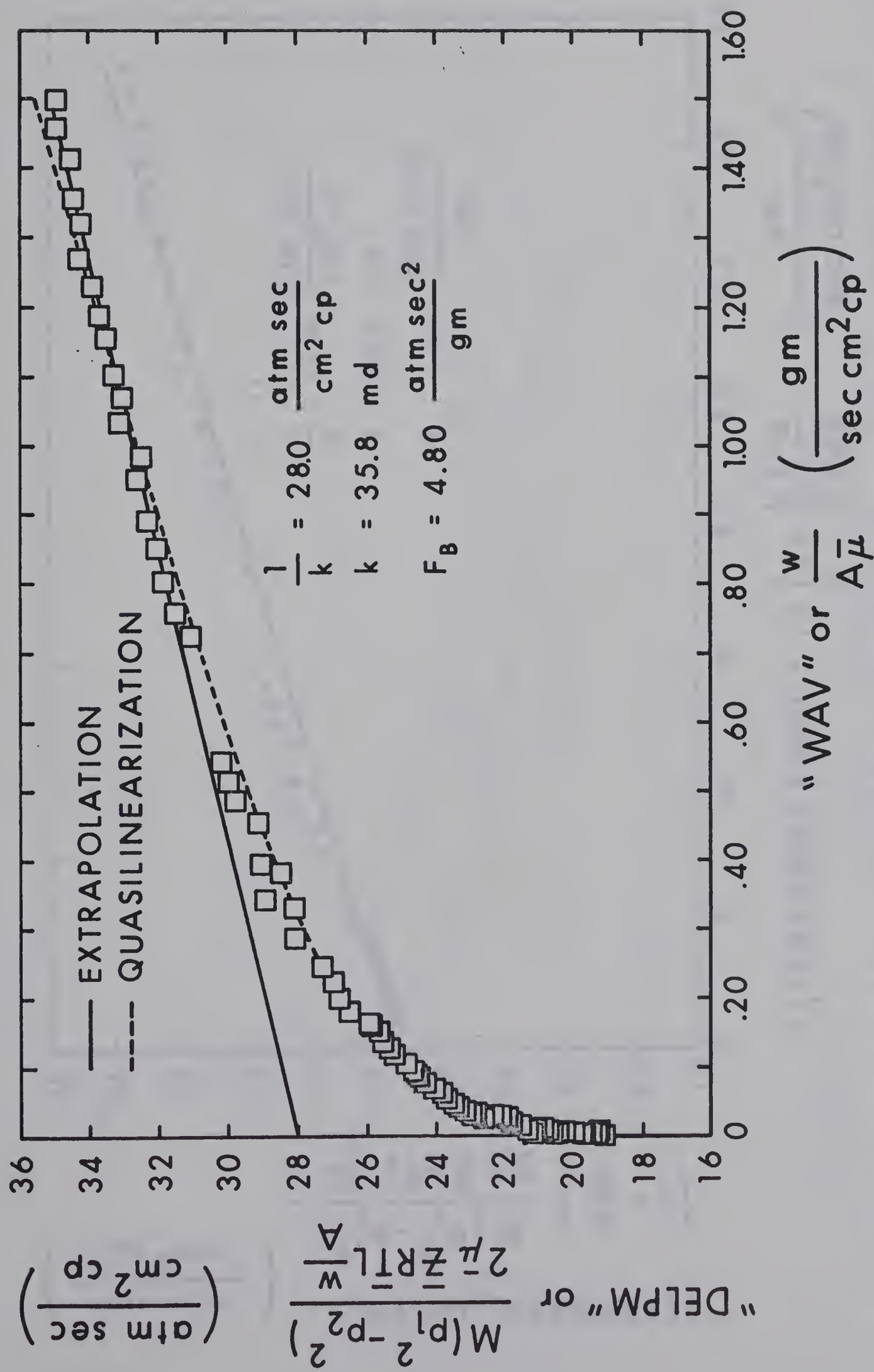


FIGURE 16 STANDARD VISCO-INERTIAL FLOW PLOT FOR CORE 2

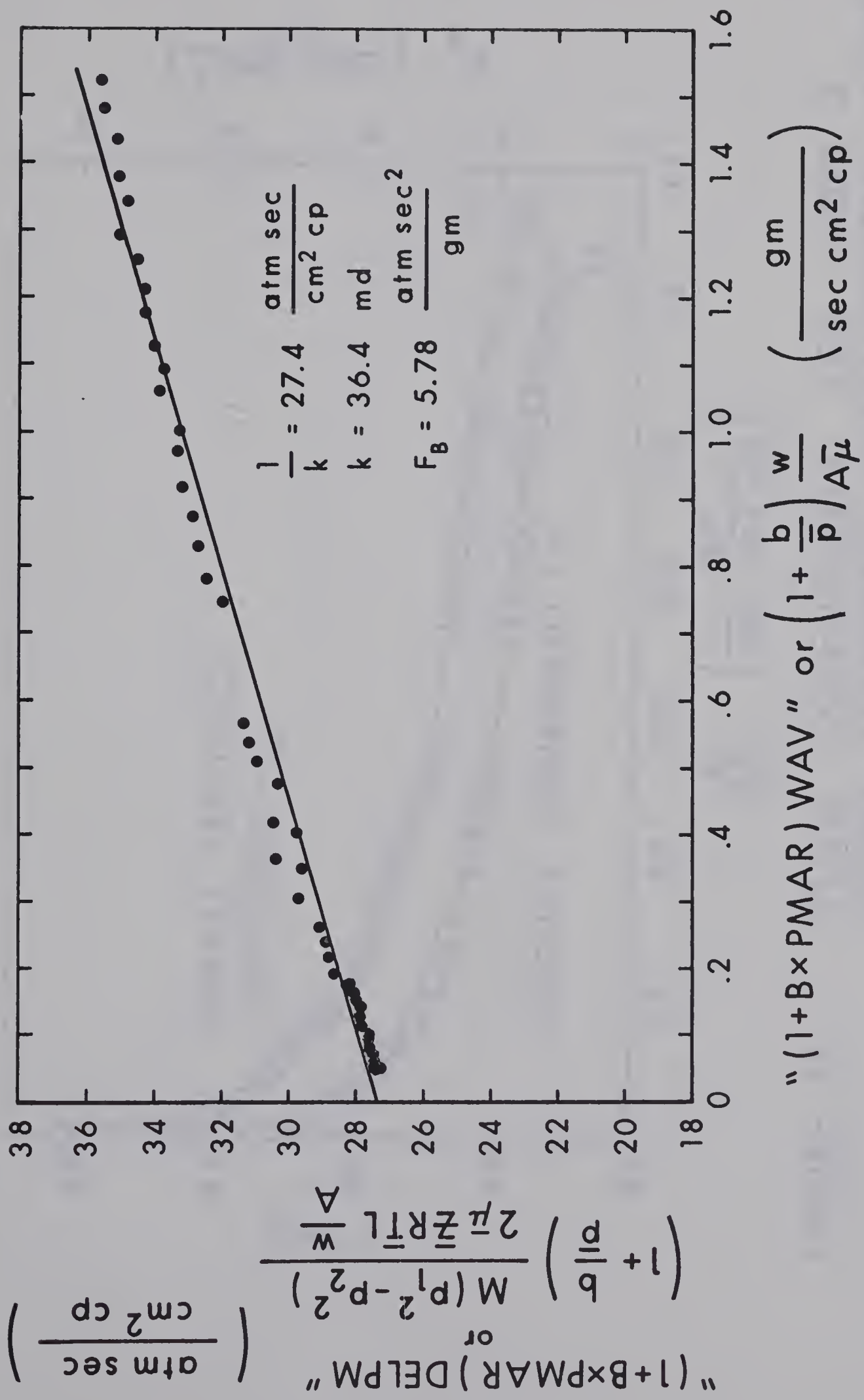


FIGURE 17

MODIFIED VISCO-INERTIAL FLOW PLOT FOR CORE 2

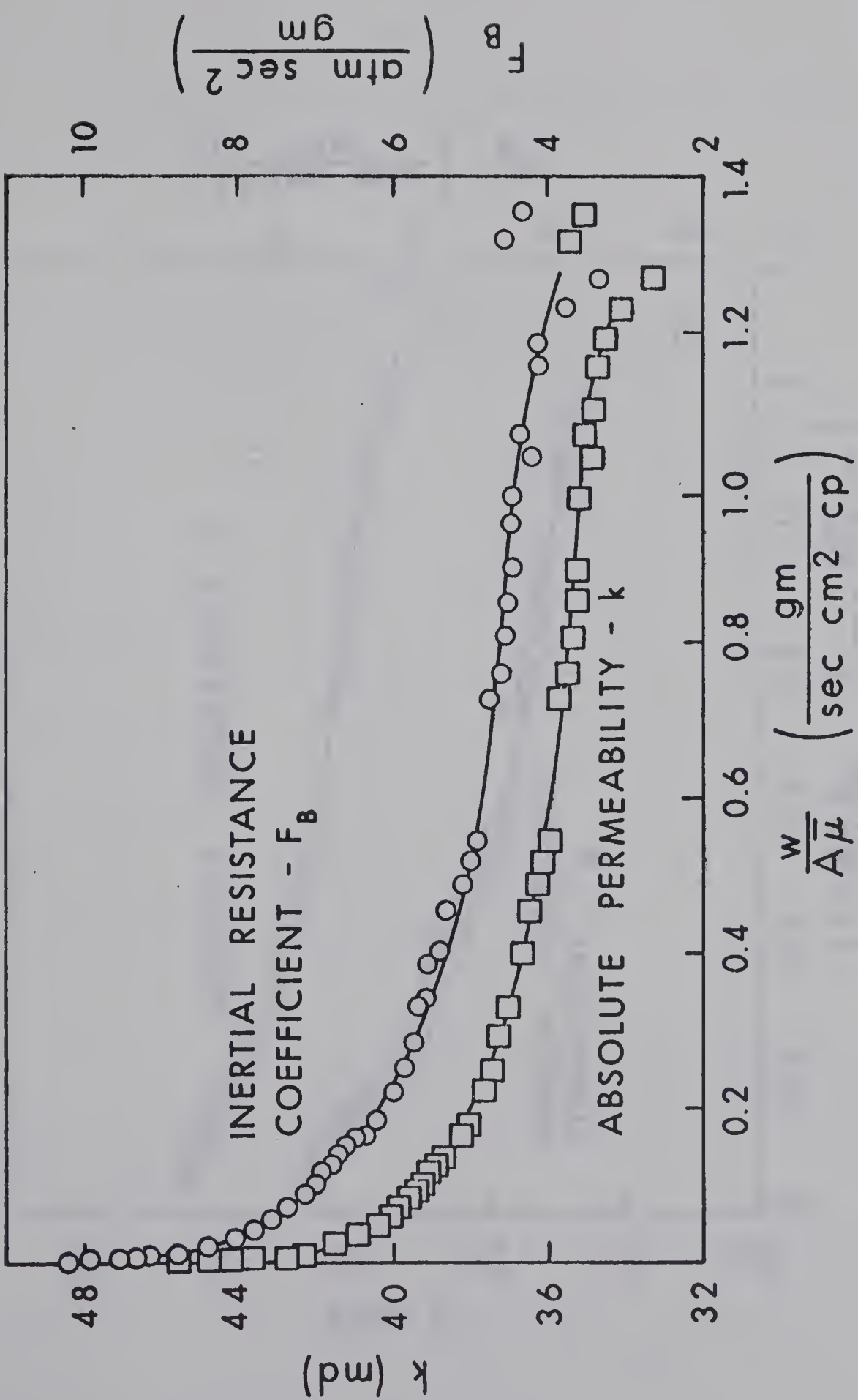


FIGURE 18 FLOW COEFFICIENTS FOR CORE 2.
USING STANDARD VISCO-INERTIAL PLOT TECHNIQUE

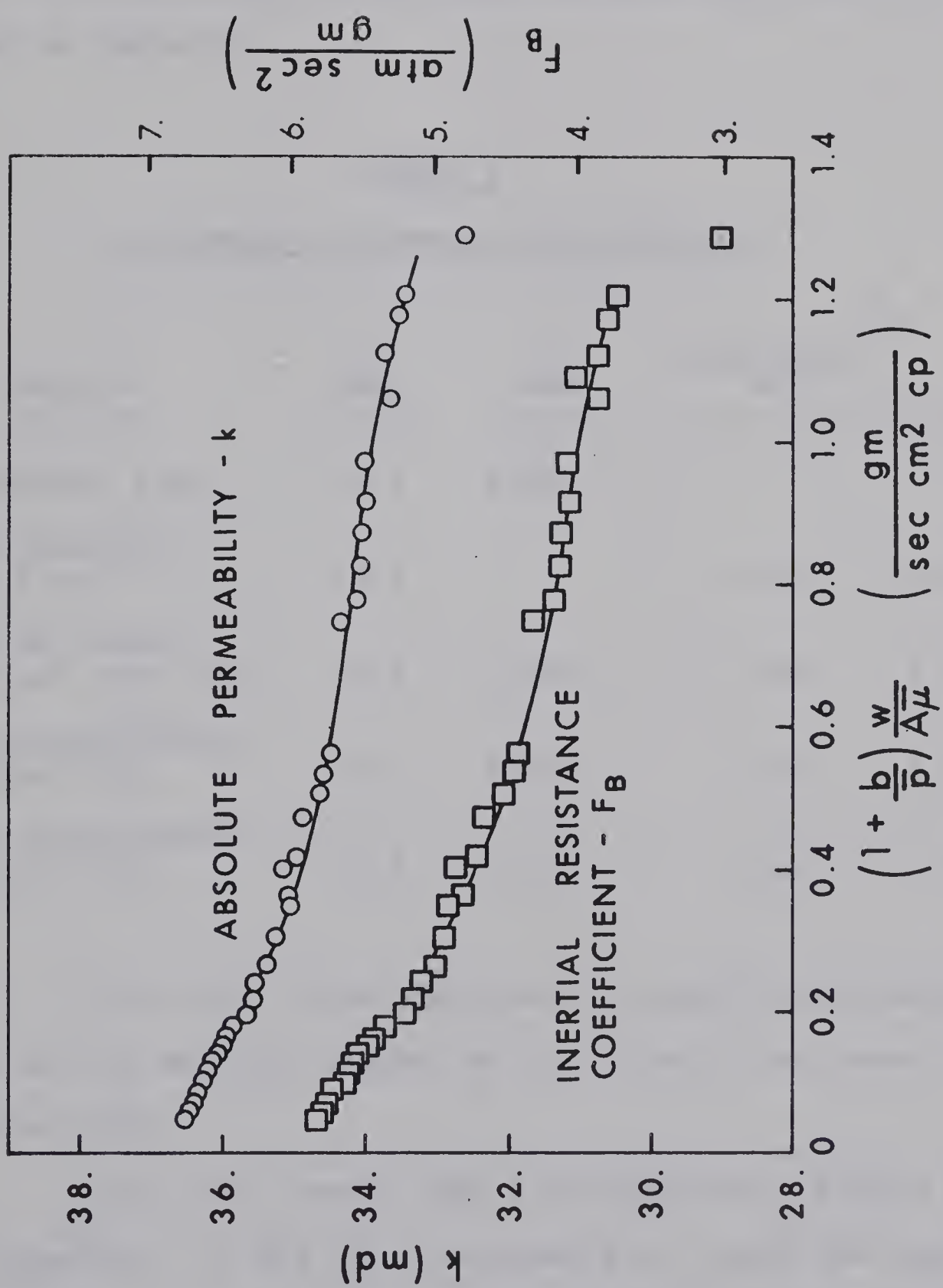


FIGURE 19 MODIFIED VISCO-INERTIAL FLOW EQUATION COEFFICIENTS FOR CORE 2.

exact to three significant figures, with 6 iterations required for the solution of Equation (28) and 9 iterations for the solution of Equation (32).

A summary of the results obtained for core 2 is presented in Table 6.

Table 6
A Summary of Results for Core 2

Method	k (md)	b (atm)	F_B ($\frac{\text{atm sec}^2}{\text{gm}}$)	(ft^{-1})
Klinkenberg Plot	36.5	0.401		
Visco-Inertial Flow Plot	35.8		4.80	1.48×10^8
Modified Visco-Inertial Flow Plot	36.4	(.401)	5.78	1.79×10^8
Quasilinearization of Eqn. (28)	36.2	0.423	5.62	1.74×10^8
Quasilinearization of Eqn. (32)	36.2	0.423	5.62	1.74×10^8

Using the values obtained by quasilinearization a check of the Reynolds Number at the cut-off indicated a value of 0.012.

Since this sample was a vertical core from a producing formation, it was found necessary to check the degree of homogeneity. Using pressure taps installed along the length

of the sample, several pressure profiles were measured. The data in Tables 16 to 19, Appendix D are exhibited graphically in Figure (20). Analysis of the data for each section, using the numerical techniques, resulted in the average values listed in Table 7.

Table 7
Permeability and Inertial Resistance
Coefficient Distribution for Core 2

	k (md)	b (atm)	F_B (atm sec ² /gm)
Section 1	13.2	.917	9.76
Section 2	92.2	.565	2.13
Section 3	254.	.208	.894
Section 4	124.	.452	1.07

In order to check that the effect observed was due to heterogeneity rather than an entrance effect, the direction of flow was reversed and a test was performed simulating one of the flow rates. The pressure profiles are compared in Figure (21).

On the premises that the numerical technique is vastly superior, the applicability of the visco-inertial theory for flow in the presence of a liquid phase was examined. Data for the Swan Hills limestone core sample 3 were taken at

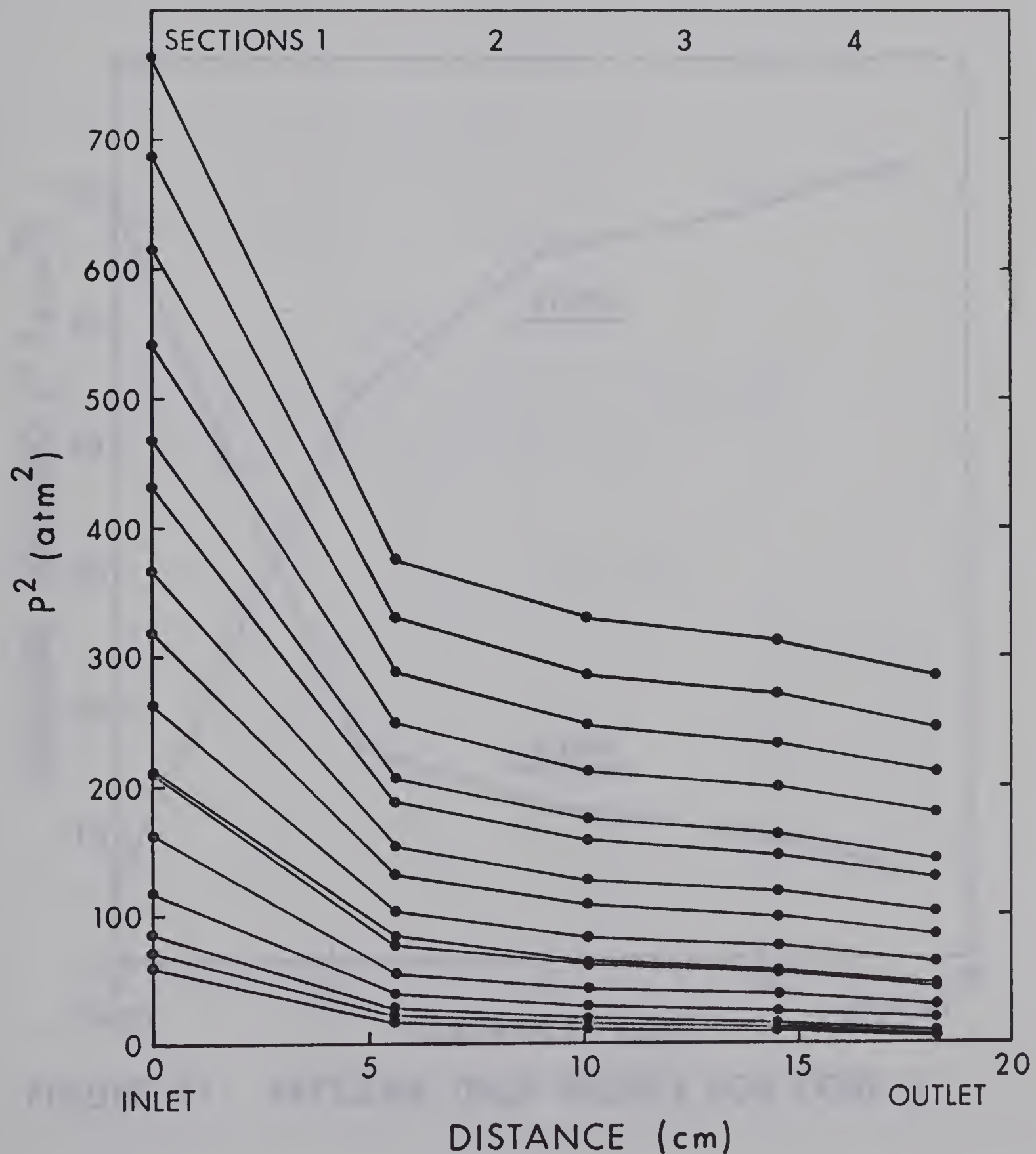


FIGURE 20 PRESSURE DROP PROFILE FOR CORE 2

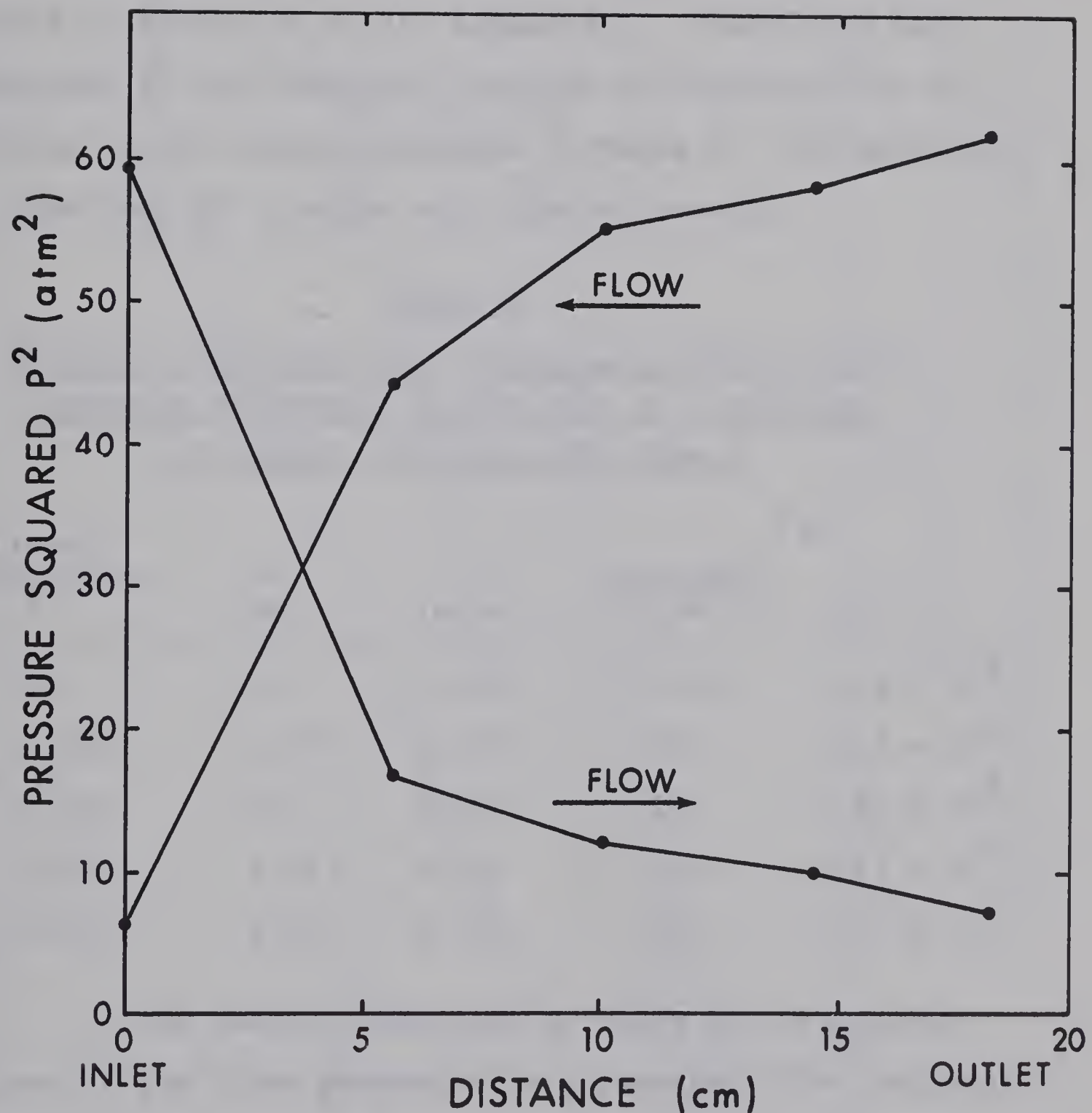


FIGURE 21 PRESSURE DROP PROFILE FOR CORE 2

four immobile liquid saturation conditions as well as for the dry core.

Basic flow data for the core, dry and at liquid saturations of 0.0765, 0.124, 0.205, and 0.253, are presented in Tables 20 to 24, Appendix D. These data were subjected to the numerical solution of Equation (32) resulting in the values presented in Table 8. The solution of Equation (28) yielded very similar results.

Table 8

Effective Permeability, Klinkenberg b-Factor and
Inertial Resistance Coefficient as a Function
of Liquid Saturation for Core 3

Liquid Saturation S	k (md)	b (psia)	$\frac{F_B}{(\frac{\text{atm sec}^2}{\text{gm}})}$	(ft^{-1})
Dry	13.0	0.649	85.5	2.64×10^9
0.0765	11.27	0.608	101.	3.12×10^9
0.124	10.0	0.501	125.	3.86×10^9
0.205	8.17	0.611	148.	4.57×10^9
0.253	6.36	0.574	228.	7.05×10^9

The results predicted by using the calculated values of the three parameters are compared with the physical observations on the visco-inertial flow plot, Figure (22). The coefficients are plotted as a function of liquid saturation in

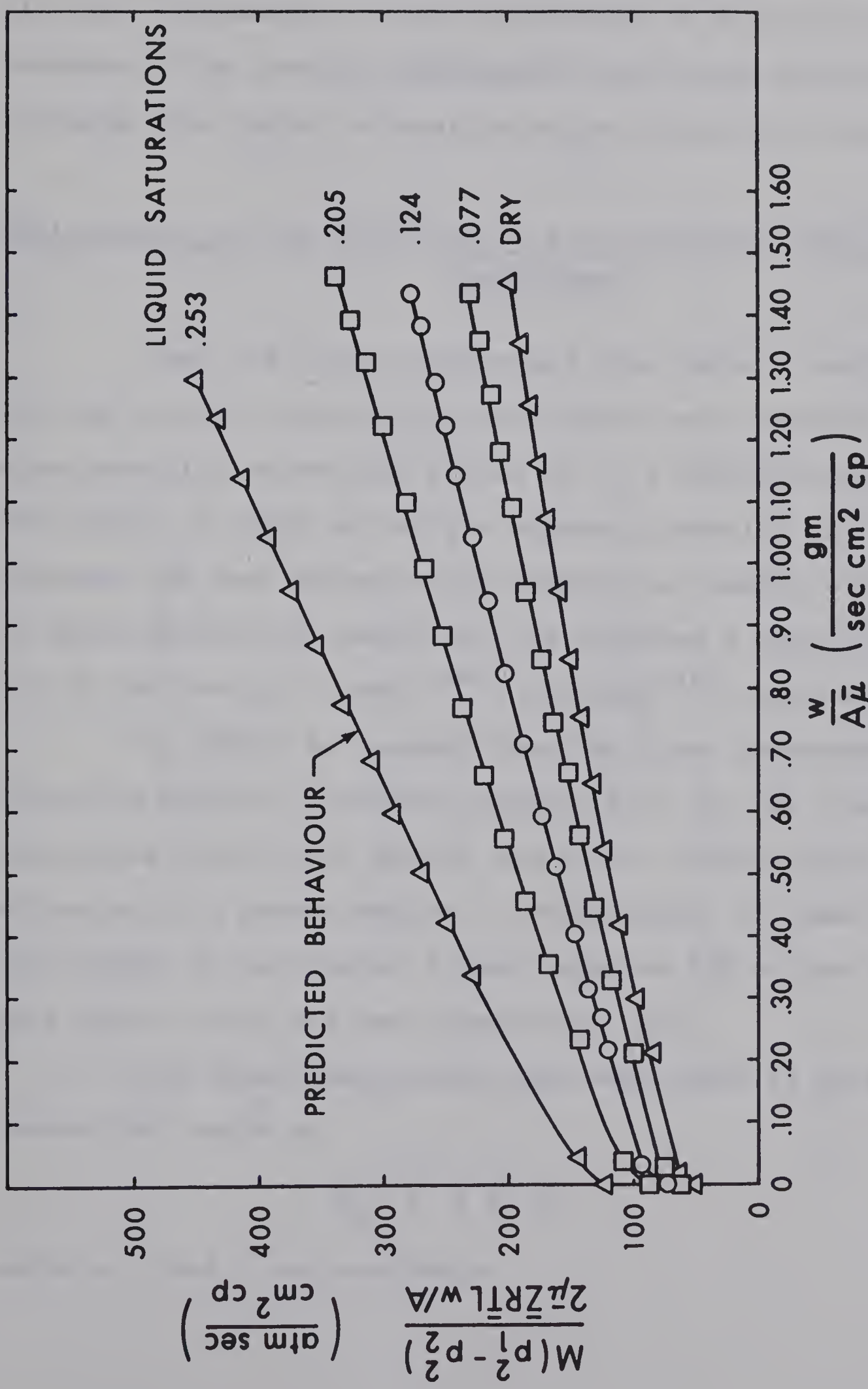


FIGURE 22 VISCO-INERTIAL FLOW PLOT FOR CORE 3.

Figure (23). The effective permeability was found to decrease steadily with every increase in the liquid saturation. Also the Klinkenberg b-factor was found to be relatively constant. The inertial resistance coefficient was found to increase with liquid saturation at an increasing rate.

Modification of the Correlation of the Inertial Resistance Coefficient

When the values determined from Sadiq's correlation for the inertial resistance coefficient were compared to the experimentally determined values of F_B a large discrepancy was noted. A check on Sadiq's approach revealed that his proposal had been formed using dimensional analysis based on semi-theoretical reasoning, and involved a least squares fit of the data of Cornell⁽⁴⁴⁾, Hamilton⁽⁴⁵⁾, and Sadiq⁽⁴⁶⁾.

It cannot be assumed that the three parameters effective porosity, absolute permeability and the inertial resistance coefficient should completely characterize the structure of a porous medium. Nevertheless, if these factors are assumed to be related a least squares fit of the basic data should yield the best predictive tool.

The relationship which has been shown to have some theoretical basis is

$$F_B = a \phi^c k^d \quad (37)$$

where a , c and d are constants.

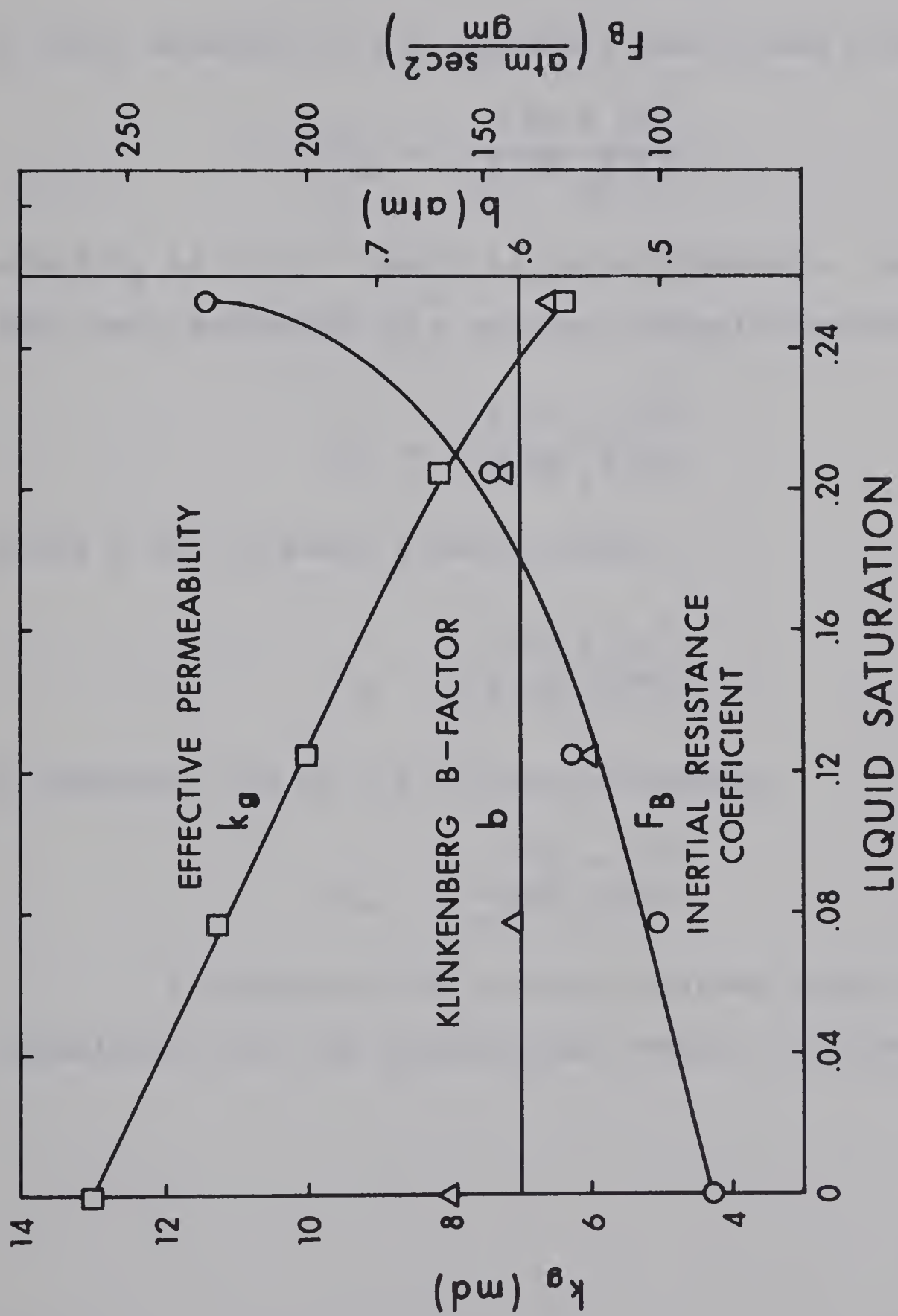


FIGURE 23
EFFECTIVE PERMEABILITY, KLINKENBERG
b-FACTOR AND INERTIAL RESISTANCE
COEFFICIENT AS A FUNCTION OF
LIQUID SATURATION FOR CORE 3.

This was linearized by taking logarithms

$$\ln F_B = \ln a + c \ln \phi + d \ln k \quad (38)$$

A least squares fit for Cornell's basic data yielded

$$F_B = \frac{2.80 \times 10^9}{\phi^{1.09} k^{1.17}} \quad (39)$$

where F_B is in ft^{-1} and k is in millidarcies. Hamilton's data were subjected to a similar analysis resulting in

$$F_B = \frac{6.56 \times 10^8}{\phi^{1.56} k^{1.22}} \quad (40)$$

while a fit of Sadiq's data yielded

$$F_B = \frac{3.40 \times 10^4}{\phi^{6.31} k^{0.50}} \quad (41)$$

A composite fit of all the data indicated

$$F_B = \frac{7.56 \times 10^8}{\phi^{1.67} k^{1.12}} \quad (42)$$

A comparison of results obtained using the proposed techniques with the experimental results is given in Table 9.

Table 9

A Comparison of Inertial Resistance
Coefficient Estimations

Sample	Experimental Value	F_B (ft^{-1})	Present Correlation
1	5.47×10^9	2.64×10^8	3.98×10^9
2	1.74×10^8	3.2×10^7	1.39×10^8
3	2.64×10^9	9.30×10^8	1.13×10^9

DISCUSSION OF RESULTS

For core 20 of Sadiq the permeability value obtained by the modified visco-inertial flow plot technique is consistent with that obtained from the Klinkenberg extrapolation of the viscous data. However, the value of the inertial resistance coefficient is approximately one-third of the value obtained using the standard visco-inertial flow plot technique. The results obtained by quasilinearization of the two modified equations compare very closely. They are quite consistent with the results obtained from the Klinkenberg and modified visco-inertial flow plots.

One important observation which may be made about the data is that not one data point can be considered free of slippage effects. Even at the highest mean pressure condition the factor $(1 + b/p)$ is found to be greater than 1.20. The significance of this observation is that the highest flow rate data have been obtained at the extreme pressure capacity of the equipment. Hence, the equipment would have to be modified especially for this sample if unaffected data were required. This indicates the superiority of schemes whereby slippage, be it especially significant or not, can be accounted for.

For the two cases in which the data of Cornell were used the lack of sufficient viscous data for a Klinkenberg extrapolation prevented the evaluation of the Klinkenberg

b-factor and hence prevented the use of the modified visco-inertial flow plot technique. Since most of the data were affected by slippage, only very few of the points could be used to determine k and F_B using the standard visco-inertial flow plot. Hence, the numerical technique was the only feasible means of solution. Application of the numerical technique to the modified forms of the visco-inertial flow equation gave results which were very consistent with those estimated by extrapolation of the visco-inertial flow plot.

The large deviations found when a comparison with Cornell's values was performed casts doubt upon the reliability of results presented by previous investigators who have used the standard technique.

In the present work, since very many data observations had been taken for both core samples 1 and 2, it was possible to distinguish a region of linearity on a back-pressure plot quite readily. As expected, the viscous data did not lie on a 45° slope in both cases. Generally the tentative viscous results were found to be quite representative, as indicated by Figures (6) and (15). These plots also indicate that the addition of several data points from the visco-inertial flow region may cause serious errors in the values obtained for the absolute permeability and the Klinkenberg b-factor.

In both cases a region of linearity could also be

distinguished on a standard visco-inertial flow plot. However, Figures(8) and (18) clearly illustrate that within the region of linearity the values of the parameters k and F_B consistently increase with decreasing $w/A\bar{\mu}$. The plots also indicate that the use of several affected data points can cause serious errors in the calculated values of k and F_B . Generally the values of k did not correspond very closely to those obtained from a Klinkenberg extrapolation.

Use of the modified visco-inertial flow plot yielded permeability values which were very consistent with the Klinkenberg extrapolation results. The values of the inertial resistance coefficient obtained by the modified visco-inertial flow plot were found to differ significantly from the standard technique values. In view of the fact that the permeability results were found to be more consistent, the inertial resistance coefficient values could be assumed to be more reliable.

The results obtained by quasilinearization of the modified equation for small pressure gradients were found to agree very well with the graphical results. In the present work results obtained by quasilinearization of the equation for high pressure gradients have been found to compare very well with results obtained from the solution of the equation for low pressure gradients. The discrepancies observed between the experimental and predicted results, which may be seen in

Figures (7) and (16), have been found to be not very great but very similar for both cores.

Sample 1 was found to have a permeability which was quite uniform with length and no significant mechanical end effects were observed. Though core 2 was found to be highly nonuniform, no end effects of any consequence were encountered as there was no noticeable change in the pressure profile at inlet or outlet with a change in the direction of flow. Hence, the discrepancies noted must be attributed to deficiencies of the basic theory in describing the physical model and poor experimental techniques. On the basis of this the merits of each method may be described.

Adequate criteria have not been developed for the delineation of the regions of linearity on the standard visco-inertial plot and the backpressure plots. Close agreement in permeability results suggests that the modified Klinkenberg and visco-inertial flow plot technique is superior to its predecessors. The shortcomings of the graphical technique is that it is time consuming and data must be split, requiring a large number of observations for good results.

Results obtained by the numerical solution of this modified equation are consistent with those obtained graphically. The modified form derived under the condition of a high pressure gradient is not amenable to graphical treatment. Comparison of the results obtained using the numerical means

with those obtained for the modified form for a small pressure gradient indicates the assumption in the derivation that the mean pressure is constant is not a serious one for this work.

The numerical technique is likely superior since all data are utilized simultaneously, and it is simple, rapid and inexpensive. Times of compilation and execution on the IBM 7040 for a typical set of data were 30 seconds and 5 seconds respectively, little more than the time required for a linear least squares fit. The only major drawback is that convergence may not occur if the initial guesses are poor. However, it is thought that the correlations presented for the absolute permeability and the Klinkenberg b-factor and the correlation developed for the inertial resistance coefficient provide adequate initial guesses. The correlation proposed for the inertial resistance coefficient has a sounder basis than any previous correlation. Nevertheless, it should be used with caution since it has been shown that the experimental values of the three parameters which have been correlated, the inertial resistance coefficient, the absolute permeability, and the effective porosity, in many cases are in serious error.

A comparison of the predicted and observed results obtained for gas flow in the presence of an immobile liquid phase indicates that all differences are very small. Hence,

the modified visco-inertial flow equation is assumed to adequately describe the phenomenon observed.

As expected, according to viscous flow investigations, the effective permeability was found to decrease uniformly with increasing liquid saturation while the Klinkenberg b-factor remained relatively constant. The inertial resistance coefficient was found to be a continuous function of saturation which increased at an increasing rate as the saturation was raised.

CONCLUSIONS AND RECOMMENDATIONS

Conclusions

The conclusions drawn as a result of this study are:

- 1) The standard visco-inertial graphical technique is adequate if there is certainty that the data are not affected by molecular streaming.
- 2) Since there is no adequate criterion for delineation of the region of linearity for the standard visco-inertial plot, where any discrepancy is anticipated or noted it is proposed that the modified graphical technique be used.
- 3) When access to a digital computer is available, use of the numerical technique is superior. The method is fairly simple, rapid and inexpensive, requiring no data splitting, hence utilizing all data simultaneously. Convergence, however, may not occur if poor initial guesses are made.
- 4) For this work the assumption that the mean pressure \bar{p} is not a function of p in deriving the modified form of the visco-inertial flow equation is not a serious one.
- 5) It has been indicated that the data used in evaluating the correlation of the inertial resistance coefficient with the absolute permeability and the effective porosity

is doubtful. Hence, the proposed correlations should be used exercising some measure of caution.

- 6) The revised correlation of the inertial resistance coefficient with the absolute permeability and the effective porosity predicts results better than any previous proposal.
- 7) The description of flow through a non-uniform sample lends itself to the identical analysis which has been applied in the case of uniform samples. A single set of parameters can be used to adequately describe the flow behavior. For all cases examined mechanical end effects were found to be negligible.
- 8) The flow theory which has been used to describe single phase gas flow is adequate for describing gas flow in the presence of an immobile liquid phase.
- 9) The effective permeability, Klinkenberg b-factor and inertial resistance coefficient are continuous functions of the saturation of an immobile liquid, with F_B increasing at an increasing rate with the liquid saturation.
- 10) Serious errors may result in using the present dry core correlations to predict the inertial resistance coefficient for gas flow in the presence of an immobile liquid saturation.

Recommendations

The following recommendations are made:

- 1) A study of pressure profiles should be performed and the consequences of nonuniformities and mechanical end effects of both machined and fractured cores should be carefully investigated.
- 2) The applicability of slip theory should be verified for purely viscous flow at very high pressure conditions.
- 3) Data reported by previous investigators should be re-evaluated by the presently proposed techniques to account for molecular streaming. Revisions to the correlations based on this data should be made accordingly.
- 4) A high quality set of standard flow calibrating devices should be made available to simplify the calibration of all flow measuring devices over their entire range.
- 5) Investigation should be made of the ramifications of non-isothermal flow.
- 6) Caution should be exercised in using the dry core correlations to predict the inertial resistance coefficient for gas flow in the presence of a second phase. Using the presently proposed techniques, flow in the presence of an immobile liquid saturation should be studied further so that the relationship between the inertial resistance coefficient and the liquid saturation may be established. Simultaneous flow of liquid and gas under visco-inertial flow conditions should also be examined.

NOMENCLATURE

A	area, L ²
b	Klinkenberg b-factor, m/Lt ²
d	collision diameter, L
F	formation resistivity factor
F _A	viscous resistance coefficient, L ⁻²
F _B	inertial resistance coefficient, L ⁻¹
k	absolute permeability, L ²
k _a	apparent permeability, L ²
k _g	effective permeability to gas, L ²
L	length, L
M	molecular weight, m
N	Avogadro's Number
N _{Re}	Reynolds Number
n	concentration of molecules per unit volume, L ⁻³
p	pressure, m/Lt ²
Q	volumetric flow rate, L ³ /t
q	volume rate of flow through a unit cross-sectional area of the solid plus fluid, L/t
R	universal gas constant, mL ² /t ² T
r	effective path radius, L
S	saturation
T	temperature, T
v	velocity, L/t
w	mass flow rate, m/t
x	distance in flow direction, L

Z compressibility factor
 λ mean free path length, L
 μ viscosity, m/Lt
 ρ density, m/L³
 ϕ porosity

Subscripts

c critical
r reduced
o reference conditions
1 inlet
2 outlet

Superscript

- average value

BIBLIOGRAPHY

1. Klinkenberg, L.J., The Permeability of Porous Media to Liquids and Gases, API Drilling and Production Practice, 200-213, 1941.
2. Katz, D.L., et al, Handbook of Natural Gas Engineering, p. 46-51, McGraw-Hill Book Company, Inc., 1959.
3. Rose, W.D., Permeability and Gas Slippage Phenomena, API Drilling and Production Practice, 209-217, 1948.
4. Nichol, L., Gas Turbulence Factor in Microvugular Carbonates, paper presented at the 17th Annual Technical Meeting of the Petroleum Society of the CIM, Edmonton, Alberta, May 1966.
5. Scheidegger, A.E., The Physics of Flow Through Porous Media, p. 127, University of Toronto Press, 1957.
6. Ergun, S., and Orning, A.A., Fluid Flow Through Randomly Packed Columns and Fluidized Beds, Ind.Eng. Chem. 41: No. 6: 1179-1184, 1949.
7. Green, L., Jr., and Duwez, P., Fluid Flow Through Porous Metals, Trans. ASME, J. App. Mech. 79: 39-45, 1951.
8. Cornell, D., and Katz, D.L., Flow of Gases Through Consolidated Porous Media, Ind.Eng.Chem. 45: No. 10: 2145-2152, October 1953.
9. Irmay, S., On the Theoretical Derivation of Darcy and Forchheimer Formulas, Transactions, American Geophysical Union, 39: No. 4: 702-707, August, 1958.
10. Tek, M.R., Development of a Generalized Darcy Equation, Pet. Trans. AIME, 210: 376-378, 1957.
11. Mackett, R.A., Viscous and Visco-Inertial Gas Flow in Limestone Cores, M.Sc. Thesis in Petroleum Engineering, University of Alberta, November 1966.
12. Cornell, D., Flow of Gases Through Consolidated Porous Media, Doctoral Dissertation Series Publication 5761, Ann Arbor, Michigan, University Microfilms, 1953.
13. Greenberg, D.B., and Weger, E., An Investigation of the Viscous and Inertia Coefficients for the Flow of Gases Through Porous Sintered Metals with High Pressure Gradients, Chem.Eng. Sci., 12: 8, 1960.

14. Hubbert, M. King, Darcy's Law and the Field Equation of Flow of Underground Fluids, Pet.Trans. AIME, 207:222, 1956.
15. Green, L., Jr., and Duwez, P., loc. cit.
16. Mackett, R.A., loc. cit.
17. Klinkenberg, L.J., loc. cit.
18. Hirschfelder, J.O., Curtiss, C.F., and Bird, R.B., Molecular Theory of Gases and Liquids, p. 10, J. Wiley and Sons, Inc., 2nd Printing, corrected, with notes added, March 1964.
19. Stewart, C.R., and Owens, W.H., A Laboratory Study of Laminar and Turbulent Flow in Heterogeneous Porosity Limestones, Pet.Trans. AIME, 213:121, 1958.
20. Rose, W.D., loc. cit.
21. Estes, R.K., and Fulton, P.F., Gas Slippage and Permeability Measurements, Pet. Trans. AIME, 207:338-342, 1956.
22. Hamm, J.D., and Eilerts, C.K., Effect of Saturation on Mobility of Low Liquid-Vapor Ratio Fluids, A pre-print of paper number SPE 1498 for the 41st Annual Fall Meeting of the Society of Petroleum Engineers of AIME, held in Dallas, Texas, Oct. 2-5, 1966.
23. Stewart, C.R., and Owens, W.H., loc. cit.
24. Iffly, R., and Naville, S., Influence of Velocity on the Permeability to Gas in a Gas-Gasoline Two-Phase Flow, Geop. 747A, Geopetrole, January 1967.
25. Nichol, L., loc. cit.
26. Klinkenberg, L.J., loc. cit.
27. Katz, D.L., et al, loc. cit.
28. Sadiq, S., The Inertial Resistance Coefficient and Other Reservoir Rock Properties, M.Sc. Thesis in Petroleum Engineering, University of Alberta, January, 1965.
29. Dranchuk, P.M., and Sadiq, S., The Interpretation of Permeability Measurements, J. Cdn. Pet. Tech., 4, No. 3, 130-133, 1965.
30. Ibid, loc. cit.

31. Cornell, D., loc. cit.
32. Ibid, p. 131 .
33. Ibid, p. 125 .
34. Sadiq, S., loc. cit.
35. Ibid, p. 60-61.
36. Bellman, R.E., and Kalaba, R.E., Quasilinearization and Non-Linear Boundary-Value Problems, p. 11, American Elsevier Publishing Co. Inc., 1965.
37. Heid, J.G., et al, Study of the Permeability of Rocks to Homogeneous Fluids, API Drilling and Production Practice, 230-246, 1950.
38. Sadiq, S., loc. cit.
39. Mackett, R.A., loc. cit.
40. Kestin, J., and Wang, H.E., The Viscosity of Five Gases: A Re-Evaluation, Trans. ASME: 80, Table 1, p. 13, 1959.
41. Hilsenrath, J., et al, Tables of Thermal Properties of Gases, National Bureau of Standards, Washington, D.C., Circular 554, Table 7-1, p. 317, 1955.
42. Dranchuk, P.M., and Kolada, L.J., Interpretation of Steady Linear Visco-Inertial Gas Flow Data, presented at 18th Annual Technical Meeting of the Petroleum Society of CIM, May, 1967.
43. Dranchuk, P.M., and Kolada, L.J., Steady Linear Gas Flow Through Porous Media, presented at the 42nd Annual Fall Meeting of the Society of Petroleum Engineers of AIME, held in Houston, Texas, Oct. 1-4, 1967.
44. Cornell, D., loc. cit.
45. Hamilton, R.J., A Study of Linear, Steady State Gas Flow Through Consolidated Porous Media. M.Sc. Thesis in Petroleum Engineering, University of Alberta, February, 1963.
46. Sadiq, S., loc.cit.

A P P E N D I X A

A MODIFIED VERSION OF THE VISCO-INERTIAL FLOW THEORY
ACCOUNTING FOR SLIPPAGE EFFECTS AT HIGH FLOW RATES

A modified Forchheimer equation has been derived and, by Equation (24), is

$$-\frac{dp}{dx} = \frac{\mu q}{k(1 + \frac{b}{p})} + F_B \rho q^2 \quad (A-1)$$

Multiplying through by ρ/μ which is equal to $PM/\mu ZRT$ by the modified gas law, and setting the constant mass flow rate/area ρq equal to w/A results in

$$\frac{-M}{\mu ZRT} p \frac{dp}{dx} = -\frac{w}{A} \frac{1}{k(1 + \frac{b}{p})} + \frac{F_B w}{\mu} \left(\frac{w}{A}\right)^2 \quad (A-2)$$

Dividing by w/A

$$\frac{-M}{\mu ZRT} \frac{w}{A} p \frac{dp}{dx} = \frac{1}{(1 + \frac{b}{p})} \left(\frac{1}{k} + \frac{F_B w}{\mu A} \left(1 + \frac{b}{p}\right)\right) \quad (A-3)$$

$$\frac{-(1 + \frac{b}{p}) p dp}{\frac{1}{k} + \frac{F_B w}{\mu A} (1 + \frac{b}{p})} = \frac{\mu ZRT \frac{w}{A}}{M} dx \quad (A-4)$$

$$\frac{-(p^2 + bp) dp}{\frac{bF_B w}{\mu A} + p(\frac{1}{k} + \frac{F_B w}{\mu A})} = \frac{\mu ZRT \frac{w}{A}}{M} dx \quad (A-5)$$

Letting $\alpha = \frac{F_B w}{\mu A}$ (A-6)

and

$$\gamma = \frac{1}{k} + \frac{F_B w}{\mu A} = \frac{1}{k} + \alpha \quad (A-7)$$

the differential equation may be written as

$$\frac{-(p^2 + bp)}{\alpha b + p\gamma} dp = \frac{\mu ZRT \frac{w}{A}}{M} dx \quad (A-8)$$

For a constant viscosity and compressibility evaluated at the arithmetic mean pressure and temperature, integration using items 91.1 and 92.1^(A1) and interchanging limits and sign results in

$$\left[\frac{p^2}{2\gamma} - \frac{\alpha bp}{\gamma} + \frac{(\alpha b)^2}{\gamma^3} \ln(\alpha b + p\gamma) + \frac{b}{\gamma^2} \left[p\gamma - \alpha b \ln(\alpha b + p\gamma) \right] \right]_{p_2}^{p_1} = \frac{\mu \bar{Z} \bar{R} \bar{T} \frac{w}{A}}{M} \left[x \right]_O^L \quad (A-9)$$

Substituting Equation (A-7)

$$\left[\frac{p^2}{2\gamma} - \frac{\alpha bp}{\gamma} + \frac{(\alpha b)^2}{\gamma^3} \ln(\alpha b + p\gamma) + \frac{bp}{\gamma^2 k} + \frac{b}{\gamma^2} \alpha p - \frac{b^2}{\gamma^2} \alpha \ln(\alpha b + p\gamma) \right]_{p_2}^{p_1} = \frac{\mu \bar{Z} \bar{R} \bar{T} L \frac{w}{A}}{M} \quad (A-10)$$

$$\begin{aligned} & \left[\frac{p^2}{2\gamma} + \left(\gamma - \frac{1}{k} \right) \frac{\alpha b^2}{\gamma^3} \ln(\alpha b + p\gamma) + \frac{b}{\gamma^2} \frac{p}{k} - \frac{\alpha b^2}{\gamma^2} \ln(\alpha b + p\gamma) \right]_{p_2}^{p_1} \\ &= \left[\frac{p^2}{2\gamma} - \frac{\alpha b^2}{k \gamma^3} \ln(\alpha b + p\gamma) + \frac{b}{\gamma^2} \frac{p}{k} \right]_{p_2}^{p_1} \\ &= \frac{\mu \bar{Z} \bar{R} \bar{T} L \frac{w}{A}}{M} \end{aligned} \quad (A-11)$$

$$\begin{aligned} \frac{(p_1^2 - p_2^2)}{2\gamma} - \frac{\alpha b^2}{k\gamma^3} \ln \frac{(\alpha b + p_1\gamma)}{(\alpha b + p_2\gamma)} + \frac{b}{\gamma^2} \frac{(p_1 - p_2)}{k} \\ = \frac{\frac{\mu Z R T L}{A} \frac{w}{M}}{2\gamma^3} \end{aligned} \quad (A-12)$$

Multiplying by $\frac{1}{(p_1^2 - p_2^2)}$

$$\begin{aligned} \gamma^2 - \frac{2\alpha b^2}{k} \frac{1}{(p_1^2 - p_2^2)} \log \frac{(\alpha b + p_1\gamma)}{(\alpha b + p_2\gamma)} + \frac{2b\gamma}{k} \frac{(p_1 - p_2)}{(p_1^2 - p_2^2)} \\ = \frac{\gamma^3 2\mu Z R T L \frac{w}{A}}{M(p_1^2 - p_2^2)} \end{aligned} \quad (A-13)$$

Realizing

$$\frac{(p_1^2 - p_2^2)}{2(p_1 - p_2)} = \bar{p} \quad (A-14)$$

$$\frac{M(p_1^2 - p_2^2)}{2\mu Z R T L \frac{w}{A}} = \frac{\gamma^3}{\gamma^2 - \frac{2\alpha b^2}{k(p_1^2 - p_2^2)} \ln \frac{(\alpha b + p_1\gamma)}{(\alpha b + p_2\gamma)} + \frac{b\gamma}{k\bar{p}}} \quad (A-15)$$

- A1. Dwight, H.B., Tables of Integrals and Other Mathematical Data, p. 18. The Macmillan Company, Third Edition, 1960.

A P P E N D I X B

DEVELOPMENT OF A GENERAL NUMERICAL PROCEDURE
TO SOLVE THE MODIFIED FORCHHEIMER EQUATIONS

In general the problem consists of solving a relationship of the form

$$f = \text{fcn}(k, b, F_B) \quad (\text{B-1})$$

which is non-linear in the three parameters k , b , and F_B .

If the equation were linear a unique solution for k , b , and F_B would be obtained if the number of observed data points $n = 3$. For $n > 3$ a least squares fit of the data would result in unbiased estimations of k , b and F_B .

The equation may be linearized through application of the Newton-Raphson approximation

$$\begin{aligned} f^j &= f_{i-1}^j + \left(\frac{\partial f}{\partial b}\right)_{i-1}^j (b_i - b_{i-1}) \\ &+ \left(\frac{\partial f}{\partial k}\right)_{i-1}^j (k_i - k_{i-1}) + \left(\frac{\partial f}{\partial F_B}\right)_{i-1}^j (F_{B_i} \\ &- F_{B_{i-1}}) + E_i^j \end{aligned} \quad (\text{B-2})$$

where

j = the j^{th} data point and $j = 1, 2, \dots, N$

i = the i^{th} iteration and $i = 1, 2, \dots, n$

f^j is the observed value of f for the j^{th} data point

$$f_{i-1}^j = \left[fcn(b, k, F_B) \right]_{i-1}^j \quad (B-3)$$

$$= \left[fcn(b_{i-1}, k_{i-1}, F_{B_{i-1}}) \right]_i^j \quad (B-4)$$

where

E_i^j = random error associated with the j^{th} data point and i^{th} iteration

Equation (B-2) may now be rewritten as

$$\begin{aligned} f^j - f_{i-1}^j + \left(\frac{\partial f}{\partial b} \right)_{i-1}^j b_{i-1} + \left(\frac{\partial f}{\partial k} \right)_{i-1}^j k_{i-1} + \left(\frac{\partial f}{\partial F_B} \right)_{i-1}^j F_{B_{i-1}} \\ = \left(\frac{\partial f}{\partial b} \right)_{i-1}^j b_i + \left(\frac{\partial f}{\partial k} \right)_{i-1}^j k_i + \left(\frac{\partial f}{\partial F_B} \right)_{i-1}^j F_{B_i} + E_i^j \end{aligned} \quad (B-5)$$

or

$$\begin{aligned} f^j - s_{i-1}^j = \left(\frac{\partial f}{\partial b} \right)_{i-1}^j b_i + \left(\frac{\partial f}{\partial k} \right)_{i-1}^j k_i \\ + \left(\frac{\partial f}{\partial F_B} \right)_{i-1}^j F_{B_i} + E_i^j \end{aligned} \quad (B-6)$$

In the event that $N = 3$ it is assumed that no random error exists or $E_i^j = 0$ for all j and i , reducing the problem to

$$\begin{aligned} f^j - s_{i-1}^j = \left(\frac{\partial f}{\partial b} \right)_{i-1}^j b_i + \left(\frac{\partial f}{\partial k} \right)_{i-1}^j k_i \\ + \left(\frac{\partial f}{\partial F_B} \right)_{i-1}^j F_{B_i} \quad j = 1, 2, 3 \end{aligned} \quad (B-7)$$

a set of three linear equations in three unknowns. In this case b_i , k_i , and F_{B_i} may be obtained by applying Cramer's Rule and generating a recurrence relation. Initial approximations b_0 , k_0 , and F_{B_0} are made to initiate calculation and iteration is continued until $i = n$ where

$$\left| \frac{b_n - b_{n-1}}{b_n} \right|, \left| \frac{k_n - k_{n-1}}{k_n} \right| \text{ and } \left| \frac{F_{B_n} - F_{B_{n-1}}}{F_{B_n}} \right| \leq \epsilon \quad (B-8)$$

for ϵ , the convergence criterion, chosen arbitrarily small.

If $N > 3$ a least squares criterion is applied and the sum of the squared errors for iteration i

$$\sum_{j=1}^N (E_i^j)^2 = \sum_{j=1}^N \left[f^j - s_{i-1}^j - \left(\frac{\partial f}{\partial b} \right)_{i-1}^j b_i - \left(\frac{\partial f}{\partial k} \right)_{i-1}^j k_i - \left(\frac{\partial f}{\partial F_B} \right)_{i-1}^j F_{B_i} \right]^2 \quad (B-9)$$

is minimized with respect to b_i , k_i , and F_{B_i} by setting

$$\frac{\partial \sum_{j=1}^N (E_i^j)^2}{\partial b_i} = \frac{\partial \sum_{j=1}^N (E_i^j)^2}{\partial k_i} = \frac{\partial \sum_{j=1}^N (E_i^j)^2}{\partial F_{B_i}} = 0 \quad (B-10)$$

The resulting equations

$$\frac{\partial \sum_{j=1}^N (E_i^j)^2}{\partial b_i} = - \sum_{j=1}^N 2 \left[f^j - s_{i-1}^j - \left(\frac{\partial f}{\partial b} \right)_{i-1}^j b_i \right. \\ \left. - \left(\frac{\partial f}{\partial k} \right)_{i-1}^j k_i - \left(\frac{\partial f}{\partial F_B} \right)_{i-1}^j F_{B,i} \right] \left(\frac{\partial f}{\partial b} \right)_{i-1}^j = 0 \quad (B-11)$$

$$\frac{\partial \sum_{j=1}^N (E_i^j)^2}{\partial k_i} = - \sum_{j=1}^N 2 \left[f^j - s_{i-1}^j - \left(\frac{\partial f}{\partial b} \right)_{i-1}^j b_i \right. \\ \left. - \left(\frac{\partial f}{\partial k} \right)_{i-1}^j k_i - \left(\frac{\partial f}{\partial F_B} \right)_{i-1}^j F_{B,i} \right] \left(\frac{\partial f}{\partial k} \right)_{i-1}^j = 0 \quad (B-12)$$

$$\frac{\partial \sum_{j=1}^N (E_i^j)^2}{\partial F_{B,i}} = - \sum_{j=1}^N 2 \left[f^j - s_{i-1}^j - \left(\frac{\partial f}{\partial b} \right)_{i-1}^j b_i \right. \\ \left. - \left(\frac{\partial f}{\partial k} \right)_{i-1}^j k_i - \left(\frac{\partial f}{\partial F_B} \right)_{i-1}^j F_{B,i} \right] \left(\frac{\partial f}{\partial F_B} \right)_{i-1}^j = 0 \quad (B-13)$$

reduce to a series of three equations, linear in three unknowns for each iteration

$$\begin{aligned}
& b_i \sum_{j=1}^N \left[\left(\frac{\partial f}{\partial b} \right)_{i-1}^j \right]^2 + k_i \sum_{j=1}^N \left(\frac{\partial f}{\partial k} \right)_{i-1}^j \left(\frac{\partial f}{\partial b} \right)_{i-1}^j \\
& + F_B b_i \sum_{j=1}^N \left(\frac{\partial f}{\partial F_B} \right)_{i-1}^j \left(\frac{\partial f}{\partial b} \right)_{i-1}^j \\
= & \sum_{j=1}^N (f^j - s_{i-1}^j) \left(\frac{\partial f}{\partial b} \right)_{i-1}^j \quad (B-14)
\end{aligned}$$

$$\begin{aligned}
& b_i \sum_{j=1}^N \left(\frac{\partial f}{\partial b} \right)_{i-1}^j \left(\frac{\partial f}{\partial k} \right)_{i-1}^j + k_i \sum_{j=1}^N \left[\left(\frac{\partial f}{\partial k} \right)_{i-1}^j \right]^2 \\
& + F_B b_i \sum_{j=1}^N \left(\frac{\partial f}{\partial F_B} \right)_{i-1}^j \left(\frac{\partial f}{\partial k} \right)_{i-1}^j \\
= & \sum_{j=1}^N (f^j - s_{i-1}^j) \left(\frac{\partial f}{\partial k} \right)_{i-1}^j \quad (B-15)
\end{aligned}$$

$$\begin{aligned}
& b_i \sum_{j=1}^N \left(\frac{\partial f}{\partial b} \right)_{i-1}^j \left(\frac{\partial f}{\partial F_B} \right)_{i-1}^j + k_i \sum_{j=1}^N \left(\frac{\partial f}{\partial k} \right)_{i-1}^j \left(\frac{\partial f}{\partial F_B} \right)_{i-1}^j \\
& + F_B b_i \sum_{j=1}^N \left[\left(\frac{\partial f}{\partial F_B} \right)_{i-1}^j \right]^2 \\
= & \sum_{j=1}^N (f^j - s_{i-1}^j) \left(\frac{\partial f}{\partial F_B} \right)_{i-1}^j \quad (B-16)
\end{aligned}$$

This system of equation may now be solved for each iteration using a method such as Cramer's Rule.

Initial approximations b_o , k_o , and F_{B_o} are made and iteration proceeds until $i = n$ where

$$\left| \frac{b_n - b_{n-1}}{b_n} \right|, \quad \left| \frac{k_n - k_{n-1}}{k_n} \right| \quad \text{and} \quad \left| \frac{F_{B_n} - F_{B_{n-1}}}{F_{B_n}} \right| \leq \varepsilon \quad (B-17)$$

for ε , the convergence criterion, chosen arbitrarily small.

A P P E N D I X C

APPLICATION OF THE NUMERICAL TECHNIQUE TO TWO
MODIFIED FORMS OF THE FORCHHEIMER EQUATION

In order to apply the numerical technique to the modified forms of the Forchheimer Equation it is necessary in each case to evaluate the partial derivatives with respect to the three constants.

The first modified equation is

$$f = \frac{M(p_1^2 - p_2^2)}{2\bar{\mu}ZRTL \frac{w}{A}} = \frac{1}{k(1 + \frac{b}{\bar{p}})} + F_B \frac{w}{A\bar{\mu}} \quad (C-1)$$

Now

$$f^j = \left[\frac{M(p_1^2 - p_2^2)}{2\bar{\mu}ZRTL \frac{w}{A}} \right]^j \quad (C-2)$$

$$f_{i-1}^j = \left[\frac{1}{k(1 + \frac{b}{\bar{p}})} + F_B \frac{w}{A\bar{\mu}} \right]_{i-1}^j \quad (C-3)$$

$$= \frac{1}{k_{i-1}(1 + b_{i-1}(\frac{1}{\bar{p}})^j)} + F_{B,i-1} \frac{w}{A\bar{\mu}} (\frac{1}{\bar{p}})^j \quad (C-4)$$

$$\left(\frac{\partial f}{\partial b} \right)_{i-1}^j = \left[\frac{-\frac{1}{\bar{p}}}{k(1 + b(\frac{1}{\bar{p}})^2)} \right]_{i-1}^j = \frac{-\frac{1}{\bar{p}}}{k_{i-1}(1 + b_{i-1}(\frac{1}{\bar{p}})^j)^2} \quad (C-5)$$

$$\left(\frac{\partial f}{\partial k} \right)_{i-1}^j = \left[\frac{-1}{k^2(1 + \frac{b}{\bar{p}})} \right]_{i-1}^j = \frac{-1}{(k_{i-1})^2(1 + b_{i-1}(\frac{1}{\bar{p}})^j)} \quad (C-6)$$

$$\left(\frac{\partial f}{\partial F_B} \right)_{i-1}^j = \left(\frac{w}{A\bar{\mu}} \right)_{i-1}^j = \left(\frac{w}{A\bar{\mu}} \right)^j \quad (C-7)$$

For the second modified version of the Forchheimer equation

$$\begin{aligned}
 f &= \frac{M(p_1^2 - p_2^2)}{2\bar{\mu}ZRTL \frac{w}{A}} \\
 &= \frac{\gamma^3}{\gamma^2 - \frac{2ab^2}{k(p_1^2 - p_2^2)} \ln \frac{(ab + p_1\gamma)}{(ab + p_2\gamma)} + \frac{b\gamma}{kp}} \\
 &= \frac{\gamma^3}{L} \tag{C-8}
 \end{aligned}$$

Now we have $p_1 = \bar{p} + \frac{(p_1 - p_2)}{2}$

$$p_2 = \bar{p} - \frac{(p_1 - p_2)}{2}$$

and

$$(p_1^2 - p_2^2) = 2\bar{p} (p_1 - p_2)$$

Setting NUM. = $\alpha b + p_1\gamma$

and DEN = $\alpha b + p_2\gamma$

$$f^j = \left[\frac{M(p_1^2 - p_2^2)}{2\bar{\mu}ZRTL \frac{w}{A}} \right]^j \tag{C-9}$$

$$f_{i-1}^j = \left[\frac{\gamma^3}{\gamma^2 - \frac{\alpha b^2}{kp(p_1 - p_2)} \ln \frac{NUM}{DEN} + \frac{b\gamma}{kp}} \right]^j_{i-1} \tag{C-10}$$

$$\begin{aligned}
\left(\frac{\partial f}{\partial b}\right)_{i-1}^j &= \left[-\frac{\gamma^3}{L^2} \left[\frac{-2\alpha b}{kp(p_1-p_2)} \ln\left(\frac{NUM}{DEN}\right) \right. \right. \\
&\quad \left. \left. - \frac{\alpha b^2}{kp(p_1-p_2)} \left(\frac{\alpha}{NUM} - \frac{\alpha}{DEN} \right) + \frac{\gamma}{kp} \right] j \right]_{i-1} \\
\left(\frac{\partial f}{\partial k}\right)_{i-1}^j &= \left[\frac{1}{L^2} \left[L \left(-\frac{3\gamma^2}{k^2} \right) - \gamma^3 \left(-\frac{2\gamma}{k^2} - \frac{\alpha b^2}{kp(p_1-p_2)} \left(\frac{-p_1}{k^2 NUM} \right. \right. \right. \right. \\
&\quad \left. \left. \left. \left. + \frac{p_2}{k^2 DEN} \right) + \ln\left(\frac{NUM}{DEN}\right) \frac{\alpha b^2}{k^2 p(p_1-p_2)} \right. \right. \right. \\
&\quad \left. \left. \left. - \frac{\alpha b}{k^2 p} - \frac{2b}{k^3 p} \right) \right] j \right]_{i-1} \\
\left(\frac{\partial F}{\partial F_B}\right)_{i-1}^j &= \left[\frac{1}{L^2} \left[L \left(3\gamma^2 \frac{w}{A\bar{\mu}} \right) - \gamma^3 \left(2\gamma \frac{w}{A\bar{\mu}} - \frac{\alpha b^2}{kp(p_1-p_2)} \right. \right. \right. \\
&\quad \left. \left. \left. \left(\frac{w}{A\bar{\mu}} (b+p_1) - \frac{w}{A\bar{\mu}} (b+p_2) \right) \right. \right. \right. \\
&\quad \left. \left. \left. + \ln\left(\frac{NUM}{DEN}\right) \frac{w}{A\bar{\mu}} \frac{b^2}{kp(p_1-p_2)} + \frac{b}{kp} \frac{w}{A\bar{\mu}} \right) \right] j \right]_{i-1}
\end{aligned}$$

The nomenclature used in the computer program is

B	Klinkenberg b-factor, b
BETA	inertial resistance coefficient, F_B
D = DELPM	$\frac{M(p_1^2 - p_2^2)}{2\bar{\mu}ZRTL w/A}$
DCALC	f_n^j
DE = DELP	$p_1 - p_2$
K	absolute permeability, k
P(I)	$\partial f / \partial k$
PM = PMAR	$1/\bar{p}$
Q(I)	$\partial f / \partial b$
R(I)	$\partial f / \partial F_B$
V(I)	f_{i-1}^j
W = WAV	$w/A\bar{\mu}$

Additional nomenclature used in the computer output is

KA	apparent permeability, k_a
P1A	p_1
P2A	p_2
QO	Q_o
TMK	\bar{T}


```

C* * * * * * * * * * * * * * * * * * * * * * * * * * * * * * * * * * * * * *
C DATA CORRELATION USING QUASILINEARIZATION
C SOLUTION OF THE EQUATION FOR HIGH PRESSURE GRADIENTS
C NSETS = NUMBER OF DATA SETS
C FMT(J) = APPROPRIATE COMMENT WHICH DESCRIBES DATA SET
C N = NUMBER OF OBSERVATIONS IN THE DATA SET
C K = PERMEABILITY , INITIAL GUESS
C B = KLINKENBERG B-FACTOR , INITIAL GUESS
C BETA = INERTIAL RESISTANCE COEFFICIENT , INITIAL GUESS
C EPSLON = CONVERGENCE CRITERION
C D=DELP, PM=PMAR, W=WAV, DE=DELP
C* * * * * * * * * * * * * * * * * * * * * * * * * * * * * * * * * * * * * *

100 FORMAT(1X,I3)
101 FORMAT(20A4)
102 FORMAT(2X,6E12.5)
103 FORMAT(2X,4E14.7)
104 FORMAT(1H0,19X,17HINITIAL GUESS ,3(2X,E11.4))
106 FORMAT(20X,13HITERATION NO.,I4,3(2X,E11.4))
107 FORMAT(1H ,18X,5(E10.4,1X),E8.2)
108 FORMAT(19X,36H PMAR WAV DELP D,
         129HELPM DCALC ERROR )
109 FORMAT(19X,37H (ATM-1) (GM/SEC CM2 CP) (ATM) ,
         129H (ATM SEC/CM2 CP) )
110 FORMAT(1H1)
113 FORMAT(1H )
114 FORMAT(1H-)
115 FORMAT(1H-,44X,1HK,12X,1HB,10X,4HBETA)
116 FORMAT(41X,36H(DARCI'S) (ATM) (ATM SEC2/GM))
      REAL FMT(20),D(100),PM(100),W(100),DE(100),V(100),NUM
      REAL Z(100),P(100),Q(100),R(100),T(100),ERROR(100),K,L
      REAL DCALC(100),X(100),K1
      READ(5,100)NSETS
      DO 1 JJ=1,NSETS
      READ(5,101) (FMT(J),J=1,20)
      WRITE(6,110)
      WRITE(6,114)
      READ(5,100)N
C SETTING THE INITIAL GUESSES
      READ(5,102)K,B,BETA,EPSLON
      DO 2 I=1,N
      READ(5,103)D(I),PM(I),W(I),DE(I)
2 CONTINUE
      WRITE(6,101)(FMT(J),J=1,20)
      WRITE(6,115)
      WRITE(6,116)
      WRITE(6,104)K,B,BETA
      WRITE(6,113)
      M=0
8 SIGPSQ=0.0
      SIGPQ=0.0
      SIGPR=0.0
      SIGQSQ=0.0
      SIGQR=0.0
      SIGRSQ=0.0

```



```
SIGPD=0.0  
SIGQD=0.0  
SIGRD=0.0  
SIGPT=0.0  
SIGQT=0.0  
SIGRT=0.0
```

C SETTING THE ELEMENTS OF THE MATRIX AND THE KNOWN VECTOR

DO 3 I=1,N

E=1./K+BETA*W(I)

NUM=BETA*B*W(I)+(1./PM(I)+DE(I)/2.)*E

DEN=BETA*B*W(I)+(1./PM(I)-DE(I)/2.)*E

L=E**2+B*PM(I)*E/K-B**2*BETA*W(I)*PM(I)/(K*DE(I))*ALOG

1(ABS(NUM/DEN))

V(I)=E**3/L

X(I)=1.0

Z(I)=1.0

P(I)=(-L*3.*E**2/K**2-E**3*(-2.*E/K**2-2.*B*PM(I)/K**3
1-B*PM(I)*BETA*W(I)/K**2-B**2*BETA*W(I)*PM(I)/(K*DE(I))
1*((-1./PM(I)-DE(I)/2.)/K**2/NUM+(1./PM(I)-DE(I)/2.)/K*
1*2/DEN)+(ALOG(ABS(NUM/DEN))) *B**2*BETA*W(I)*PM(I)/K**2
1/DE(I)))/L**2

Q(I)=(-E**3*(PM(I)/K*E-B**2*BETA*PM(I)*W(I)/K/DE(I)*(B
1ETA*W(I)/NUM-BETA*W(I)/DEN)-(ALOG(ABS(NUM/DEN)))*2.*B*
1BETA*PM(I)*W(I)/K/DE(I)))/L**2

R(I)=(L*3.*E**2*W(I)-E**3*(2.*E*W(I)+B*PM(I)*W(I)/K-B*
1*2*BETA*W(I)*PM(I)/K/DE(I)*((B*W(I)+W(I)*(1./PM(I)+DE(
1I)/2.))/NUM-(B*W(I)+(1./PM(I)-DE(I)/2.)*W(I))/DEN)-ALU
1G(ABS(NUM/DEN))*B**2*W(I)*PM(I)/K/DE(I)))/L**2

T(I)=V(I)*X(I)*Z(I)-K*P(I)-B*Q(I)-BETA*R(I)

SIGPSQ=SIGPSQ+P(I)**2

SIGPQ=SIGPQ+P(I)*Q(I)

SIGPR=SIGPR+P(I)*R(I)

SIGQSQ=SIGQSQ+Q(I)**2

SIGQR=SIGQR+Q(I)*R(I)

SIGRSQ=SIGRSQ+R(I)**2

SIGPD=SIGPD+P(I)*D(I)

SIGQD=SIGQD+Q(I)*D(I)

SIGRD=SIGRD+R(I)*D(I)

SIGPT=SIGPT+P(I)*T(I)

SIGQT=SIGQT+Q(I)*T(I)

SIGRT=SIGRT+R(I)*T(I)

3 CONTINUE

B1=SIGPD-SIGPT

B2=SIGQD-SIGQT

B3=SIGRD-SIGRT

C SOLUTION USING CRAMER'S RULE

DET(SIGPSQ*(SIGQSQ*SIGRSQ-SIGQR*SIGQR)-SIGPQ*(SIGPQ*S
1SIGRSQ-SIGQR*SIGPR)+SIGPR*(SIGPQ*SIGQR-SIGQSQ*SIGPR))

DET(SIGPQ*(SIGQR*B3-SIGRSQ*B2)-SIGQSQ*(SIGPR*B3-SIGR
1SQ*B1)+SIGQR*(SIGPR*B2-SIGQR*B1))

DET(SIGPSQ*(SIGQR*B3-SIGRSQ*B2)-SIGPQ*(SIGPR*B3-SIGR
1SQ*B1)+SIGPR*(SIGPR*B2-SIGQR*B1))

DET(SIGPSQ*(SIGQSQ*B3-SIGQR*B2)-SIGPQ*(SIGPQ*B3-SIGQ
1R*B1)+SIGPR*(SIGPQ*B2-SIGQSQ*B1))


```

K1=FNDET/DDET
B1=SNDET/DDET
BETA1=TNDET/DDET
M=1+M
C A CHECK ON THE CONVERGENCE OF THE SOLUTION
IF(ABS((K1-K)/K).LE.EPSLN ) GO TO 4
GO TO 7
4 IF (ABS((B1-B)/B).LE.EPSLN ) GO TO 5
GO TO 7
5 IF (ABS((BETA1-BETA)/BETA).LE.EPSLN ) GO TO 6
7 IF(ABS(K1-K).GT.(2.*ABS(K))) K1=K+2.*K*K1/ABS(K1)
IF(ABS(B1-B).GT.(2.*ABS(B))) B1=B+2.*B*B1/ABS(B1)
IF(ABS(BETA1-BETA).GT.(2.*ABS(BETA))) BETA1=BETA+2.*BETA
1*BETA1/ABS(BETA1)
WRITE(6,106)M,K1,B1,BETA1
K=K1
B=B1
BETA=BETA1
IF(M.EQ.100) GO TO 6
GO TO 8
6 WRITE(6,106)M,K1,B1,BETA1
WRITE(6,114)
WRITE(6,108)
WRITE(6,109)
WRITE(6,113)
DO 9 I=1,N
IF(((I+M).EQ.43).OR.((I+M).EQ.92)) GO TO 11
GO TO 10
11 WRITE(6,110)
WRITE(6,114)
WRITE(6,101) (FMT(J),J=1,20)
WRITE(6,114)
WRITE(6,108)
WRITE(6,109)
WRITE(6,113)
10 DCALC(I)=V(I)*X(I)*Z(I)
ERROR(I)=ABS(DCALC(I)-D(I))
WRITE(6,107)PM(I),W(I),DE(I),D(I),DCALC(I),ERROR(I)
9 CONTINUE
1 CONTINUE
STOP
END

```


A P P E N D I X D

TABULATED DATA

TABLE 10 EXPERIMENTAL GAS FLOW DATA FOR CORE 1

ENDFACE DATA FOR SANDSTONE SAMPLE

RUN	P1A (ATM)	P2A (ATM)	TMK (K)	QD (CC/SEC)	DELP2 (ATM2)
1	30.84	2.291	300.13	0.1566E 03	0.9456E 03
2	33.14	2.534	301.01	0.1775E 03	0.1092E 04
3	9.96	0.981	300.16	0.1925E 02	0.9700E 02
4	12.50	1.020	300.06	0.2898E 02	0.1504E 03
5	13.84	1.064	300.14	0.3613E 02	0.1905E 03
6	15.50	1.119	300.14	0.4461E 02	0.2391E 03
7	17.56	1.216	300.13	0.5635E 02	0.3069E 03
8	21.24	1.432	300.27	0.7875E 02	0.4489E 03
9	24.54	1.686	299.92	0.1040E 03	0.5992E 03
10	27.48	1.948	300.26	0.1270E 03	0.7513E 03
11	29.45	2.150	300.28	0.1446E 03	0.8628E 03
12	26.21	1.840	300.41	0.1173E 03	0.6868E 03
13	22.80	1.546	300.45	0.9049E 02	0.5175E 03
14	19.26	1.308	300.52	0.6625E 02	0.3693E 03
15	1.84	0.922	300.80	0.6523E 00	0.2542E 01
16	1.12	0.922	300.80	0.1136E 00	0.3981E 00
17	38.29	3.140	301.08	0.2292E 03	0.1457E 04
18	43.72	3.680	301.36	0.2890E 03	0.1896E 04
19	48.62	4.628	301.71	0.3498E 03	0.2342E 04
20	52.06	5.198	301.84	0.3946E 03	0.2683E 04
21	55.39	5.709	301.64	0.4358E 03	0.3036E 04
22	54.10	7.291	302.23	0.5640E 03	0.4050E 04
23	59.92	6.483	302.03	0.4987E 03	0.3548E 04
24	49.91	4.833	301.69	0.3660E 03	0.2468E 04
25	46.14	4.263	301.27	0.3194E 03	0.2110E 04
26	40.80	3.498	300.91	0.2570E 03	0.1652E 04
27	35.45	3.200	300.56	0.2001E 03	0.1247E 04
28	35.49	3.205	300.40	0.1996E 03	0.1249E 04
29	33.07	2.540	300.24	0.1770E 03	0.1087E 04
30	21.16	1.427	300.09	0.7889E 02	0.4459E 03
31	53.06	5.450	299.76	0.4162E 03	0.2850E 04
32	71.59	8.733	300.25	0.6849E 03	0.5049E 04
33	68.90	8.206	300.01	0.6434E 03	0.4680E 04
34	66.74	7.814	299.90	0.6100E 03	0.4393E 04
35	64.26	7.355	299.72	0.5721E 03	0.4075E 04
36	61.30	6.904	299.64	0.5350E 03	0.3779E 04
37	57.71	6.173	299.51	0.4759E 03	0.3292E 04
38	54.51	5.620	299.47	0.4324E 03	0.2940E 04
39	8.50	0.900	300.20	0.1433E 02	0.7138E 02
40	1.31	0.920	300.53	0.2366E 00	0.8728E 00
41	1.63	0.920	300.54	0.4748E 00	0.1822E 01
42	2.01	0.921	300.65	0.7976E 00	0.3191E 01
43	2.75	0.923	300.56	0.1585E 01	0.5718E 01
44	4.33	0.926	300.62	0.3893E 01	0.1788E 02

TABLE 10 EXPERIMENTAL GAS FLOW DATA FOR CORE 1

ENDFACE DATA FOR SANDSTONE SAMPLE

FUN	P1A (ATM)	P2A (ATM)	TMR (K)	Q0 (CC/SEC)	DELP2 (ATM2)
45	3.65	0.934	300.54	0.2788E 01	0.1243E 02
46	1.50	0.923	300.68	0.3729E 00	0.1402E 01
47	1.40	0.922	300.71	0.3024E 00	0.1122E 01
48	2.42	0.926	300.56	0.1215E 01	0.5023E 01

TABLE 10 EXPERIMENTAL GAS FLOW DATA FOR CORE 1

ENDFACE DATA FOR SANDSTONE SAMPLE

RUN	DELP (ATM)	PMAK (ATM-1)	KA (MD)	DELPM (ATM SEC/CM ² CP)	WAV (GM/SEC CM ² CP)
1	0.2854E 02	0.6037E-01	0.2161E 01	0.4028E 03	0.1630E 00
2	0.3061E 02	0.5606E-01	0.2133E 01	0.4688E 03	0.1840E 00
3	0.8917E 01	0.1838E 00	0.2567E 01	0.3896E 03	0.2023E-01
4	0.1128E 02	0.1500E 00	0.2494E 01	0.4010E 03	0.3043E-01
5	0.1278E 02	0.1342E 00	0.2456E 01	0.4072E 03	0.3790E-01
6	0.1438E 02	0.1203E 00	0.2418E 01	0.4136E 03	0.4676E-01
7	0.1634E 02	0.1065E 00	0.2381E 01	0.4199E 03	0.5902E-01
8	0.1980E 02	0.8823E-01	0.2280E 01	0.4385E 03	0.8230E-01
9	0.2285E 02	0.7627E-01	0.2254E 01	0.4437E 03	0.1086E 00
10	0.2553E 02	0.6796E-01	0.2203E 01	0.4538E 03	0.1323E 00
11	0.2730E 02	0.6329E-01	0.2186E 01	0.4574E 03	0.1505E 00
12	0.2443E 02	0.7114E-01	0.2227E 01	0.4490E 03	0.1223E 00
13	0.2125E 02	0.8215E-01	0.2277E 01	0.4392E 03	0.9445E-01
14	0.1795E 02	0.9723E-01	0.2333E 01	0.4286E 03	0.6926E-01
15	0.9129E 00	0.7237E 00	0.3321E 01	0.3011E 03	0.6869E-03
16	0.1952E 00	0.9808E 00	0.3691E 01	0.2709E 03	0.1196E-03
17	0.3915E 02	0.4827E-01	0.2071E 01	0.4827E 03	0.2370E 00
18	0.3984E 02	0.4202E-01	0.2018E 01	0.4954E 03	0.2983E 00
19	0.4399E 02	0.3756E-01	0.1983E 01	0.5042E 03	0.3591E 00
20	0.4686E 02	0.3493E-01	0.1959E 01	0.5106E 03	0.4041E 00
21	0.4968E 02	0.3273E-01	0.1913E 01	0.5228E 03	0.4457E 00
22	0.5581E 02	0.2801E-01	0.1869E 01	0.5350E 03	0.5730E 00
23	0.5343E 02	0.3012E-01	0.1882E 01	0.5313E 03	0.5082E 00
24	0.4568E 02	0.3053E-01	0.1971E 01	0.5074E 03	0.3755E 00
25	0.4187E 02	0.3968E-01	0.2002E 01	0.4994E 03	0.3287E 00
26	0.3730E 02	0.4515E-01	0.2053E 01	0.4871E 03	0.2661E 00
27	0.3225E 02	0.5174E-01	0.2103E 01	0.4755E 03	0.2074E 00
28	0.3228E 02	0.5169E-01	0.2092E 01	0.4779E 03	0.2070E 00
29	0.3053E 02	0.5016E-01	0.2127E 01	0.4702E 03	0.1839E 00
30	0.1974E 02	0.8853E-01	0.2297E 01	0.4352E 03	0.8249E-01
31	0.4821E 02	0.3384E-01	0.1922E 01	0.5202E 03	0.4280E 00
32	0.3286E 02	0.2450E-01	0.1810E 01	0.5525E 03	0.6959E 00
33	0.6070E 02	0.2594E-01	0.1829E 01	0.5469E 03	0.6552E 00
34	0.5693E 02	0.2083E-01	0.1843E 01	0.5425E 03	0.6223E 00
35	0.5690E 02	0.2793E-01	0.1859E 01	0.5379E 03	0.5848E 00
36	0.5496E 02	0.2909E-01	0.1873E 01	0.5339E 03	0.5484E 00
37	0.5154E 02	0.3131E-01	0.1904E 01	0.5252E 03	0.4886E 00
38	0.4869E 02	0.3320E-01	0.1933E 01	0.5172E 03	0.4448E 00
39	0.7543E 01	0.2114E 00	0.2596E 01	0.3852E 03	0.1507E-01
40	0.3712E 00	0.8964E 00	0.3503E 01	0.2855E 03	0.2494E-03
41	0.7156E 00	0.7832E 00	0.3367E 01	0.2970E 03	0.5004E-03
42	0.1089E 01	0.6025E 00	0.3232E 01	0.3094E 03	0.8401E-03
43	0.1028E 01	0.5443E 00	0.3051E 01	0.3277E 03	0.1070E-02
44	0.3402E 01	0.3866E 00	0.2819E 01	0.3248E 03	0.4097E-02

TABLE 10

EXPERIMENTAL GAS FLOW DATA FOR CORE 1

ENDFACE DATA FOR SANDSTONE SAMPLE

RUN	DELP (ATM)	PMAR (ATM-1)	KA (MD)	DELPm (ATM SEC/CM ² CP)	WAV (GM/SEC CM ² CP)
45	0.2714E 01	0.4366E 00	0.2901E 01	0.3447E 03	0.2936E-02
46	0.5782E 00	0.8252E 00	0.3440E 01	0.2907E 03	0.3929E-03
47	0.4622E 00	0.8598E 00	0.3487E 01	0.2868E 03	0.3186E-03
48	0.1499E 01	0.5969E 00	0.3126E 01	0.3199E 03	0.1280E-02

TABLE 11 EXPERIMENTAL GAS FLOW DATA FOR CORE 1

DATA FOR SANDSTONE SAMPLE FROM SECTION 1

RUN	P1A (ATM)	P2A (ATM)	T(K)	QG (CC/SEC)	DELP2 (ATM2)
1	30.84	26.481	300.13	0.1566E 03	0.2496E 03
2	33.14	28.479	301.01	0.1775E 03	0.2872E 03
3	9.90	8.494	300.16	0.1925E 02	0.2581E 02
4	12.30	10.570	300.15	0.2898E 02	0.3969E 02
5	13.04	11.880	300.14	0.3613E 02	0.5054E 02
6	15.50	13.334	300.14	0.4461E 02	0.6255E 02
7	17.56	15.095	300.13	0.5635E 02	0.8055E 02
8	21.24	18.157	300.27	0.7875E 02	0.1213E 03
9	24.54	21.117	299.92	0.1040E 03	0.1561E 03
10	27.48	23.583	300.26	0.1270E 03	0.1989E 03
11	29.45	25.319	300.28	0.1446E 03	0.2264E 03
12	20.27	22.597	300.41	0.1173E 03	0.1796E 03
13	22.80	19.586	300.45	0.9049E 02	0.1363E 03
14	19.20	16.558	300.52	0.6625E 02	0.9689E 02

TABLE II EXPERIMENTAL GAS FLOW DATA FOR CORE 1

DATA FOR SANDSTONE SAMPLE FROM SECTION 1

RUN	DELP (ATM)	PMAR (ATM-1)	KA (MD)	DELPM (ATM SEC/CM ² CP)	WAV (GM/SEC CM ² CP)
1	0.4355E 01	0.3489E-01	0.1952E 01	0.5123E 03	0.1611E 00
2	0.4661E 01	0.3246E-01	0.1936E 01	0.5166E 03	0.1817E 00
3	0.1403E 01	0.1087E 00	0.2283E 01	0.4381E 03	0.2017E-01
4	0.1735E 01	0.8743E-01	0.2238E 01	0.4468E 03	0.3029E-01
5	0.1965E 01	0.7775E-01	0.2194E 01	0.4559E 03	0.3772E-01
6	0.2169E 01	0.6936E-01	0.2191E 01	0.4563E 03	0.4650E-01
7	0.2467E 01	0.6124E-01	0.2153E 01	0.4645E 03	0.5805E-01
8	0.2079E 01	0.5077E-01	0.2005E 01	0.4987E 03	0.8167E-01
9	0.3419E 01	0.4381E-01	0.2058E 01	0.4859E 03	0.1076E 00
10	0.3396E 01	0.3917E-01	0.1982E 01	0.5045E 03	0.1310E 00
11	0.4134E 01	0.3652E-01	0.1986E 01	0.5036E 03	0.1488E 00
12	0.3674E 01	0.4093E-01	0.2028E 01	0.4932E 03	0.1211E 00
13	0.3215E 01	0.4718E-01	0.2055E 01	0.4865E 03	0.9367E-01
14	0.2705E 01	0.2583E-01	0.2112E 01	0.4736E 03	0.6878E-01

TABLE 12 EXPERIMENTAL GAS FLOW DATA FOR CORE 1

DATA FOR SANSTONE SAMPLE FROM SECTION 2

RUN	P1A (ATM)	P2A (ATM)	TMK (K)	Q0 (CC/SEC)	DELP2 (ATM2)
1	26.48	22.228	300.13	0.1560E 03	0.2071E 03
2	28.48	24.107	301.01	0.1775E 03	0.2299E 03
3	8.49	7.103	300.16	0.1925E 02	0.2170E 02
4	10.57	8.831	300.15	0.2898E 02	0.3373E 02
5	11.88	9.947	300.14	0.3613E 02	0.4218E 02
6	13.33	11.138	300.14	0.4461E 02	0.5374E 02
7	15.09	12.635	300.13	0.5635E 02	0.6821E 02
8	16.16	15.200	300.27	0.7875E 02	0.9862E 02
9	21.12	17.677	299.92	0.1040E 03	0.1334E 03
10	23.58	19.759	300.26	0.1270E 03	0.1658E 03
11	25.32	21.229	300.28	0.1446E 03	0.1904E 03
12	22.60	16.915	300.41	0.1173E 03	0.1528E 03
13	19.59	16.405	300.45	0.9049E 02	0.1145E 03
14	16.56	13.853	300.52	0.6625E 02	0.8226E 02

TABLE 12

EXPERIMENTAL GAS FLOW DATA FOR CORE 1

DATA FOR SANDSTONE SAMPLE FROM SECTION 2

RUN	DELP (ATM)	PMAR (ATM-1)	KA (MD)	DELPM (ATM SEC/CM2 CP)	WAV (GM/SEC CM2 CP)
1	0.4253E 01	0.4106E-01	0.2028E 01	0.4932E 03	0.1618E 00
2	0.4372E 01	0.3803E-01	0.2084E 01	0.4798E 03	0.1825E 00
3	0.1392E 01	0.1282E 00	0.2347E 01	0.4261E 03	0.2019E-01
4	0.1739E 01	0.1031E 00	0.2277E 01	0.4392E 03	0.3034E-01
5	0.1933E 01	0.9163E-01	0.2271E 01	0.4402E 03	0.3779E-01
6	0.2190E 01	0.8173E-01	0.2203E 01	0.4538E 03	0.4660E-01
7	0.2460E 01	0.7212E-01	0.2196E 01	0.4554E 03	0.5878E-01
8	0.2757E 01	0.6996E-01	0.2129E 01	0.4697E 03	0.8190E-01
9	0.3440E 01	0.5155E-01	0.2077E 01	0.4813E 03	0.1079E 00
10	0.3824E 01	0.4614E-01	0.2052E 01	0.4874E 03	0.1315E 00
11	0.4090E 01	0.4297E-01	0.2036E 01	0.4910E 03	0.1494E 00
12	0.3681E 01	0.4818E-01	0.2055E 01	0.4865E 03	0.1215E 00
13	0.3181E 01	0.5557E-01	0.2112E 01	0.4735E 03	0.9395E-01
14	0.2705E 01	0.6577E-01	0.2148E 01	0.4656E 03	0.6895E-01

TABLE 13 EXPERIMENTAL GAS FLOW DATA FOR CORE 1

DATA FOR SANDSTONE SAMPLE FROM SECTION 3

RUN	P1A (ATM)	P2A (ATM)	TMR (K)	Q0 (CC/SEC)	DELP2 (ATM2)
1	22.23	17.635	300.13	0.1566E 03	0.1831E 03
2	24.11	19.150	301.01	0.1775E 03	0.2144E 03
3	7.10	5.585	300.16	0.1925E 02	0.1925E 02
4	8.83	6.938	300.15	0.2898E 02	0.2986E 02
5	9.95	7.822	300.14	0.3613E 02	0.3776E 02
6	11.14	8.783	300.14	0.4461E 02	0.4690E 02
7	12.63	9.960	300.13	0.5635E 02	0.6032E 02
8	15.26	12.024	300.27	0.7875E 02	0.8647E 02
9	17.68	13.989	299.92	0.1040E 03	0.1168E 03
10	19.70	15.650	300.26	0.1270E 03	0.1453E 03
11	21.23	16.330	300.28	0.1446E 03	0.1674E 03
12	18.92	14.993	300.41	0.1173E 03	0.1330E 03
13	16.40	12.994	300.45	0.9049E 02	0.1003E 03
14	13.85	10.944	300.52	0.6625E 02	0.7213E 02

TABLE 13

EXPERIMENTAL GAS FLUX DATA FOR CORE 1

DATA FOR SANDSTONE SAMPLE FROM SECTION 3

RUN	DELP (ATM)	PMAR (ATM-1)	KA (MD)	DELPM (ATM SEC/CM ² CP)	WAV (GM/SEC CM ² CP)
1	0.4593E 01	0.5017E-01	0.2285E 01	0.4376E 03	0.1625E 00
2	0.4557E 01	0.4024E-01	0.2225E 01	0.4493E 03	0.1834E 00
3	0.1517E 01	0.1576E 00	0.2043E 01	0.3784E 03	0.2022E-01
4	0.1393E 01	0.1268E 00	0.2568E 01	0.3893E 03	0.3039E-01
5	0.2125E 01	0.1126E 00	0.2534E 01	0.3947E 03	0.3786E-01
6	0.2354E 01	0.1004E 00	0.2520E 01	0.3968E 03	0.4669E-01
7	0.2669E 01	0.8349E-01	0.2478E 01	0.4035E 03	0.5892E-01
8	0.3170E 01	0.7346E-01	0.2422E 01	0.4128E 03	0.8213E-01
9	0.3588E 01	0.6316E-01	0.2367E 01	0.4225E 03	0.1083E 00
10	0.4103E 01	0.5647E-01	0.2332E 01	0.4287E 03	0.1320E 00
11	0.4399E 01	0.5255E-01	0.2307E 01	0.4335E 03	0.1500E 00
12	0.3923E 01	0.5898E-01	0.2354E 01	0.4248E 03	0.1219E 00
13	0.3411E 01	0.6803E-01	0.2405E 01	0.4159E 03	0.9424E-01
14	0.2909E 01	0.8066E-01	0.2444E 01	0.4092E 03	0.6913E-01

TABLE 14 EXPERIMENTAL GAS FLOW DATA FOR CURE 1

DATA FOR SANDSTONE SAMPLE FROM SECTION 4

RUN	P1A (ATM)	P2A (ATM)	TMK (K)	Q0 (CC/SEC)	DELP2 (ATM2)
1	17.63	2.291	300.13	0.1556E 03	0.3057E 03
2	19.15	2.534	301.01	0.1775E 03	0.3603E 03
3	5.59	0.981	300.16	0.1925E 02	0.3023E 02
4	6.94	1.026	300.15	0.2898E 02	0.4708E 02
5	7.82	1.064	300.14	0.3613E 02	0.6006E 02
6	8.70	1.119	300.14	0.4461E 02	0.7590E 02
7	9.97	1.216	300.13	0.5635E 02	0.9784E 02
8	12.02	1.452	300.27	0.7875E 02	0.1425E 03
9	13.99	1.686	299.92	0.1040E 03	0.1929E 03
10	15.06	1.948	300.26	0.1270E 03	0.2413E 03
11	16.83	2.150	300.28	0.1446E 03	0.2786E 03
12	14.99	1.340	300.41	0.1173E 03	0.2214E 03
13	12.99	1.546	300.45	0.9049E 02	0.1664E 03
14	10.94	1.308	300.52	0.6625E 02	0.1181E 03

TABLE 14

EXPERIMENTAL GAS FLOW DATA FOR CORE 1

DATA FOR SANSTUNE SAMPLE FROM SECTION 4

RUN	DELP (ATM)	PMAR (ATM-1)	KA (MD)	DELPM (ATM SEC/CM ² CP)	WAV (GM/SEC CM ² CP)
1	0.1534E 02	0.1004E 00	0.2304E 01	0.4230E 03	0.1640E 00
2	0.1602E 02	0.9224E-01	0.2286E 01	0.4375E 03	0.1852E 00
3	0.4004E 01	0.3046E 00	0.2924E 01	0.3420E 03	0.2027E-01
4	0.5912E 01	0.2911E 00	0.2828E 01	0.3536E 03	0.3050E-01
5	0.6729E 01	0.2251E 00	0.2764E 01	0.3618E 03	0.3801E-01
6	0.7604E 01	0.2020E 00	0.2702E 01	0.3701E 03	0.4690E-01
7	0.8749E 01	0.1789E 00	0.2649E 01	0.3775E 03	0.5922E-01
8	0.1059E 02	0.1486E 00	0.2545E 01	0.3929E 03	0.8264E-01
9	0.1230E 02	0.1276E 00	0.2480E 01	0.4032E 03	0.1091E 00
10	0.1371E 02	0.1136E 00	0.2428E 01	0.4118E 03	0.1331E 00
11	0.1468E 02	0.1054E 00	0.2395E 01	0.4175E 03	0.1514E 00
12	0.1315E 02	0.1188E 00	0.2446E 01	0.4089E 03	0.1229E 00
13	0.1145E 02	0.1376E 00	0.2508E 01	0.3988E 03	0.9487E-01
14	0.9630E 01	0.1632E 00	0.2587E 01	0.3865E 03	0.6952E-01

TABLE 15

EXPERIMENTAL GAS FLOW DATA FOR CORE 2

ENDFACE DATA FOR SANDSTONE SAMPLE

RUN	P1A (ATM)	P2A (ATM)	TMK (K)	Q0 (CC/SEC)	DELP2 (ATM2)
1	1.70	0.949	300.25	0.8468E 01	0.1982E 01
2	1.58	0.946	300.29	0.6841E 01	0.1596E 01
3	1.45	0.941	300.34	0.5343E 01	0.1218E 01
4	1.36	0.939	300.31	0.4215E 01	0.9719E 00
5	1.33	0.937	300.37	0.4022E 01	0.8970E 00
6	1.29	0.935	300.34	0.3528E 01	0.7858E 00
7	1.26	0.934	300.40	0.3149E 01	0.7153E 00
8	1.21	0.927	300.23	0.2713E 01	0.5964E 00
9	1.16	0.926	300.31	0.2213E 01	0.4843E 00
10	1.11	0.914	300.26	0.1799E 01	0.3965E 00
11	1.08	0.913	300.27	0.1557E 01	0.3432E 00
12	1.14	0.937	299.98	0.9208E 01	0.2156E 01
13	1.70	0.936	299.98	0.8704E 01	0.2008E 01
14	1.62	0.933	300.01	0.7499E 01	0.1744E 01
15	1.50	0.929	299.97	0.6054E 01	0.1378E 01
16	1.54	0.925	299.90	0.4782E 01	0.1077E 01
17	1.51	0.923	299.89	0.3826E 01	0.8548E 00
18	1.34	0.918	299.59	0.4205E 01	0.9411E 00
19	1.28	0.926	300.10	0.3500E 01	0.7868E 00
20	1.22	0.925	300.00	0.2850E 01	0.6269E 00
21	4.03	1.386	300.26	0.7171E 02	0.1952E 02
22	1.75	0.937	299.59	0.9275E 01	0.2180E 01
23	2.17	0.959	299.71	0.1562E 02	0.3796E 01
24	2.59	0.991	299.82	0.2288E 02	0.5710E 01
25	2.80	1.010	299.51	0.2690E 02	0.6798E 01
26	2.38	0.973	299.61	0.1909E 02	0.4709E 01
27	1.96	0.946	299.65	0.1233E 02	0.2944E 01
28	2.98	1.031	300.48	0.3087E 02	0.7831E 01
29	1.06	0.928	300.31	0.1243E 01	0.2705E 00
30	1.05	0.928	300.28	0.1070E 01	0.2317E 00
31	1.02	0.927	300.30	0.8746E 00	0.1885E 00
32	1.01	0.927	300.08	0.7830E 00	0.1688E 00
33	1.00	0.927	300.20	0.6991E 00	0.1493E 00
34	1.00	0.933	300.24	0.5633E 00	0.1210E 00
35	0.98	0.932	299.91	0.3992E 00	0.3656E-01
36	0.97	0.931	300.12	0.3053E 00	0.6598E-01
37	0.02	3.300	299.97	0.2310E 03	0.7051E 02
38	10.74	4.279	300.03	0.3087E 03	0.9697E 02
39	11.73	4.905	299.87	0.3577E 03	0.1135E 03
40	13.10	5.726	300.20	0.4243E 03	0.1384E 03
41	28.72	17.475	299.98	0.1331E 04	0.5196E 03
42	17.85	9.022	300.04	0.6748E 03	0.2374E 03
43	27.41	16.413	300.32	0.1245E 04	0.4821E 03
44	26.07	15.304	300.41	0.1162E 04	0.4454E 03

TABLE 15

EXPERIMENTAL GAS FLUX DATA FOR CORE 2

ENDFACE DATA FOR SANDSTONE SAMPLE

RUN	P1A (ATM)	P2A (ATM)	TMR (K)	QD (CC/SEC)	DELP2 (ATM2)
45	24.84	14.358	299.90	0.1080E 04	0.4111E 03
46	24.03	13.712	299.80	0.1038E 04	0.3893E 03
47	14.33	6.492	300.74	0.4825E 03	0.1632E 03
48	19.28	9.963	300.53	0.7571E 03	0.2720E 03
49	20.69	11.031	300.33	0.8397E 03	0.3063E 03
50	19.97	10.507	300.19	0.7995E 03	0.2885E 03
51	18.47	9.405	300.06	0.7126E 03	0.2526E 03
52	23.02	12.909	299.54	0.9741E 03	0.3635E 03
53	13.79	6.139	300.08	0.4565E 03	0.1524E 03
54	12.09	5.050	300.17	0.3710E 03	0.1207E 03
55	11.07	4.397	299.93	0.3193E 03	0.1031E 03
56	9.94	3.704	300.11	0.2691E 03	0.8455E 02
57	3.34	1.084	300.39	0.3854E 02	0.9989E 01
58	3.92	1.203	300.40	0.5248E 02	0.1392E 02
59	4.45	1.339	300.21	0.6660E 02	0.1802E 02
60	4.84	1.453	300.07	0.7790E 02	0.2133E 02
61	5.41	1.645	300.15	0.9532E 02	0.2653E 02
62	5.82	1.803	300.26	0.1089E 03	0.3064E 02
63	6.10	1.921	300.27	0.1186E 03	0.3353E 02
64	5.37	2.031	300.25	0.1280E 03	0.3648E 02
65	6.70	2.173	300.25	0.1397E 03	0.4015E 02
66	7.04	2.326	300.24	0.1522E 03	0.4414E 02
67	3.08	1.048	300.25	0.3273E 02	0.8381E 01
68	3.64	1.139	300.26	0.4500E 02	0.1196E 02
69	4.15	1.253	300.28	0.5803E 02	0.1552E 02
70	7.04	2.347	300.43	0.1521E 03	0.4408E 02
71	5.67	1.539	300.47	0.8494E 02	0.2335E 02
72	3.47	1.103	300.55	0.4161E 02	0.1082E 02
73	2.96	1.035	300.40	0.3022E 02	0.7664E 01
74	2.68	1.005	300.77	0.2461E 02	0.6194E 01
75	2.48	0.987	300.65	0.2089E 02	0.5194E 01
76	2.24	0.972	300.61	0.1745E 02	0.4280E 01
77	7.53	2.569	300.27	0.1687E 03	0.5006E 02
78	8.00	2.799	300.36	0.1878E 03	0.5623E 02
79	8.51	3.057	300.41	0.2087E 03	0.6309E 02
80	21.72	12.019	299.02	0.8933E 03	0.3272E 03
81	22.28	12.495	300.35	0.9261E 03	0.3403E 03
82	23.64	13.543	300.23	0.1006E 04	0.3755E 03
83	25.51	15.026	299.84	0.1120E 04	0.4251E 03
84	26.81	15.979	299.42	0.1196E 04	0.4632E 03
85	28.06	16.993	300.18	0.1279E 04	0.4988E 03
86	29.60	18.299	299.90	0.1378E 04	0.5450E 03
87	30.17	18.755	299.34	0.1415E 04	0.5587E 03
88	14.84	6.894	300.23	0.5095E 03	0.1727E 03

TABLE 15

EXPERIMENTAL GAS FLOW DATA FOR CORE 2

ENLFACE DATA FOR SANSTONE SAMPLE

RUN	DELP (ATM)	PMAR (ATM-1)	KA (MD)	DELPM (ATM SEC/CM2 CP)	WAV (GM/SEC CM2 CP)
1	0.7488E 00	0.7556E 00	0.4759E 02	0.2101E 02	0.9150E-02
2	0.6322E 00	0.7925E 00	0.4777E 02	0.2093E 02	0.7392E-02
3	0.5091E 00	0.8361E 00	0.4889E 02	0.2045E 02	0.5772E-02
4	0.4224E 00	0.8693E 00	0.4832E 02	0.2069E 02	0.4555E-02
5	0.3951E 00	0.8810E 00	0.4998E 02	0.2001E 02	0.4346E-02
6	0.3534E 00	0.8994E 00	0.5003E 02	0.1999E 02	0.3812E-02
7	0.3259E 00	0.9112E 00	0.4908E 02	0.2037E 02	0.3402E-02
8	0.2755E 00	0.9372E 00	0.5067E 02	0.1973E 02	0.2933E-02
9	0.2324E 00	0.9597E 00	0.5090E 02	0.1964E 02	0.2391E-02
10	0.1960E 00	0.9885E 00	0.5052E 02	0.1979E 02	0.1944E-02
11	0.1718E 00	0.1001E 01	0.5052E 02	0.1979E 02	0.1683E-02
12	0.8040E 00	0.7465E 00	0.4751E 02	0.2105E 02	0.9950E-02
13	0.7625E 00	0.7595E 00	0.4822E 02	0.2074E 02	0.9412E-02
14	0.6841E 00	0.7846E 00	0.4784E 02	0.2090E 02	0.8109E-02
15	0.5680E 00	0.8247E 00	0.4887E 02	0.2046E 02	0.6547E-02
16	0.4650E 00	0.8635E 00	0.4936E 02	0.2026E 02	0.5173E-02
17	0.3834E 00	0.8970E 00	0.4975E 02	0.2010E 02	0.4139E-02
18	0.4176E 00	0.8875E 00	0.4958E 02	0.2017E 02	0.4553E-02
19	0.3564E 00	0.9059E 00	0.4950E 02	0.2020E 02	0.3784E-02
20	0.2925E 00	0.9331E 00	0.5057E 02	0.1978E 02	0.3083E-02
21	0.3244E 01	0.3324E 00	0.4098E 02	0.2440E 02	0.7737E-01
22	0.8115E 00	0.7446E 00	0.4722E 02	0.2118E 02	0.1004E-01
23	0.1212E 01	0.6388E 00	0.4570E 02	0.2188E 02	0.1690E-01
24	0.1590E 01	0.5590E 00	0.4448E 02	0.2248E 02	0.2475E-01
25	0.1780E 01	0.5254E 00	0.4390E 02	0.2278E 02	0.2910E-01
26	0.1405E 01	0.5969E 00	0.4501E 02	0.2222E 02	0.2066E-01
27	0.1013E 01	0.6885E 00	0.4650E 02	0.2150E 02	0.1334E-01
28	0.1951E 01	0.4983E 00	0.4400E 02	0.2273E 02	0.3332E-01
29	0.1558E 00	0.1004E 01	0.5122E 02	0.1952E 02	0.1344E-02
30	0.1174E 00	0.1014E 01	0.5147E 02	0.1943E 02	0.1157E-02
31	0.9661E-01	0.1025E 01	0.5168E 02	0.1935E 02	0.9452E-03
32	0.8696E-01	0.1030E 01	0.5164E 02	0.1936E 02	0.8474E-03
33	0.7730E-01	0.1035E 01	0.5215E 02	0.1918E 02	0.7558E-03
34	0.6277E-01	0.1037E 01	0.5184E 02	0.1929E 02	0.6090E-03
35	0.4534E-01	0.1048E 01	0.5126E 02	0.1951E 02	0.4319E-03
36	0.3477E-01	0.1054E 01	0.5149E 02	0.1942E 02	0.3301E-03
37	0.5723E 01	0.1023E 00	0.3655E 02	0.2736E 02	0.2487E 00
38	0.6458E 01	0.1332E 00	0.3556E 02	0.2811E 02	0.3319E 00
39	0.6825E 01	0.1202E 00	0.3520E 02	0.2841E 02	0.3845E 00
40	0.7342E 01	0.1061E 00	0.3435E 02	0.2911E 02	0.4552E 00
41	0.1125E 02	0.4329E-01	0.2897E 02	0.3451E 02	0.1411E 01
42	0.8832E 01	0.7441E-01	0.3215E 02	0.3110E 02	0.7270E 00
43	0.1100E 02	0.4563E-01	0.2925E 02	0.3419E 02	0.1320E 01
44	0.1070E 02	0.4834E-01	0.2952E 02	0.3387E 02	0.1233E 01

TABLE 15

EXPERIMENTAL GAS FLOW DATA FOR CORE 2

ENDFACE DATA FOR SANDSTONE SAMPLE

RUN	DELP (ATM)	PMAR (ATM-1)	KA (MD) (ATM SEC/CM ² CP)	DELPM (GM/SEC CM ² CP)	WAV
45	0.1049E 02	0.5102E-01	0.2980E 02	0.3356E 02	0.1156E 01
46	0.1032E 02	0.5259E-01	0.3002E 02	0.3331E 02	0.1105E 01
47	0.7839E 01	0.9604E-01	0.3325E 02	0.3007E 02	0.5164E 00
48	0.9295E 01	0.6835E-01	0.3137E 02	0.3187E 02	0.8078E 00
49	0.9550E 01	0.6306E-01	0.3090E 02	0.3236E 02	0.8954E 00
50	0.9465E 01	0.6562E-01	0.3119E 02	0.3206E 02	0.8533E 00
51	0.9054E 01	0.7175E-01	0.3169E 02	0.3156E 02	0.7617E 00
52	0.1012E 02	0.5566E-01	0.3011E 02	0.3321E 02	0.1039E 01
53	0.7648E 01	0.1004E 00	0.3355E 02	0.2980E 02	0.4898E 00
54	0.7043E 01	0.1167E 00	0.3440E 02	0.2907E 02	0.3984E 00
55	0.6669E 01	0.1294E 00	0.3459E 02	0.2891E 02	0.3433E 00
56	0.6172E 01	0.1460E 00	0.3557E 02	0.2811E 02	0.2895E 00
57	0.2257E 01	0.4520E 00	0.4304E 02	0.2323E 02	0.4160E-01
58	0.2717E 01	0.3904E 00	0.4207E 02	0.2377E 02	0.5662E-01
59	0.3112E 01	0.3455E 00	0.4122E 02	0.2426E 02	0.7188E-01
60	0.3389E 01	0.3177E 00	0.4072E 02	0.2456E 02	0.8414E-01
61	0.3762E 01	0.2836E 00	0.4007E 02	0.2496E 02	0.1028E 00
62	0.4019E 01	0.2623E 00	0.3968E 02	0.2520E 02	0.1175E 00
63	0.4180E 01	0.2493E 00	0.3948E 02	0.2533E 02	0.1273E 00
64	0.4342E 01	0.2380E 00	0.3916E 02	0.2554E 02	0.1379E 00
65	0.4526E 01	0.2254E 00	0.3886E 02	0.2573E 02	0.1506E 00
66	0.4713E 01	0.2136E 00	0.3849E 02	0.2598E 02	0.1639E 00
67	0.2031E 01	0.4846E 00	0.4353E 02	0.2297E 02	0.3535E-01
68	0.2502E 01	0.4185E 00	0.4253E 02	0.2351E 02	0.4923E-01
69	0.2880E 01	0.3713E 00	0.4171E 02	0.2397E 02	0.6263E-01
70	0.4695E 01	0.2130E 00	0.3858E 02	0.2592E 02	0.1638E 00
71	0.3532E 01	0.3025E 00	0.4063E 02	0.2461E 02	0.9157E-01
72	0.2505E 01	0.4374E 00	0.4295E 02	0.2328E 02	0.4489E-01
73	0.1921E 01	0.5012E 00	0.4400E 02	0.2273E 02	0.3262E-01
74	0.1679E 01	0.5421E 00	0.4442E 02	0.2251E 02	0.2655E-01
75	0.1497E 01	0.5762E 00	0.4491E 02	0.2226E 02	0.2224E-01
76	0.1314E 01	0.6140E 00	0.4553E 02	0.2196E 02	0.1884E-01
77	0.4958E 01	0.1981E 00	0.3765E 02	0.2656E 02	0.1817E 00
78	0.3204E 01	0.1851E 00	0.3735E 02	0.2678E 02	0.2022E 00
79	0.3454E 01	0.1729E 00	0.3701E 02	0.2702E 02	0.2246E 00
80	0.9700E 01	0.5928E-01	0.3066E 02	0.3262E 02	0.9534E 00
81	0.9785E 01	0.5751E-01	0.3071E 02	0.3256E 02	0.9860E 00
82	0.1010E 02	0.5379E-01	0.3024E 02	0.3307E 02	0.1070E 01
83	0.1049E 02	0.4934E-01	0.2970E 02	0.3367E 02	0.1190E 01
84	0.1083E 02	0.4675E-01	0.2907E 02	0.3440E 02	0.1272E 01
85	0.1107E 02	0.4439E-01	0.2903E 02	0.3444E 02	0.1350E 01
86	0.1136E 02	0.4170E-01	0.2861E 02	0.3495E 02	0.1400E 01
87	0.1142E 02	0.4088E-01	0.2857E 02	0.3500E 02	0.1500E 01
88	0.7948E 01	0.9202E-01	0.3308E 02	0.3023E 02	0.5458E 00

TABLE 16 EXPERIMENTAL GAS FLOW DATA FOR CORE 2

DATA FOR SANDSTONE SAMPLE FROM SECTION 1

RUN	P1A (ATM)	P2A (ATM)	TMK (K)	Q0 (CC/SEC)	DELP2 (ATM2)
1	10.93	6.305	300.30	0.3315E 03	0.7976E 02
2	9.28	5.113	299.84	0.2506E 03	0.5999E 02
3	14.47	8.771	299.92	0.5074E 03	0.1324E 03
4	12.67	7.410	300.16	0.4110E 03	0.1055E 03
5	7.70	4.093	299.81	0.1811E 03	0.4253E 02
6	8.52	4.603	299.40	0.2161E 03	0.5133E 02
7	14.55	8.855	299.08	0.5100E 03	0.1334E 03
8	10.24	10.115	299.49	0.6044E 03	0.1614E 03
9	17.89	11.441	299.56	0.6999E 03	0.1891E 03
10	19.16	12.394	299.42	0.7713E 03	0.2137E 03
11	20.75	13.670	299.51	0.8656E 03	0.2436E 03
12	23.28	15.762	299.22	0.1020E 04	0.2936E 03
13	24.81	17.055	299.74	0.1115E 04	0.3248E 03
14	26.21	18.195	299.46	0.1203E 04	0.3558E 03
15	27.64	19.420	299.12	0.1296E 04	0.3866E 03
16	21.65	14.350	298.88	0.9183E 03	0.2627E 03

TABLE 16

EXPERIMENTAL GAS FLOW DATA FOR CORE 2

DATA FOR SANOSTONE SAMPLE FROM SECTION 1

KUN	DELP (ATM)	PMAK (ATM-1)	KA (MU)	DELPM (ATM SEC/CM ² CP)	WAV (GM/SEC CM ² CP)
1	0.4627E 01	0.1160E 00	0.1436E 02	0.6962E 02	0.3559E 00
2	0.4108E 01	0.1389E 00	0.1437E 02	0.6957E 02	0.2696E 00
3	0.5699E 01	0.8606E-01	0.1324E 02	0.7553E 02	0.5437E 00
4	0.5257E 01	0.9962E-01	0.1348E 02	0.7419E 02	0.4414E 00
5	0.5606E 01	0.1696E 00	0.1404E 02	0.6829E 02	0.1952E 00
6	0.5913E 01	0.1525E 00	0.1445E 02	0.6922E 02	0.2329E 00
7	0.5699E 01	0.8544E-01	0.1314E 02	0.7607E 02	0.5476E 00
8	0.6124E 01	0.7589E-01	0.1292E 02	0.7738E 02	0.6474E 00
9	0.5447E 01	0.6819E-01	0.1279E 02	0.7817E 02	0.7486E 00
10	0.6771E 01	0.6337E-01	0.1248E 02	0.8015E 02	0.8243E 00
11	0.7077E 01	0.5811E-01	0.1230E 02	0.8127E 02	0.9237E 00
12	0.7519E 01	0.5123E-01	0.1203E 02	0.8311E 02	0.1037E 01
13	0.7757E 01	0.4777E-01	0.1194E 02	0.8374E 02	0.1185E 01
14	0.6012E 01	0.4504E-01	0.1175E 02	0.8508E 02	0.1278E 01
15	0.8217E 01	0.4250E-01	0.1164E 02	0.8593E 02	0.1375E 01
16	0.7298E 01	0.3556E-01	0.1200E 02	0.8289E 02	0.9808E 00

TABLE 17 EXPERIMENTAL GAS FLOW DATA FOR CORE 2

DATA FOR SANDSTONE SAMPLE FROM SECTION 2

RUN	P1A (ATM)	P2A (ATM)	TMR (K)	Q0 (CC/SEC)	DELP2 (ATM2)
1	6.30	5.502	300.30	0.3315E 03	0.9480E 01
2	5.11	4.592	299.84	0.2506E 03	0.6850E 01
3	8.77	7.828	299.92	0.5074E 03	0.1564E 02
4	7.41	6.550	300.16	0.4116E 03	0.1193E 02
5	4.09	3.446	299.81	0.1811E 03	0.4874E 01
6	4.60	3.909	299.40	0.2161E 03	0.5908E 01
7	8.86	7.896	299.08	0.5100E 03	0.1607E 02
8	10.11	9.135	299.49	0.6044E 03	0.1880E 02
9	11.44	10.400	299.56	0.6999E 03	0.2274E 02
10	12.39	11.326	299.42	0.7713E 03	0.2534E 02
11	13.67	12.578	299.51	0.8650E 03	0.2867E 02
12	15.76	14.585	299.22	0.1020E 04	0.3572E 02
13	17.05	15.817	299.74	0.1115E 04	0.4071E 02
14	18.19	16.960	299.46	0.1203E 04	0.4342E 02
15	19.42	18.185	299.12	0.1296E 04	0.4644E 02
16	14.35	15.231	298.88	0.9183E 03	0.3087E 02

TABLE 17

EXPERIMENTAL GAS FLOW DATA FOR CORE 2

DATA FOR SANDSTONE SAMPLE FROM SECTION 2

RUN	DELP (ATM)	PMAR (ATM-1)	KA (MD)	DELPM (ATM SEC/CM ² CP)	wAV (GM/SEC CM ² CP)
1	0.8029E 00	0.1694E 00	0.9477E 02	0.1055E 02	0.3567E 00
2	0.7213E 00	0.2104E 00	0.9868E 02	0.1013E 02	0.2702E 00
3	0.9424E 00	0.1205E 00	0.8787E 02	0.1138E 02	0.5454E 00
4	0.8540E 00	0.1432E 00	0.9352E 02	0.1069E 02	0.4426E 00
5	0.0464E 00	0.2053E 00	0.1003E 03	0.9972E 01	0.1955E 00
6	0.0941E 00	0.2350E 00	0.9848E 02	0.1015E 02	0.2334E 00
7	0.9594E 00	0.1119E 00	0.8554E 02	0.1169E 02	0.5493E 00
8	0.9759E 00	0.1039E 00	0.8666E 02	0.1154E 02	0.6495E 00
9	0.1041E 01	0.9157E-01	0.8336E 02	0.1200E 02	0.7511E 00
10	0.1068E 01	0.8432E-01	0.8242E 02	0.1213E 02	0.8273E 00
11	0.1092E 01	0.7620E-01	0.8189E 02	0.1221E 02	0.9272E 00
12	0.1177E 01	0.6590E-01	0.7743E 02	0.1291E 02	0.1091E 01
13	0.1238E 01	0.6084E-01	0.7459E 02	0.1341E 02	0.1190E 01
14	0.1235E 01	0.5689E-01	0.7539E 02	0.1326E 02	0.1283E 01
15	0.1235E 01	0.5319E-01	0.7584E 02	0.1319E 02	0.1382E 01
16	0.1119E 01	0.7251E-01	0.8041E 02	0.1244E 02	0.9846E 00

TABLE 13 EXPERIMENTAL GAS FLOW DATA FOR CURE 2
DATA FOR SANDSTONE SAMPLE FROM SECTION 3

RUN	P1A (ATM)	P2A (ATM)	TMK (K)	Q0 (CC/SEC)	DELP2 (ATM2)
1	5.00	5.148	300.30	0.3315E 03	0.3768E 01
2	4.39	4.093	299.84	0.2506E 03	0.2540E 01
3	7.83	7.478	299.92	0.5074E 03	0.5364E 01
4	6.56	6.185	300.16	0.4116E 03	0.4725E 01
5	3.45	3.149	299.81	0.1811E 03	0.1903E 01
6	3.91	3.599	299.40	0.2161E 03	0.2325E 01
7	7.07	7.486	299.08	0.5100E 03	0.5931E 01
8	9.13	8.720	299.49	0.6044E 03	0.7411E 01
9	10.40	9.961	299.56	0.6999E 03	0.8937E 01
10	11.33	10.880	299.42	0.7713E 03	0.9897E 01
11	12.58	12.113	299.51	0.8656E 03	0.1147E 02
12	14.58	14.112	299.22	0.1020E 04	0.1357E 02
13	15.82	15.345	299.74	0.1115E 04	0.1468E 02
14	16.96	16.477	299.46	0.1203E 04	0.1627E 02
15	18.18	17.684	299.12	0.1296E 04	0.1794E 02
16	19.23	18.777	298.88	0.9183E 03	0.1181E 02

TABLE 16

EXPERIMENTAL GAS FLOW DATA FOR CORE 2

DATA FOR SANDSTONE SAMPLE FROM SECTION 3

RUN	DELP (ATM)	PMAR (ATM-1)	KA (MD)	DELPM (ATM SEC/CM ² CP)	WAV (GM/SEC CM ² CP)
1	0.3538E 00	0.1878E 00	0.2383E 03	0.4196E 01	0.3569E 00
2	0.2954E 00	0.2357E 00	0.2662E 03	0.3756E 01	0.2703E 00
3	0.3504E 00	0.1307E 00	0.2561E 03	0.3904E 01	0.5457E 00
4	0.3709E 00	0.1570E 00	0.2360E 03	0.4238E 01	0.4429E 00
5	0.2977E 00	0.3033E 00	0.2488E 03	0.4019E 01	0.1956E 00
6	0.3096E 00	0.2664E 00	0.2502E 03	0.3997E 01	0.2335E 00
7	0.3862E 00	0.1302E 00	0.2317E 03	0.4316E 01	0.5496E 00
8	0.4151E 00	0.1120E 00	0.2204E 03	0.4536E 01	0.6499E 00
9	0.4389E 00	0.9823E-01	0.2120E 03	0.4717E 01	0.7517E 00
10	0.4457E 00	0.9007E-01	0.2109E 03	0.4741E 01	0.8279E 00
11	0.4644E 00	0.8100E-01	0.2046E 03	0.4887E 01	0.9278E 00
12	0.4729E 00	0.6969E-01	0.2037E 03	0.4909E 01	0.1092E 01
13	0.4712E 00	0.6418E-01	0.2057E 03	0.4839E 01	0.1191E 01
14	0.4865E 00	0.5981E-01	0.2011E 03	0.4974E 01	0.1284E 01
15	0.5001E 00	0.5576E-01	0.1962E 03	0.5097E 01	0.1383E 01
16	0.4542E 00	0.7690E-01	0.2100E 03	0.4761E 01	0.9853E 00

TABLE 19

EXPERIMENTAL GAS FLOW DATA FOR CORE 2

DATA FOR SANDSTONE SAMPLE FROM SECTION 4

RUN	P1A (ATM)	P2A (ATM)	TMR (K)	Q _U (CC/SEC)	DELP2 (ATM2)
1	5.15	4.561	300.30	0.3315E 03	0.5698E 01
2	4.09	3.506	299.84	0.2506E 03	0.4460E 01
3	7.48	6.806	299.92	0.5074E 03	0.9598E 01
4	6.19	5.531	300.16	0.4116E 03	0.7106E 01
5	3.15	2.664	299.81	0.1811E 03	0.2818E 01
6	3.60	3.072	299.40	0.2161E 03	0.3518E 01
7	7.49	6.839	299.08	0.5100E 03	0.9260E 01
8	8.72	8.048	299.49	0.6044E 03	0.1127E 02
9	9.96	9.272	299.56	0.6999E 03	0.1325E 02
10	10.88	10.191	299.42	0.7713E 03	0.1452E 02
11	12.11	11.399	299.51	0.8656E 03	0.1680E 02
12	14.11	13.363	299.22	0.1020E 04	0.2057E 02
13	15.35	14.563	299.74	0.1115E 04	0.2340E 02
14	16.48	15.686	299.46	0.1203E 04	0.2544E 02
15	17.68	16.919	299.12	0.1296E 04	0.2649E 02
16	12.78	12.045	298.88	0.9183E 03	0.1816E 02

TABLE 19

EXPERIMENTAL GAS FLOW DATA FOR CORE 2

DATA FOR SANDSTONE SAMPLE FROM SECTION 4

RUN	DEL F (ATM)	PMAR (ATM-1)	KA (MD)	DELPM (ATM SEC/CM ² CP)	WAV (GM/SEC CM ² CP)
1	0.5869E 00	0.2060E 00	0.1303E 03	0.7677E 01	0.3571E 00
2	0.5869E 00	0.2632E 00	0.1253E 03	0.7978E 01	0.2704E 00
3	0.6720E 00	0.1400E 00	0.1183E 03	0.8453E 01	0.5459E 00
4	0.6039E 00	0.1700E 00	0.1297E 03	0.7712E 01	0.4431E 00
5	0.4848E 00	0.3441E 00	0.1433E 03	0.6979E 01	0.1957E 00
6	0.5274E 00	0.2998E 00	0.1366E 03	0.7319E 01	0.2336E 00
7	0.6464E 00	0.1396E 00	0.1226E 03	0.8155E 01	0.5499E 00
8	0.5720E 00	0.1193E 00	0.1198E 03	0.8345E 01	0.6503E 00
9	0.6890E 00	0.1040E 00	0.1182E 03	0.8463E 01	0.7520E 00
10	0.6890E 00	0.9492E-01	0.1188E 03	0.8415E 01	0.8283E 00
11	0.7145E 00	0.8506E-01	0.1154E 03	0.8664E 01	0.9283E 00
12	0.7485E 00	0.7279E-01	0.1111E 03	0.9003E 01	0.1093E 01
13	0.7825E 00	0.6687E-01	0.1071E 03	0.9333E 01	0.1192E 01
14	0.7910E 00	0.6218E-01	0.1062E 03	0.9412E 01	0.1285E 01
15	0.7655E 00	0.5780E-01	0.1098E 03	0.9108E 01	0.1384E 01
16	0.7315E 00	0.8057E-01	0.1129E 03	0.8896E 01	0.9859E 00

TABLE 20

EXPERIMENTAL GAS FLOW DATA FOR CURE 3

ENDFACE DATA FOR LIMESTONE SAMPLE - DRY

RUN	P1A (ATM)	P2A (ATM)	TMK (K)	Q0 (CC/SEC)	DELP2 (ATM2)
1	28.39	6.092	299.04	0.4870E 03	0.7609E 03
2	61.29	17.862	299.37	0.1341E 04	0.3437E 04
3	57.58	16.552	299.05	0.1248E 04	0.3041E 04
4	54.07	15.307	298.80	0.1153E 04	0.2690E 04
5	50.74	14.130	298.93	0.1063E 04	0.2375E 04
6	47.66	13.048	298.62	0.9796E 03	0.2103E 04
7	43.66	11.073	299.22	0.8735E 03	0.1770E 04
8	39.65	10.187	298.83	0.7698E 03	0.1468E 04
9	36.20	9.214	299.23	0.6638E 03	0.1229E 04
10	32.33	7.938	299.40	0.5859E 03	0.9824E 03
11	23.35	5.190	299.28	0.3744E 03	0.5182E 03
12	18.38	3.801	299.47	0.2681E 03	0.3235E 03
13	14.40	2.780	299.56	0.1884E 03	0.1997E 03
14	1.33	0.930	299.61	0.1433E 01	0.9040E 00
15	3.81	0.970	299.65	0.1724E 02	0.1361E 02

TABLE 20

EXPERIMENTAL GAS FLOW DATA FOR CORE 3

ENDFACE DATA FOR LIMESTONE SAMPLE - DRY

RUN	DELP (ATM)	PMAR (ATM-1)	KA (MD)	DELPM (ATM SEC/CM ² CP)	WAV (GM/SEC CM ² CP)
1	0.2169E 02	0.5702E-01	0.8103E 01	0.1234E 03	0.5394E 00
2	0.4342E 02	0.2527E-01	0.5036E 01	0.1985E 03	0.1454E 01
3	0.4102E 02	0.2698E-01	0.5272E 01	0.1897E 03	0.1358E 01
4	0.3877E 02	0.2883E-01	0.5486E 01	0.1823E 03	0.1259E 01
5	0.3661E 02	0.3083E-01	0.5720E 01	0.1748E 03	0.1163E 01
6	0.3463E 02	0.3294E-01	0.5929E 01	0.1687E 03	0.1074E 01
7	0.3199E 02	0.3614E-01	0.6288E 01	0.1590E 03	0.9593E 00
8	0.2946E 02	0.4013E-01	0.6649E 01	0.1504E 03	0.8484E 00
9	0.2703E 02	0.4400E-01	0.7059E 01	0.1417E 03	0.7544E 00
10	0.2439E 02	0.4966E-01	0.7557E 01	0.1323E 03	0.6477E 00
11	0.1815E 02	0.7006E-01	0.9102E 01	0.1099E 03	0.4163E 00
12	0.1458E 02	0.9016E-01	0.1043E 02	0.9587E 02	0.2989E 00
13	0.1162E 02	0.1164E 00	0.1185E 02	0.8436E 02	0.2104E 00
14	0.4000E 00	0.8850E 00	0.1999E 02	0.5002E 02	0.1597E-02
15	0.2845E 01	0.4180E 00	0.1596E 02	0.6262E 02	0.1922E-01

TABLE 21

EXPERIMENTAL GAS FLOW DATA FOR CURE 3

DATA FOR LIMESTONE SAMPLE - LIQUID SATURATION .0765

RUN	P1A (ATM)	P2A (ATM)	TMK (K)	QJ (CC/SEC)	DELP2 (ATM2)
1	15.49	2.751	299.28	0.1867E 03	0.2321E 03
2	21.27	4.176	299.51	0.2944E 03	0.4349E 03
3	65.54	17.574	299.22	0.1329E 04	0.3961E 04
4	62.10	16.499	298.42	0.1252E 04	0.3584E 04
5	53.71	15.409	298.78	0.1163E 04	0.3209E 04
6	55.19	14.273	298.49	0.1081E 04	0.2842E 04
7	51.82	13.225	298.56	0.9980E 03	0.2510E 04
8	46.65	11.591	298.51	0.8681E 03	0.2042E 04
9	42.46	10.298	298.53	0.7675E 03	0.1697E 04
10	38.40	9.074	298.95	0.6740E 03	0.1399E 04
11	35.22	8.107	298.84	0.5993E 03	0.1174E 04
12	31.20	6.937	299.18	0.5071E 03	0.9255E 03
13	20.44	5.583	299.18	0.4032E 03	0.6678E 03
14	1.48	0.935	299.83	0.1733E 01	0.1331E 01
15	5.12	1.031	299.83	0.2657E 02	0.2525E 02

TABLE 21

EXPERIMENTAL GAS FLOW DATA FOR CURE 3

DATA FOR LIMESTONE SAMPLE - LIQUID SATURATION .0765

RUN	DELP (ATM)	PMAR (ATM-1)	KA (MD)(ATM SEC/CM ² CP)	DELPM (GM/SEC CM ² CP)	WAV
1	0.1270E 02	0.1095E 00	0.1010E 02	0.9902E 02	0.2086E 00
2	0.1709E 02	0.7860E-01	0.8532E 01	0.1172E 03	0.3277E 00
3	0.4777E 02	0.2412E-01	0.4335E 01	0.2307E 03	0.1439E 01
4	0.4560E 02	0.2545E-01	0.4481E 01	0.2223E 03	0.1361E 01
5	0.4330E 02	0.2698E-01	0.4668E 01	0.2142E 03	0.1272E 01
6	0.4092E 02	0.2879E-01	0.4855E 01	0.2059E 03	0.1180E 01
7	0.3860E 02	0.3075E-01	0.5071E 01	0.1972E 03	0.1092E 01
8	0.3506E 02	0.3434E-01	0.5401E 01	0.1852E 03	0.9535E 00
9	0.3217E 02	0.3791E-01	0.5731E 01	0.1745E 03	0.8453E 00
10	0.2941E 02	0.4200E-01	0.6108E 01	0.1637E 03	0.7433E 00
11	0.2711E 02	0.4616E-01	0.6452E 01	0.1550E 03	0.6625E 00
12	0.2427E 02	0.5244E-01	0.6928E 01	0.1443E 03	0.5615E 00
13	0.2066E 02	0.6246E-01	0.7613E 01	0.1314E 03	0.4477E 00
14	0.5500E 00	0.8264E 00	0.1641E 02	0.6090E 02	0.1932E-02
15	0.4099E 01	0.3246E 00	0.1326E 02	0.7538E 02	0.2961E-01

TABLE 22

EXPERIMENTAL GAS FLOW DATA FOR CURE 3

DATA FOR LIMESTONE SAMPLE - LIQUID SATURATION .124

RUN	P1A (ATM)	P2A (ATM)	TMR (K)	Q0 (CC/SEC)	DELP2 (ATM2)
1	17.35	2.858	299.86	0.1938E 03	0.2929E 03
2	22.42	3.954	299.99	0.2820E 03	0.4867E 03
3	71.96	17.644	300.39	0.1338E 04	0.4867E 04
4	69.07	16.936	299.43	0.1281E 04	0.4483E 04
5	65.26	15.848	299.67	0.1196E 04	0.4007E 04
6	62.16	14.963	299.26	0.1127E 04	0.3640E 04
7	58.69	13.969	298.94	0.1048E 04	0.3249E 04
8	54.54	12.792	299.23	0.9540E 03	0.2811E 04
9	50.12	11.533	299.21	0.8568E 03	0.2379E 04
10	45.15	10.138	299.03	0.7491E 03	0.1936E 04
11	40.32	8.771	299.09	0.6446E 03	0.1549E 04
12	35.08	7.342	299.65	0.5361E 03	0.1177E 04
13	31.47	6.379	299.83	0.4626E 03	0.9497E 03
14	26.37	5.048	299.86	0.3618E 03	0.6697E 03
15	19.78	3.470	299.90	0.2415E 03	0.3794E 03
16	1.74	0.936	300.23	0.2370E 01	0.2162E 01
17	5.94	1.039	300.30	0.2870E 02	0.3423E 02

TABLE 22

EXPERIMENTAL GAS FLOW DATA FOR CORE 3

DATA FOR LIMESTONE SAMPLE - LIQUID SATURATION .124

RUN	DELP (ATM)	PMAR (ATM-1)	KA (MD)	DELPM (ATM SEC/CM ² CP)	WAV (GM/SEC CM ² CP)
1	0.1449E 02	0.9896E-01	0.8339E 01	0.1199E 03	0.2160E 00
2	0.1843E 02	0.7571E-01	0.7324E 01	0.1365E 03	0.3133E 00
3	0.5451E 02	0.2232E-01	0.3590E 01	0.2786E 03	0.1439E 01
4	0.5215E 02	0.2326E-01	0.3704E 01	0.2700E 03	0.1384E 01
5	0.4941E 02	0.2466E-01	0.3864E 01	0.2588E 03	0.1295E 01
6	0.4720E 02	0.2593E-01	0.3988E 01	0.2507E 03	0.1224E 01
7	0.4472E 02	0.2753E-01	0.4157E 01	0.2417E 03	0.1142E 01
8	0.4175E 02	0.2970E-01	0.4349E 01	0.2299E 03	0.1041E 01
9	0.3858E 02	0.3244E-01	0.4603E 01	0.2172E 03	0.9379E 00
10	0.3501E 02	0.3618E-01	0.4925E 01	0.2030E 03	0.8229E 00
11	0.3155E 02	0.4074E-01	0.5285E 01	0.1892E 03	0.7102E 00
12	0.2774E 02	0.4715E-01	0.5787E 01	0.1728E 03	0.5917E 00
13	0.2509E 02	0.5284E-01	0.6181E 01	0.1618E 03	0.5115E 00
14	0.2132E 02	0.6366E-01	0.6838E 01	0.1462E 03	0.4012E 00
15	0.1651E 02	0.8601E-01	0.8035E 01	0.1245E 03	0.2688E 00
16	0.8070E 00	0.7465E 00	0.1382E 02	0.7233E 02	0.2643E-02
17	0.4903E 01	0.2865E 00	0.1059E 02	0.9455E 02	0.3200E-01

TABLE 23

EXPERIMENTAL GAS FLOW DATA FOR CORE 3

DATA FOR LIMESTONE SAMPLE - LIQUID SATURATION .205

RUN	P1A (ATM)	P2A (ATM)	TMR (K)	QD (CC/SEC)	DELP2 (ATM2)
1	79.45	17.174	299.38	0.1364E 04	0.6017E 04
2	75.50	16.269	298.57	0.1291E 04	0.5436E 04
3	72.30	15.486	298.61	0.1227E 04	0.4988E 04
4	67.54	14.261	298.70	0.1128E 04	0.4358E 04
5	61.83	12.819	298.39	0.1009E 04	0.3658E 04
6	57.03	11.537	298.84	0.9087E 03	0.3118E 04
7	51.90	10.315	298.58	0.8049E 03	0.2593E 04
8	46.86	9.042	298.88	0.7000E 03	0.2114E 04
9	41.02	7.763	299.19	0.5977E 03	0.1672E 04
10	36.82	6.627	299.34	0.5059E 03	0.1312E 04
11	31.68	5.443	299.24	0.4106E 03	0.9741E 03
12	26.37	4.279	299.36	0.3176E 03	0.6773E 03
13	19.64	2.932	299.32	0.2077E 03	0.3770E 03
14	2.00	0.940	299.81	0.2776E 01	0.3108E 01
15	6.55	1.062	299.85	0.3066E 02	0.4177E 02

TABLE 23

EXPERIMENTAL GAS FLOW DATA FOR CORE 3

DATA FOR LIMESTONE SAMPLE - LIQUID SATURATION .205

RUN	DELP (ATM)	PMAR (ATM-1)	KA (MD)	DELPM (ATM SEC/CM ² CP)	WAV (GM/SEC CM ² CP)
1	0.3228E 02	0.2070E-01	0.2954E 01	0.3385E 03	0.1404E 01
2	0.2923E 02	0.2179E-01	0.2071E 01	0.3256E 03	0.1393E 01
3	0.5082E 02	0.2278E-01	0.3175E 01	0.3150E 03	0.1327E 01
4	0.5328E 02	0.2445E-01	0.3330E 01	0.3003E 03	0.1223E 01
5	0.4901E 02	0.2679E-01	0.3530E 01	0.2833E 03	0.1099E 01
6	0.4544E 02	0.2915E-01	0.3728E 01	0.2682E 03	0.9921E 00
7	0.4164E 02	0.3212E-01	0.3952E 01	0.2530E 03	0.8821E 00
8	0.3781E 02	0.3578E-01	0.4212E 01	0.2374E 03	0.7691E 00
9	0.3585E 02	0.4050E-01	0.4543E 01	0.2201E 03	0.6583E 00
10	0.3019E 02	0.4603E-01	0.4892E 01	0.2044E 03	0.5585E 00
11	0.2624E 02	0.5387E-01	0.5328E 01	0.1877E 03	0.4548E 00
12	0.2209E 02	0.6525E-01	0.5917E 01	0.1690E 03	0.3527E 00
13	0.1671E 02	0.8862E-01	0.6928E 01	0.1443E 03	0.2316E 00
14	0.1058E 01	0.6807E 00	0.1126E 02	0.8876E 02	0.3096E-02
15	0.5488E 01	0.2627E 00	0.9250E 01	0.1081E 03	0.3418E-01

TABLE 24 EXPERIMENTAL GAS FLOW DATA FOR CORE 3

DATA FOR LIMESTONE SAMPLE - LIQUID SATURATION .253

RUN	P1A (ATM)	P2A (ATM)	TMK (K)	QD (CC/SEC)	DELP2 (ATM2)
1	85.44	15.226	298.29	0.1209E 04	0.7067E 04
2	81.46	14.444	297.89	0.1146E 04	0.6426E 04
3	76.05	13.328	298.28	0.1052E 04	0.5605E 04
4	70.53	12.218	298.19	0.9593E 03	0.4826E 04
5	65.57	11.184	297.90	0.8750E 03	0.4174E 04
6	61.04	10.259	298.32	0.7976E 03	0.3621E 04
7	55.66	9.153	298.56	0.7068E 03	0.3007E 04
8	50.19	8.081	298.24	0.6223E 03	0.2454E 04
9	45.42	7.115	298.42	0.5428E 03	0.2013E 04
10	39.98	6.047	299.06	0.4564E 03	0.1562E 04
11	32.08	5.115	299.03	0.3813E 03	0.1205E 04
12	29.81	4.141	298.85	0.3036E 03	0.8714E 03
13	2.05	0.943	299.06	0.3950E 01	0.6149E 01
14	0.60	1.072	299.01	0.4032E 02	0.7288E 02

TABLE 24

EXPERIMENTAL GAS FLOW DATA FOR CORE 3

DATA FOR LIMESTONE SAMPLE - LIQUID SATURATION .253

RUN	DELP (ATM)	PMAR (ATM-1)	KA (MD)	DELPM (ATM SEC/CM ² CP)	WAV (GM/SEC CM ² CP)
1	0.7021E 02	0.1987E-01	0.2220E 01	0.4505E 03	0.1298E 01
2	0.6701E 02	0.2086E-01	0.2303E 01	0.4342E 03	0.1236E 01
3	0.6272E 02	0.2238E-01	0.2420E 01	0.4133E 03	0.1138E 01
4	0.5832E 02	0.2417E-01	0.2553E 01	0.3917E 03	0.1042E 01
5	0.5438E 02	0.2606E-01	0.2677E 01	0.3735E 03	0.9534E 00
6	0.5078E 02	0.2805E-01	0.2813E 01	0.3555E 03	0.8707E 00
7	0.4643E 02	0.3088E-01	0.2996E 01	0.3337E 03	0.7737E 00
8	0.4211E 02	0.3432E-01	0.3217E 01	0.3109E 03	0.6840E 00
9	0.3831E 02	0.3807E-01	0.3415E 01	0.2928E 03	0.5981E 00
10	0.3593E 02	0.4345E-01	0.3704E 01	0.2700E 03	0.5036E 00
11	0.2997E 02	0.4976E-01	0.4001E 01	0.2499E 03	0.4219E 00
12	0.2507E 02	0.5891E-01	0.4388E 01	0.2279E 03	0.3371E 00
13	0.1710E 01	0.5562E 00	0.8100E 01	0.1234E 03	0.4404E-02
14	0.7032E 01	0.2067E 00	0.6967E 01	0.1433E 03	0.4495E-01

B29883